The Pennsylvania State University

The Graduate School

Department of Aerospace Engineering

DRAG COEFFICIENT ESTIMATION USING SATELLITE ATTITUDE AND ORBIT DATA

A Thesis in

Aerospace Engineering

by

2Lt. Christopher L. Hassa, USAF

Submitted in Partial Fulfillment
of the Requirements
for the Degree of

Master of Science

December 2013

The thesis of 2Lt. Christopher L. Hassa was reviewed and approved* by the following:

David B. Spencer
Professor of Aerospace Engineering
Thesis Co-Advisor

Sven G. Bilén
Associate Professor of Engineering Design, Electrical Engineering, and Aerospace Engineering
Thesis Co-Advisor

George A. Lesieutre
Professor of Aerospace Engineering
Head of the Department of Aerospace Engineering

*Signatures are on file in the Graduate School

Disclaimer:

The views expressed in this article are those of the author and do not reflect the official policy or position of the United States Air Force, Department of Defense, or the U.S. Government.

ABSTRACT

The coefficient of drag for spacecraft in a variety of orbits and solar cycle conditions is generally assumed to be a constant value of 2.2. The research herein revisits the validity of this assumption and chooses to directly calculate the coefficient of drag using orbital data gathered from NASA's *Swift* spacecraft. In order to accomplish this task, an accurate cross-sectional area calculation algorithm is generated and an atmospheric model is utilized. The area algorithm accurately predicts the operational cross-sectional area of *Swift* at any given orientation. The density model used is the NRLMSISE-00 atmospheric model, which, when compared to the internally calculated density values assuming the coefficient of drag is 2.2, show large amounts of error.

The uncertainty of the density at the altitude of *Swift* leads to an extended analysis of its orbital decay, giving the best estimate of a no-earlier-than deorbit date of mid-2022 to early 2023. This analysis proved inconclusive, however, as no single model followed the actual decay of *Swift*, implying that the coefficient of drag may change over the mission's duration.

The results of the calculation of the coefficient of drag clearly show that no single value can be assumed as correct. However, some of these results also fall outside of the expected bounds of the coefficient of drag, implying that additional research is required to incorporate additional variables to properly determine what values of the coefficient of drag to use and when.

Table of Contents

List of Figures

List of Tables

Acknowledgments

To God from whom all blessings flow. To the *Swift* FOT for taking the time to teach me about *Swift* and allowing me to help you fly the bird for the past year and a half. To my thesis advisors Drs. Sven Bilén and David Spencer for helping me settle on a topic and ensuring I finished in a timely manner. To the United States Air Force for giving me the opportunity to attend Penn State. To all my friends and family for keeping me grounded and calm.

Chapter 1

1.1 Introduction

For a satellite with no direct means of propulsion, drag is the most significant of the perturbing forces in Low Earth Orbit (LEO). Drag is the result of the particles in a fluid interacting with an object as it passes through the fluid. In space, the atmosphere can be modeled as a fluid and a spacecraft as the object in question. Scientists have been trying to understand the atmosphere and its effects on spacecraft since the launch of *Sputnik 1* in October of 1957. Mathematical models were developed in order to explain the altitude loss of spacecraft in orbit. As more spacecraft were launched, more detailed models of the atmosphere were generated. However, an additional aspect of spacecraft drag must be understood in order to properly develop the next generation of atmospheric models: the coefficient of drag.

The coefficient of drag depends on the geometry of the spacecraft, or more specifically, the geometry that a spacecraft presents to the atmospheric flow. Unfortunately, any spacecraft that changes its attitude in relation to its orbital plane also changes the cross sectional area that it exposes to the flow, thereby changing its coefficient of drag. For example, if a plate were placed perpendicularly in a free-molecular flow and under hypervelocity conditions, the coefficient of drag takes on an upper bound of $c_D = 4$, but if the plate were inclined to 45°, the coefficient of drag takes on a lower bound of $c_D = 2$ [Vallado and Finkleman, 2013]. This variation can lead to

drastic changes in altitude predictions and can incorrectly determine the date of reentry of a dying spacecraft.

Few studies are available that accurately define the cross-sectional area of a spacecraft as it orbits the Earth. This limits the fidelity of drag coefficient models and, by extension, orbit decay models. The area problem is a difficult one in that it depends on knowing accurate pointing information for the satellite. Depending on the mission, the attitude can vary greatly in a matter of seconds. For these reasons, a simplified model is most desirable; therefore, NASA's *Swift* mission was selected as the focus for this study.

NASA's *Swift* spacecraft is a medium-class Explorer mission with a constant mass of 1470 kg. It possesses reaction wheels and magnetic torque rods as its means of attitude control. There is no propulsion on board, so there is no method for station-keeping. Launched from Cape Canaveral, Florida, *Swift* has been on orbit since 20 November 2004. Since launch, it has since been successfully operated by the Flight Operations Team (FOT) and Science Operations Team (SOT) at the Pennsylvania State University. The engineers that make up the FOT are charged with maintaining the health and safety of the spacecraft and as such are tasked with tracking the lifetime trends of critical housekeeping data. They are also responsible for maintaining archives of all state of health data for the entire mission, allowing for quick access to attitude data sampled at a varying rate of 5–30 Hz.[1]

Even though *Swift* already provides a pre-simplified model for analysis, several assumptions still must be explicitly stated or made. These include a constant mass; *Swift*

[1] *Swift* CDR and operational documents

has no propulsion system or other method of changing its mass, so, barring a collision with space debris or the extreme accumulation of oxidation, this assumption holds for *Swift*'s 1470-kg mass. *Swift* has two solar arrays, which are attached as self-actuating wings. Both arrays are always supposed to point normal to the Sun, regardless of where *Swift* is pointing; however, this is not entirely accurate. The solar arrays perform their maneuver at the beginning of a slew to a new target and for long slews this introduces a small amount of error. *Swift* slews to approximately 100 targets each day, and long slews of this nature are rare enough so this error can be deemed negligible in the larger picture.

According to the trends generated by the engineers operating *Swift*, recreated in Figure 1.1, the altitude of the spacecraft has decreased by approximately 12 km of its 590 km over the ten years it has been in LEO, shown with ±3 standard deviations, to give an estimate of the error associated with this source of data.

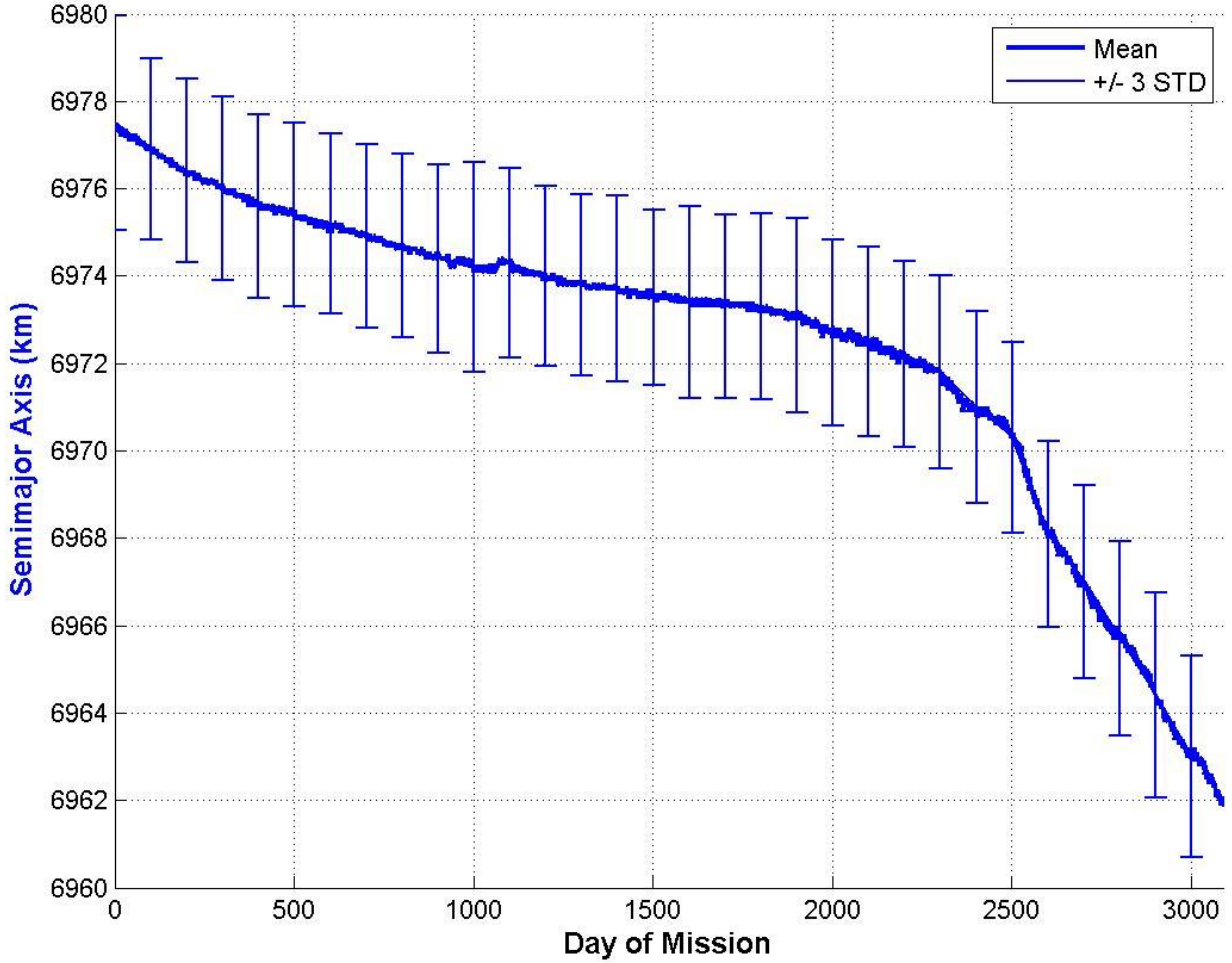

Figure 1.1. Mission Duration versus Mean Semimajor Axis

1.2 Contributions of this Thesis

This thesis discusses the validity of the assumption of a constant value for the coefficient of drag in relation to the decay of a spacecraft in orbit. It shows possible errors in the NRLMSISE-00 atmospheric model and encourages a study of how the coefficient of drag is defined as spacecraft change their attitude as well as their altitude.

1.3 Thesis Overview

This thesis begins by discussing the history of the coefficient of drag and the relevant mathematics for calculating it in Chapter 2.1. Then it discusses the approach taken to accomplish these calculations in Chapter 2.2. Chapter 3 discusses the determination of the cross-sectional area of *Swift*, the utilization of the atmospheric model, the integration of on-orbit data into the analysis, the prediction of the orbital lifetime of *Swift*, and the results of the calculations of the coefficient of drag, each in their own section. Finally, the thesis presents its final conclusions and some possible topics for future studies in Chapter 4.

Chapter 2

2.1 Background

Drag is the mechanical force on a solid object moving through a fluid. Drag results from the difference in velocities between the two and, in space, these velocity differences can be quite large. It always acts opposite to the direction of motion and, therefore, if the fluid is viscous enough, causes a measureable change to the object's velocity. In order to more effectively describe how objects move through a fluid, the concept "ballistic coefficient" was developed, which incorporates the object's mass and area as well as its coefficient of drag which depends on the geometry of the object.

The coefficient of drag as it applies to spacecraft was first developed as a mathematical construct when Cook [1965; 1966] made an estimate of 2.2 for spherical spacecraft in low-altitude orbits. As a first-order model, this estimate served its purpose quite well. It was validated with theoretical laboratory work in gas-surface interactions by Goodman and Wuchman [1976], Trilling [1967], Saltsburg et al. [1967], and Bird [1994]. The estimate for the coefficient of drag fits closest for spherical satellites, but as spacecraft began to grow in complexity and adopt various shapes and sizes, this model needed to be updated. Working with 35 years' worth of atmospheric data upon which to base the updated estimate, Moe and Moe [2005] present values for the coefficient of drag with respect to spacecraft geometry and altitude (see Figure 2.1). These new values were modeled and tested by Gaposchkin [1994], Pardini and Anselmo [2001], and Zuppardi [2004]; however, each acknowledges that there are uncertainties associated with each

model, and Vallado and Finkleman [2013] summarize several of the cumulative effects in their Table 2 (presented here as Table 2.1).

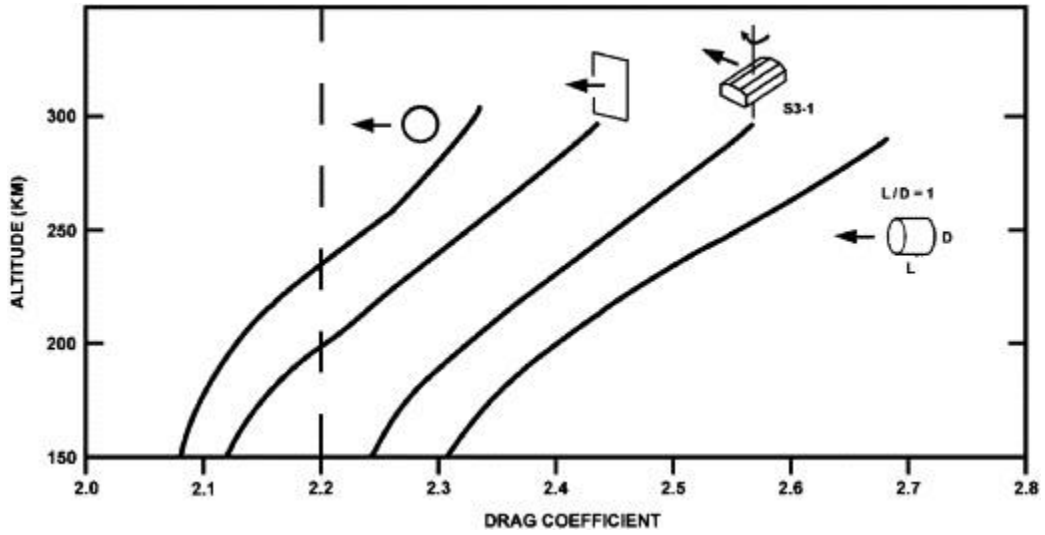

Figure 2.1. Drag Coefficients versus Altitude and Shape [from Moe and Moe, 2005]

Table 2.1. Cumulative Uncertainty Effects [from Vallado and Finkleman, 2013]

	Topic	Summary of Topic	Effect
Atmospheric Model Development			
	Indices	Which indices available when developed? How were they used? Span of time indices available	
	Data used in generation	Satellites were limited in atmospheric model development	
	Orbital Class	Atmospheric model is only good for certain orbital classes	
	Fidelity	Many studies, no conclusive "winner"	10-15% or more inaccuracy
Atmospheric Model Use			
	Which Model	Jacchia, MSIS, DTM, JB08, etc.	100 to 50,000 m in 4 days
	Implementation	Code implements technical approach exactly?	??
	Accuracy	Inherent inaccuracy of the model	10-15%
	Data Indices Availability	Publically available? Time span available	??
	Data Correction	Observed vs adjusted	6,000 m in 4 days
	Daily vs Hourly values	Frequency of updates to indices	3,000 m in 4 days
	Interpolation	Interpolate or not Which parameters to interpolate, or all? Method of interpolation	10-5,000 m in 4 days 3,000 in 4 days 10-20 m
	Which Index to use	Use a_p or K_p preferentially?	??
	Time lags	6.7 hours, other	??
	Time of observation	1700 vs 2000 UTC for $F_{10.7}$	1,000 m in 4 days
	Averages	Centered or trailing?	10,000 m in 4
	Prediction	Source, Schatten, ESA, Oltrogge, Other? Variability over time Short term accuracy	120 – 150 SFU (long) Varies 1-5 SFU (short)
	Winds		??
	All previous categories		
Satellite Parameters			
	Mass	Accuracy	5 – 10%?
	Area	Time varying?	??
	c_D	Aerodynamics, gas dynamics, continuum flow	??
	Model detail	Sphere, plate models, detailed CAD	??
	Attitude known	Consider a 10 m long 3 m diameter cylinder end vs side	424% difference
	Materials	Interaction to atmosphere – DSMC method?	??
	Maneuvers	Known or unknown Magnitude, direction	Can be very large 100's of km
Orbit Propagation			
	Input state accuracy	Example 1m initial error in the position	5,000 – 10,000 m in 7 days (extrapolated)
	Integrator type		Small
	Force model fidelity	Drag force is 10 – 100 km or more effect in 4 days	Varies
	All previous categories		
Orbit Determination			
	Obs Quality	Not tested	
	Obs Quantity	Phillips Lab (1995) report	400 m at epoch
	Solution method BLS	Not tested	??
	Solution EKF		
	Force Models	Using a different atmospheric model	500-10000+ m in 7 days
	All previous categories		

The errors presented in Table 2.1 can stack and lead to a model with significant error. Fortunately, some of the largest sources of error can be mitigated by simply knowing accurate attitude and mass data for the spacecraft in question. But, as Moe and Moe [2005] point out, the data from the past 35 years have only helped to define the first 300 km of atmosphere. Beyond that altitude, atmospheric models such as Jacchia 71 and MSIS 90 greatly overestimate the ambient density [Chao et al., 1997]. There is a great need to understand the higher altitudes to properly model the decay of other LEO spacecraft.

The widely accepted equation for the acceleration of spacecraft due to drag is

$$\vec{a}_{\text{drag}} = -\frac{1}{2}\frac{c_D A}{m}\rho v_{\text{rel}}^2 \frac{\vec{v}_{\text{rel}}}{\|\vec{v}_{\text{rel}}\|}, \tag{2.1}$$

which can be rearranged to form an approximate equation for the coefficient of drag,

$$c_D = \frac{-2m}{A\rho}\frac{\|\vec{v}_{\text{rel}}\|}{v_{\text{rel}}^2}\frac{\vec{a}_{\text{drag}}}{\vec{v}_{\text{rel}}}. \tag{2.2}$$

Determining the values that make up the first term in Equation 2.2 is extremely difficult in practice, but they are of vital importance in determining the coefficient of drag. The mass term is discussed in Chapter 1.1, and the density and area terms are discussed in Chapter 3.2 and Chapter 3.1, respectively.

The second term in Equation 2.2 is the relative velocity vector. In order to study the effects of drag on a spacecraft, a relevant form of velocity must first be derived. The spacecraft velocity is often measured in the Earth Centered Inertial (ECI) coordinate frame. ECI, shown in Figure 2.2, is defined by an orthogonal pair of vectors on the axis of Earth's rotation and its equator and a third orthogonal vector fixed on the vernal equinox. For this analysis, the vernal equinox is based on the J2000 epoch.

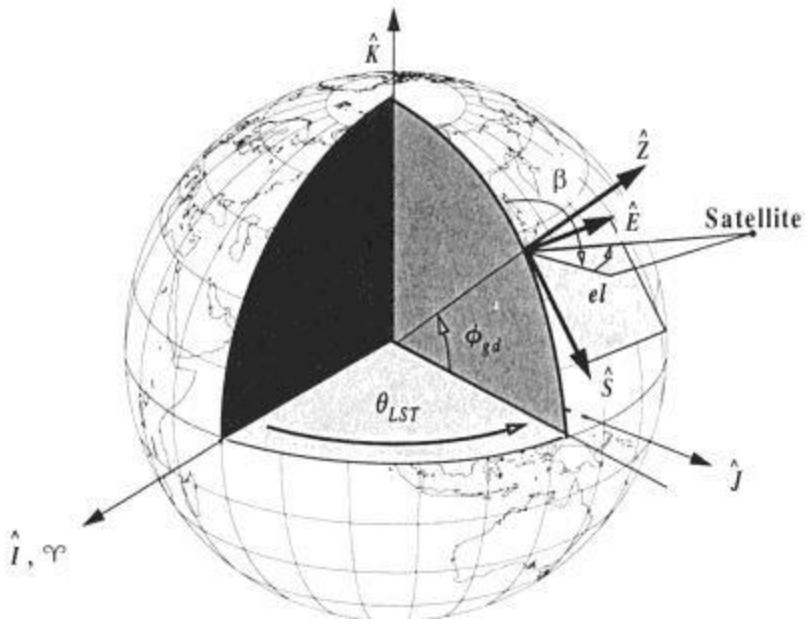

Figure 2.2. ECI Coordinate Frame [from Vallado, 2007]

The ECI coordinate frame does not provide any insight as to how the spacecraft is moving relative to its orbit, so the velocity vector must undergo a coordinate transformation via a direction cosine matrix. The new coordinate frame is called the perifocal coordinate frame, or PQW, and is expressed as

$$\vec{v}_{\mathrm{PQW}} = \begin{bmatrix} \cos\omega & \sin\omega & 0 \\ -\sin\omega & \cos\omega & 0 \\ 0 & 0 & 1 \end{bmatrix} \begin{bmatrix} 1 & 0 & 0 \\ 0 & \cos i & \sin i \\ 0 & -\sin i & \cos i \end{bmatrix} \begin{bmatrix} \cos\Omega & \sin\Omega & 0 \\ -\sin\Omega & \cos\Omega & 0 \\ 0 & 0 & 1 \end{bmatrix} \vec{v}_{\mathrm{ECI}}. \qquad (2.3)$$

The PQW coordinate frame, shown in Figure 2.3, is a 3–1–3 rotation around ω, the argument of perigee, i, the inclination, and Ω, the right ascension of the ascending node. This coordinate frame has its origin still at the center of Earth, but takes the spacecraft's orbit as its fundamental plane. The principal axis is directed towards perigee, the narrowest point in the spacecraft's orbit; the other axes are in the general direction of motion and normal to the plane formed by the two former axes.

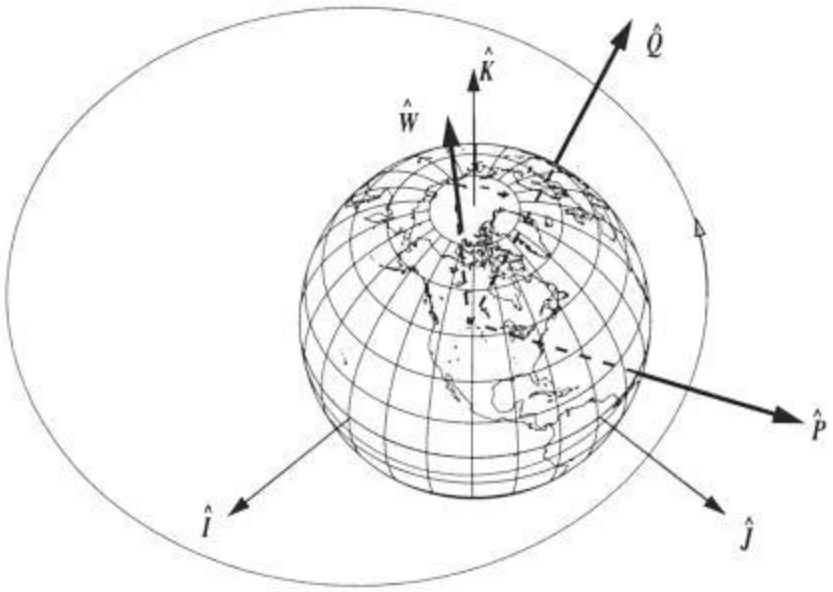

Figure 2.3. PQW Coordinate Frame [from Vallado, 2007]

The PQW coordinate frame provides a closer to a useful form of a velocity vector, but it is still a measurement based on Earth, not on the spacecraft's actual motion. This drives the use of yet another coordinate frame that is now centered on the spacecraft. This coordinate frame, RSW, is one such satellite coordinate systems. This frame is also referenced when speaking about along-track or cross-track displacements or positions, and is defined by

$$\vec{v}_{\mathrm{RSW}} = \begin{bmatrix} \cos\upsilon & \sin\upsilon & 0 \\ -\sin\upsilon & \cos\upsilon & 0 \\ 0 & 0 & 1 \end{bmatrix} \vec{v}_{\mathrm{PQW}}. \tag{2.4}$$

The RSW coordinate frame, shown in Figure 2.4, is a rotation around υ, the true anomaly. This coordinate frame is defined with its principal axis along the radius vector pointing from the center of the Earth to the spacecraft. Its second axis is in the direction

of the velocity vector but is only parallel to it at perigee, apogee, or in a circular orbit. Its third axis is normal to the orbital plane.

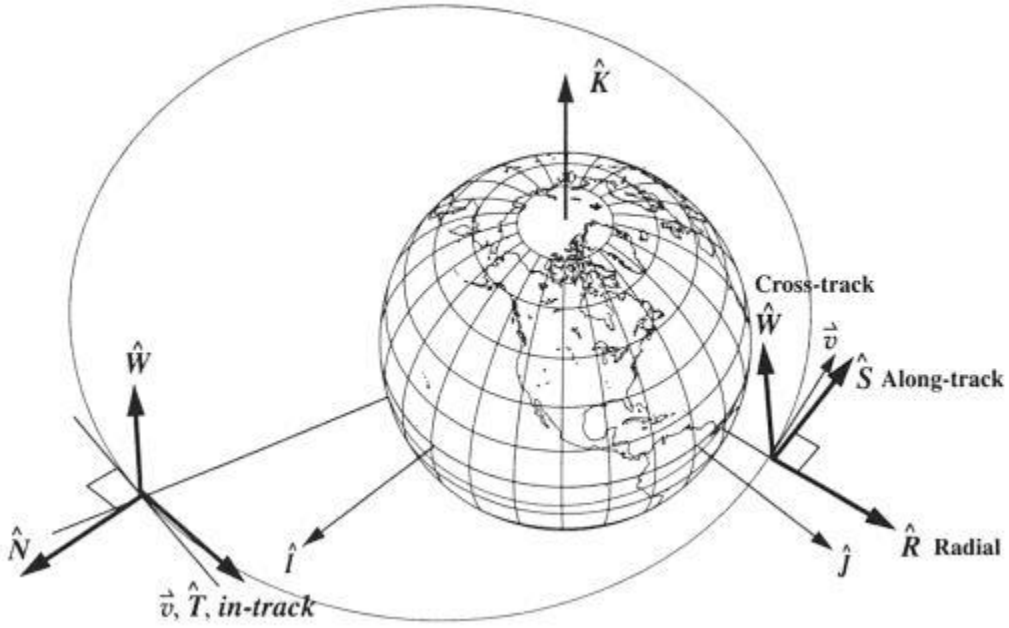

Figure 2.4. RSW and NTW Coordinate Frames [from Vallado, 2007]

The issue with the RSW coordinate frame is that the velocity vector still is not along one axis, which makes it difficult to directly generate a relative velocity vector. Thus, the final coordinate frame, NTW, a second form of the satellite coordinate systems, is introduced.

$$\vec{v}_{\text{NTW}} = \begin{bmatrix} \cos\phi_{\text{fpa}} & \sin\phi_{\text{fpa}} & 0 \\ -\sin\phi_{\text{fpa}} & \cos\phi_{\text{fpa}} & 0 \\ 0 & 0 & 1 \end{bmatrix} \vec{v}_{\text{RSW}}. \tag{2.5}$$

The NTW coordinate frame, shown in Figure 2.4, is a rotation about ϕ_{fpa}, the flight path angle. This coordinate frame is defined with its principal axis normal to the velocity vector. Its second axis is tangential to the orbit and in line with the velocity vector. The

third axis is normal to the orbital plane. This coordinate frame is useful in determining the in-track displacements. However, because the time between data points is very small, the flight path angle between the two points is also very small, approximately 1×10^{-14} radians. Therefore, by the theorem of small angles, these two can be estimated as the same, i.e.,

$$\vec{v}_{\mathrm{NTW}} = \begin{bmatrix} 1 & 0 & 0 \\ 0 & 1 & 0 \\ 0 & 0 & 1 \end{bmatrix} \vec{v}_{\mathrm{RSW}}. \tag{2.5}$$

Now that the velocity vector is in a useful form, it can be compared to the incoming velocity of the atmosphere, which must be subtracted to determine the relative velocity, i.e.,

$$\vec{v}_{\mathrm{rel}} = \vec{v}_{\mathrm{spacecraft}} - \vec{v}_{\mathrm{ambient}}. \tag{2.6}$$

The ambient velocity is derived from the motion of a location on a vector from the center of Earth, making it entirely based on the rotation of Earth. It acts directly opposite the direction of motion. This form of velocity is now ready for calculations of the coefficient of drag.

There is one more step that can be taken to help facilitate the area analysis: convert the velocity into a roll, pitch, yaw coordinate frame, RPY as

$$\vec{v}_{\mathrm{RPY}} = \begin{bmatrix} -1 & 0 & 0 \\ 0 & 1 & 0 \\ 0 & 0 & -1 \end{bmatrix} \vec{v}_{\mathrm{RSW}}. \tag{2.7}$$

The RPY coordinate frame is a rotation about –180°. This coordinate frame is also centered on the spacecraft but its axes follow the more commonly used roll, pitch, and yaw attitude definition angles.

The third term in Equation 2.2 is difficult to deal with as there is no direct way to divide vectors. Therefore, the square root of the magnitude of the vectors is taken, i.e.,

$$\frac{\vec{a}_{\text{drag}}}{\vec{v}_{\text{rel}}} = \sqrt{\frac{\vec{a}_{\text{drag}} \cdot \vec{a}_{\text{drag}}}{\vec{v}_{\text{rel}} \cdot \vec{v}_{\text{rel}}}}\,. \tag{2.8}$$

All terms in Equation 2.2 are now defined, and can now be written as

$$c_D = \frac{-2m}{A\rho} \frac{\|\vec{v}_{\text{rel}}\|}{v_{\text{rel}}^2} \sqrt{\frac{\vec{a}_{\text{drag}} \cdot \vec{a}_{\text{drag}}}{\vec{v}_{\text{rel}} \cdot \vec{v}_{\text{rel}}}}\,. \tag{2.9}$$

This now defines the equation for the coefficient of drag to be employed in this work.

2.2 Approach

This research sets out to accomplish several tasks: 1) generate a functional area determination algorithm that accurately predicts the cross sectional area of NASA's *Swift* spacecraft in any orientation; 2) develop a method to incorporate state-of-health data including attitude and altitude measurements into a drag analysis; 3) predict the orbital lifetime of *Swift*; and 4) discuss the validity of current assumptions regarding the coefficient of drag.

In order to accomplish each of these tasks, the following approach is taken. First, the following four groups of data were acquired: atmospheric density data from the US Naval Research Laboratory's Mass Spectrometer and Incoherent Scatter radar atmospheric model extending through the Exosphere, released in 2000 (NRLMSISE-00) in the region of the expected altitude of *Swift* with some buffer to both sides—it must include the total mass density the model predicts; position and velocity vectors in the Earth-Centered-Inertial coordinate frame from *Swift* gathered by the *Swift* FOT; quaternion data from *Swift* gathered by the *Swift* FOT; and altitude data from *Swift* also gathered by the *Swift* FOT.

The data analysis begins by analyzing the position and velocity vectors. The goal is to generate a relative velocity vector using the method described in Chapter 2.1. In order to eliminate some errors in the position and velocity data, averages over every minute of the *Swift* mission are taken.

Next, an analysis of the quaternions is done and they are converted into the Euler angles roll, pitch, and yaw, as described in Chapter 2.1. These angles are then used to

determine the cross sectional area, generally outlined in Chapter 3.1. Again to avoid some error in the analysis, this data was binned into averages over every minute of the mission duration.

The altitude data gathered from *Swift* and the atmospheric density data gathered from NRLMSISE-00, as described in Chapter 3.2 are paired. The hour-based average of the altitude from the *Swift* data is used as the altitude level that feeds into the atmospheric model, allowing for selection of the appropriate density value. This can only be averaged over every hour of the mission duration as that is the limit to the scale of the atmospheric model.

Finally, the coefficient of drag is calculated in parallel with the lifetime decay predictions. The prediction of the *Swift* orbital lifetime is described in Chapter 3.4. The calculations of the coefficient of drag follow the method discussed in Chapter 2.2. These results are presented in Chapter 3.5. The coefficient of drag information is also binned into hourly averages. In order to generate a control group to study the variability of the density throughout the analysis, a value for density is also directly calculated in parallel with the coefficient of drag. These results are discussed in Chapter 3.2.

All code generated for this analysis is written in m-code for MATLAB R2012a. All of the code and the analyzed data reside with the *Swift* FOT. Figure 2.5 is a visual representation of the process used in this analysis.

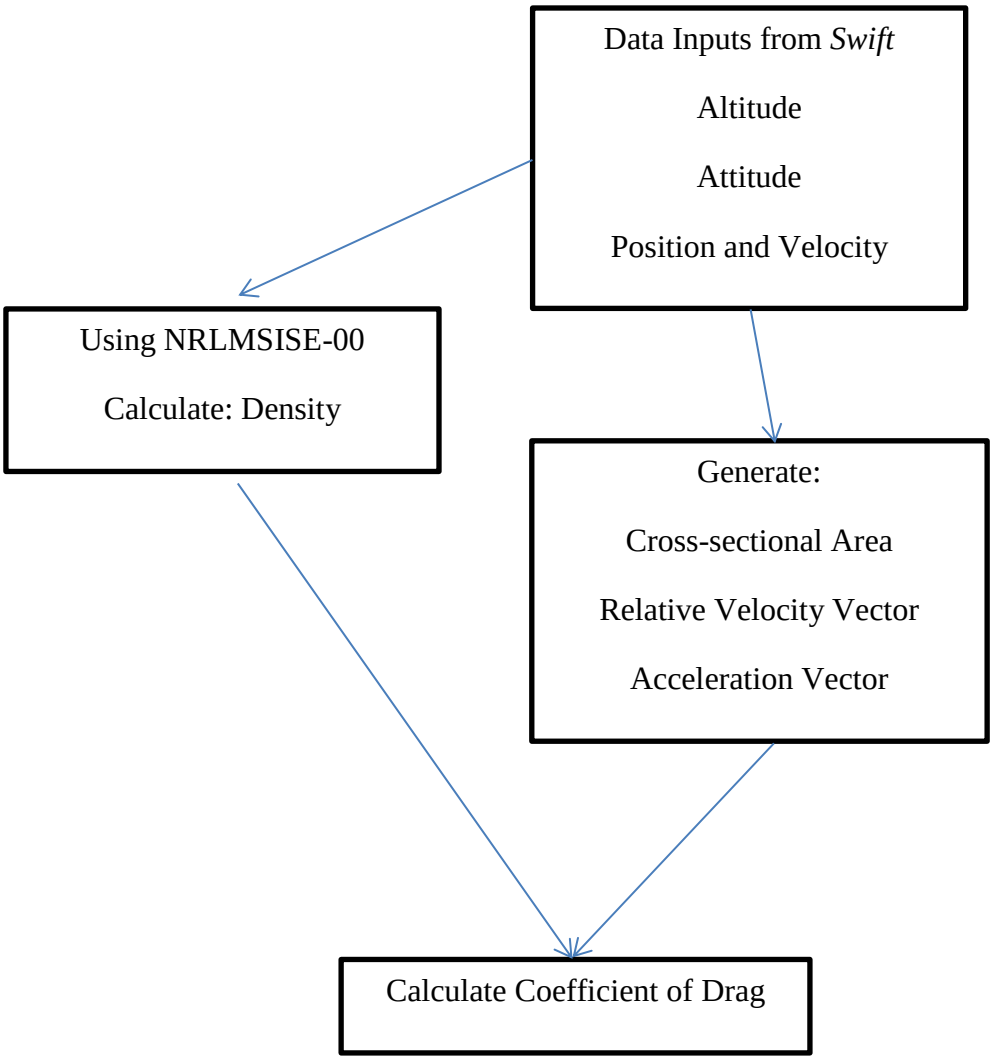

Figure 2.5. Visual Flow of Process

Chapter 3

3.1 Determining the Cross-sectional Area of *Swift*

One of the more complex tasks in determining the coefficient of drag is the development of an accurate model for the cross-sectional area of a spacecraft. When analyzing a spacecraft that has not yet launched, the best thing to do is take a maximum area and a minimum area and simply study these two boundary conditions. If the spacecraft has a simple shape, or has its cross-sectional area actively controlled, then determining the area is a simple task; however, when the spacecraft is much more complex, this task becomes more difficult.

For this analysis, a simplified, but dimensionally accurate, computer aided design (CAD) model of *Swift* was developed using SolidWorks, as shown in Figure 3.1. Accurate measurements of *Swift*'s cross-sectional area were generated and analyzed for patterns in order to facilitate an automated process to calculate the cross-sectional area. This led to the successful development of a cross-sectional area model for the spacecraft, which required the input of the roll, pitch, and yaw attitude definition angles.

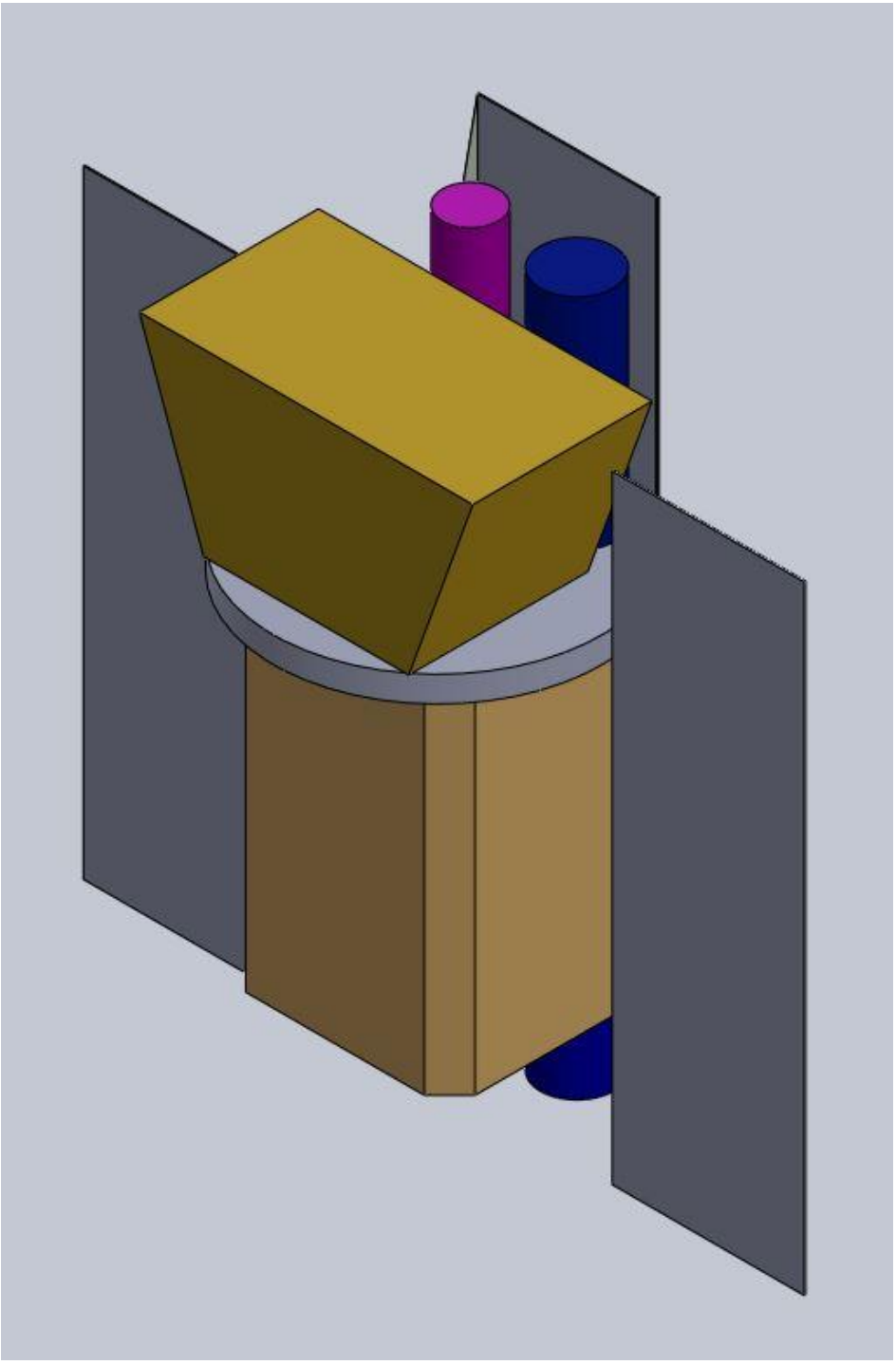

Figure 3.1. CAD Model of *Swift*

Roll, pitch, and yaw—also known as the Euler angles—are measured from the spacecraft-centered axes and are one form of attitude determination and slew calculation. However, roll, pitch, and yaw measurements are not readily available from *Swift* because *Swift* uses quaternions to perform its maneuvers. Fortunately, in orbital mechanics any Cartesian coordinate frame can be transformed into another with the same origin by rotating about a sequence of three angles about each of the coordinate axes. The most commonly used coordinate transformation uses the classical Euler angle sequence, also known as a 3–1–3, as it rotates around the third axis, then the first, then the third again. It can be proven that these three rotations can in fact be combined into a unique solution that makes a single rotation about one axis, the Euler axis, and one angle, the principal angle [Curtis, 2010]. The relation of a Cartesian coordinate frame to the Euler axis and principal angle, sometimes also called the Euler angle, is shown in relation to the Cartesian coordinate system $\vec{x}_A,\ \vec{y}_A,\ \vec{z}_A$ in Figure 3.2. A quaternion is defined by three components of a vector and a scalar part and kept as a single vector, i.e.,

$$\mathbf{Q} = \begin{bmatrix} q_1 \\ q_2 \\ q_3 \\ q_4 \end{bmatrix} \tag{3.1}$$

Here, q_1, q_2, q_3 make up the vector portion and q_4 is the scalar part. The scalar part can be found in the q_1 place instead, but not here.

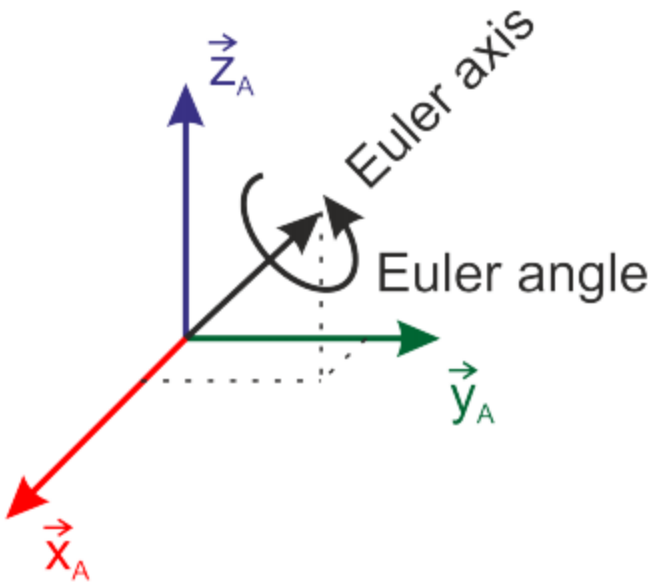

Figure 3.2. Euler Axis and Angle [from Groÿekatthöfer and Yoon, 2012]

With that knowledge in hand, the relationships for the angles of roll, pitch, and yaw are defined as

$$\text{Roll} = \tan^{-1}\left(-\frac{2(q_2q_4+q_3q_1)}{q_1^2-q_2^2-q_3^2+q_4^2}\right), \tag{3.2}$$

$$\text{Pitch} = \sin^{-1}\left(-2(q_3q_4 - q_2q_1)\right), \tag{3.3}$$

$$\text{Yaw} = \tan^{-1}\left(-\frac{2(q_2q_3+q_4q_1)}{q_1^2-q_2^2+q_3^2-q_4^2}\right). \tag{3.4}$$

With roll, pitch, and yaw now defined, the cross-sectional area can be easily calculated. Due to publication restrictions, the actual values of area are not presented, but rather a normalized form of cross-sectional area based on the standard operating area—that is, the area that incorporates the solar array approximation—is shown in Figures 3.3 through 3.12 on an hourly basis. Upon inspection, these figures indicate that the cross sectional area oscillates around 75–80% of the standard operating area of *Swift*. This will be an important result when the decay of *Swift* is discussed in Chapter 3.4.

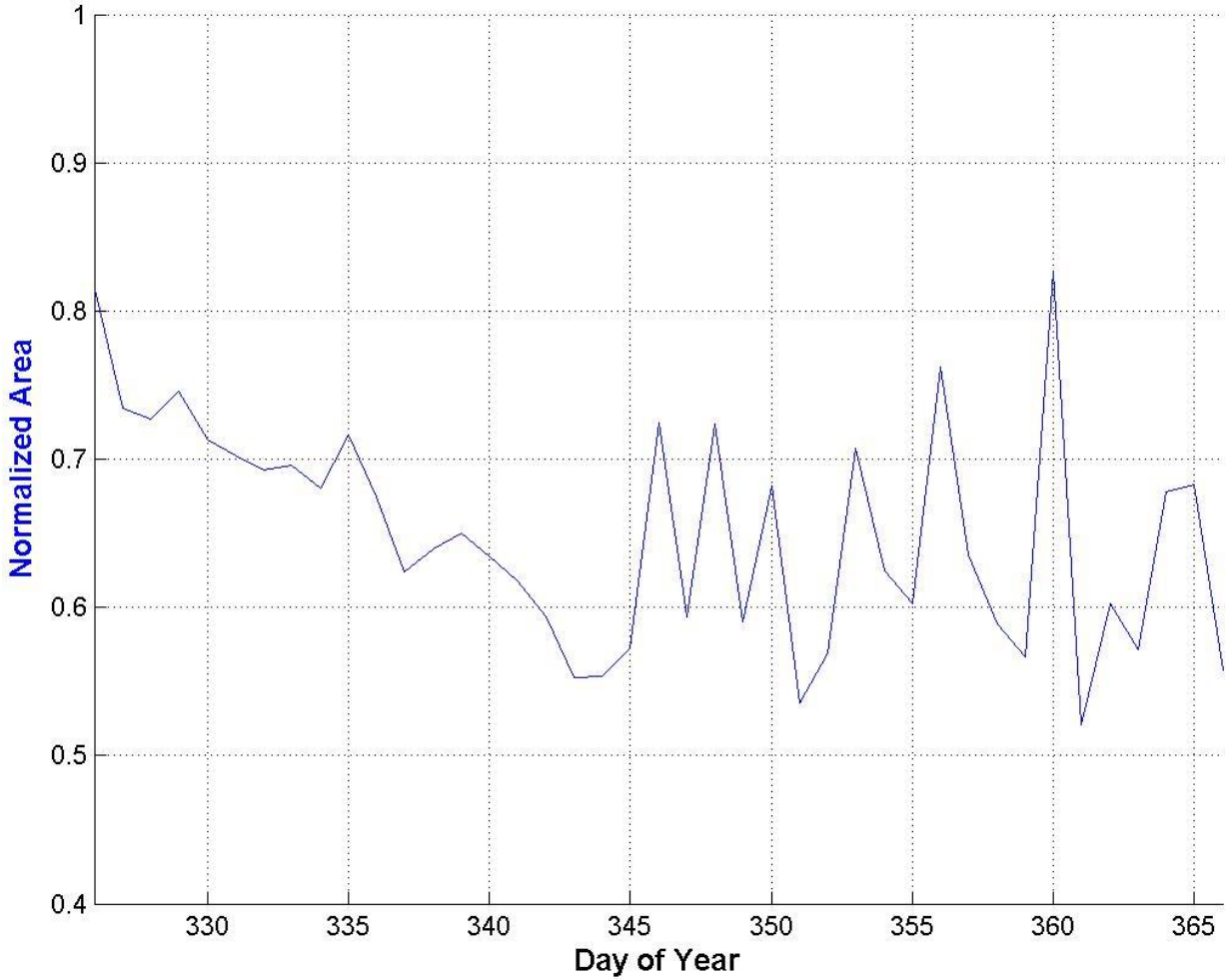

Figure 3.3. 2004 Normalized Area

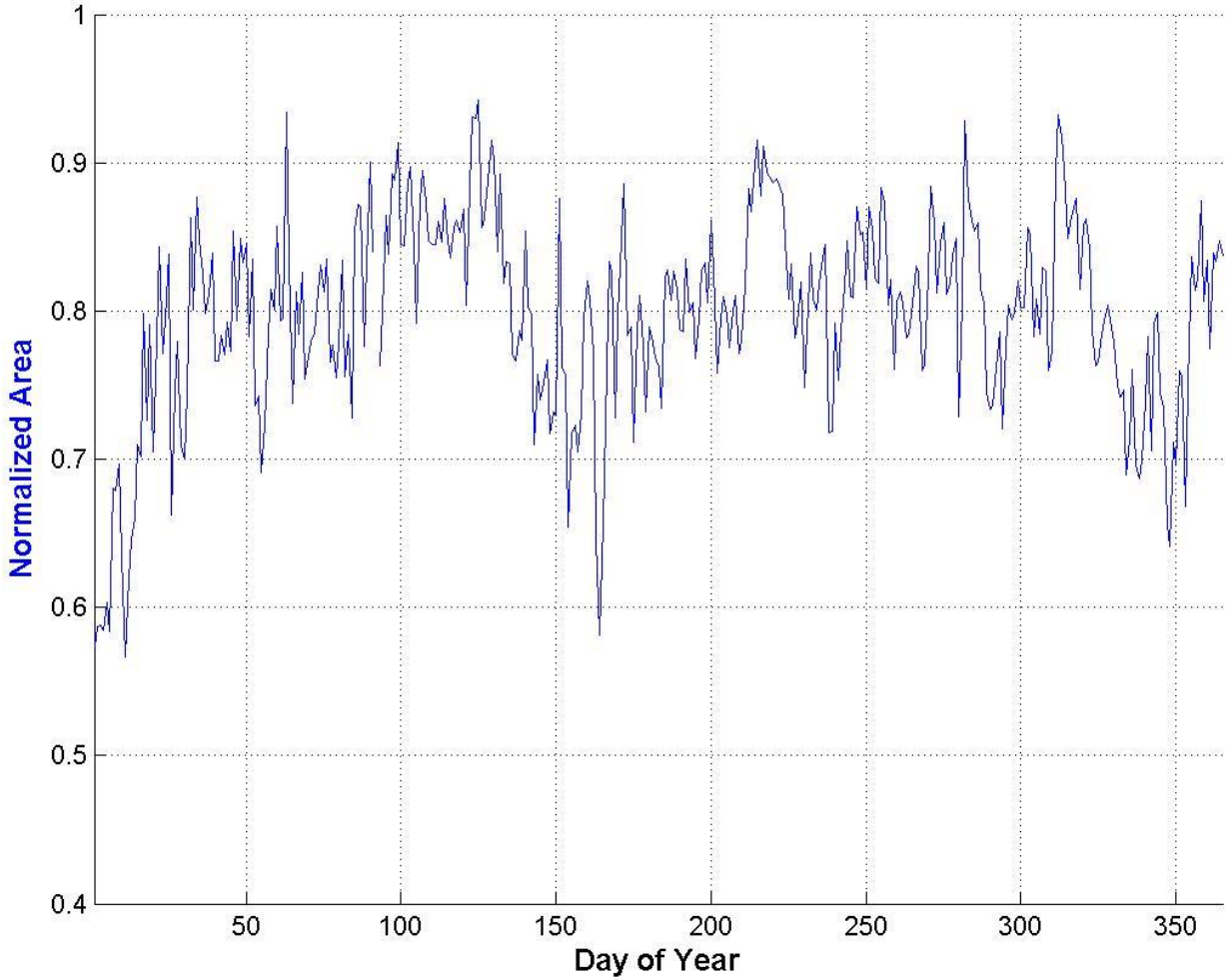

Figure 3.4. 2005 Normalized Area

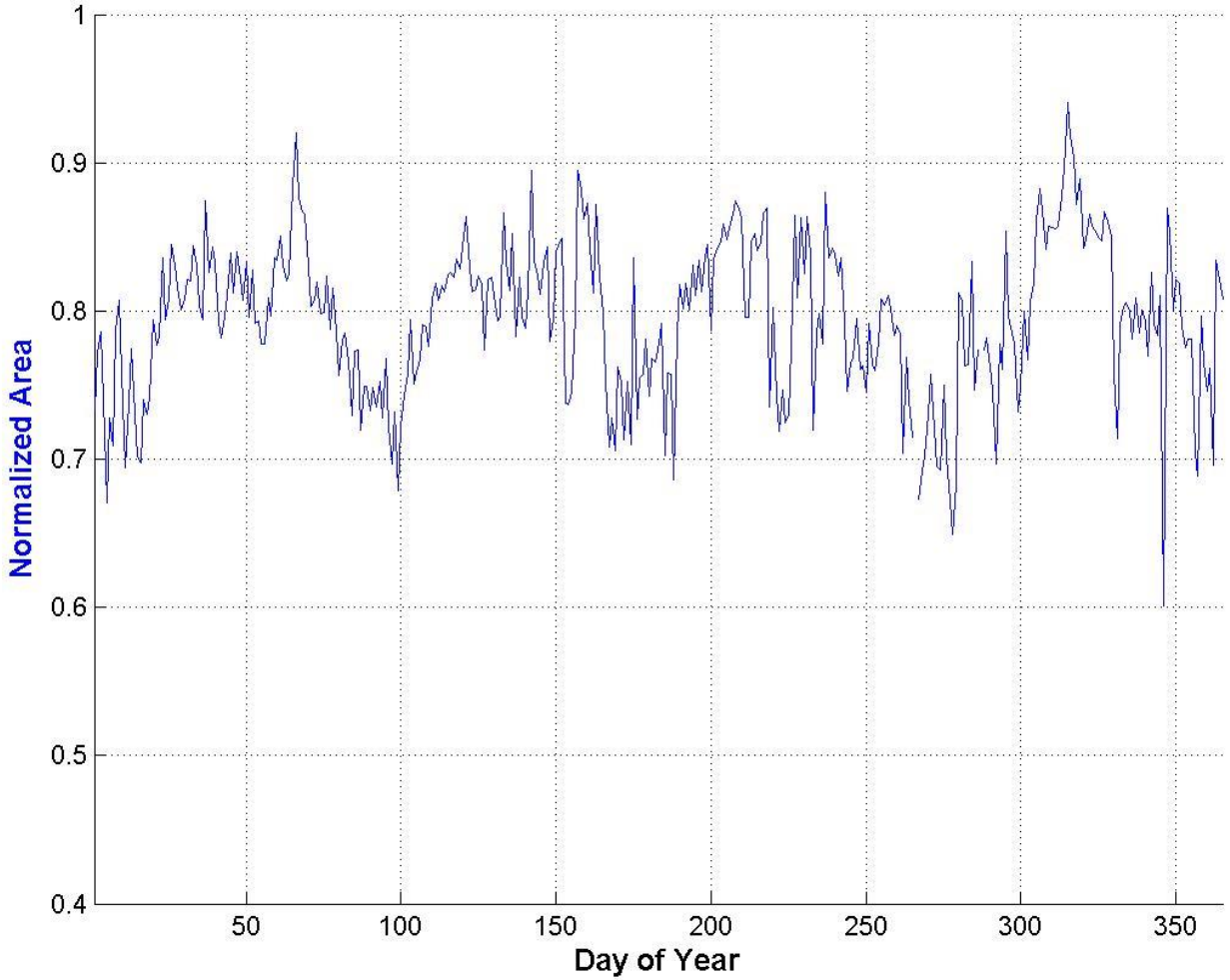

Figure 3.5. 2006 Normalized Area

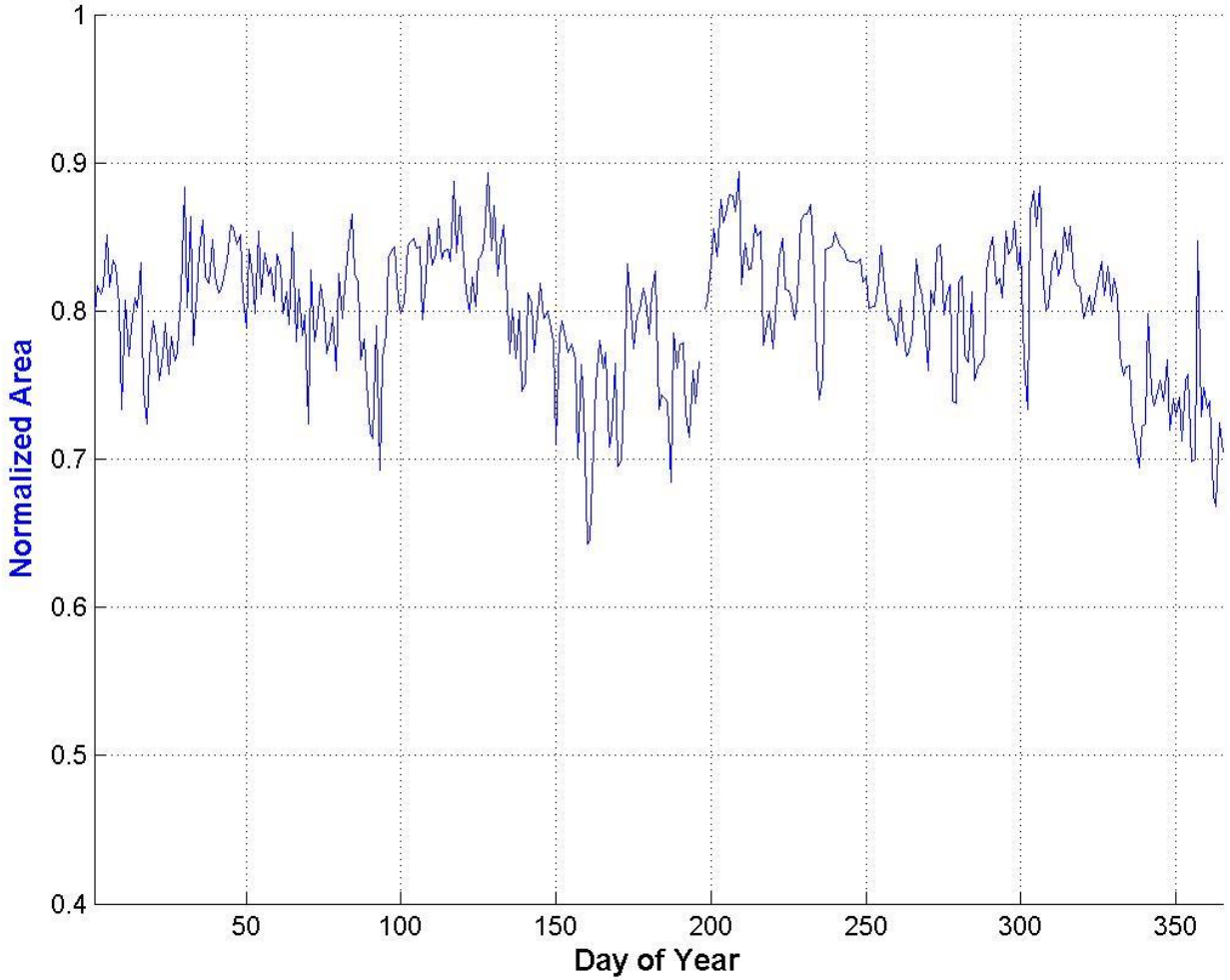

Figure 3.6. 2007 Normalized Area

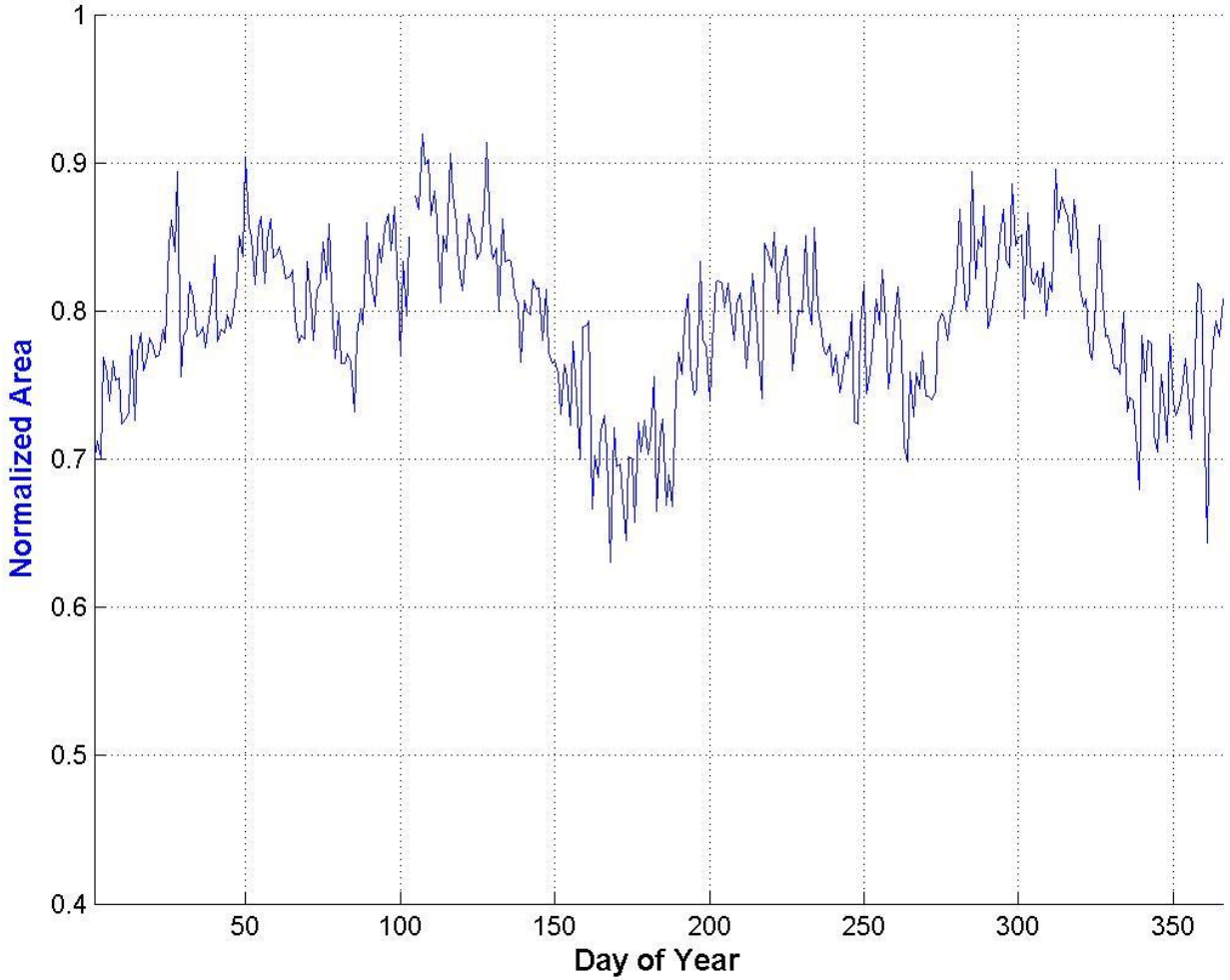

Figure 3.7. 2008 Normalized Area

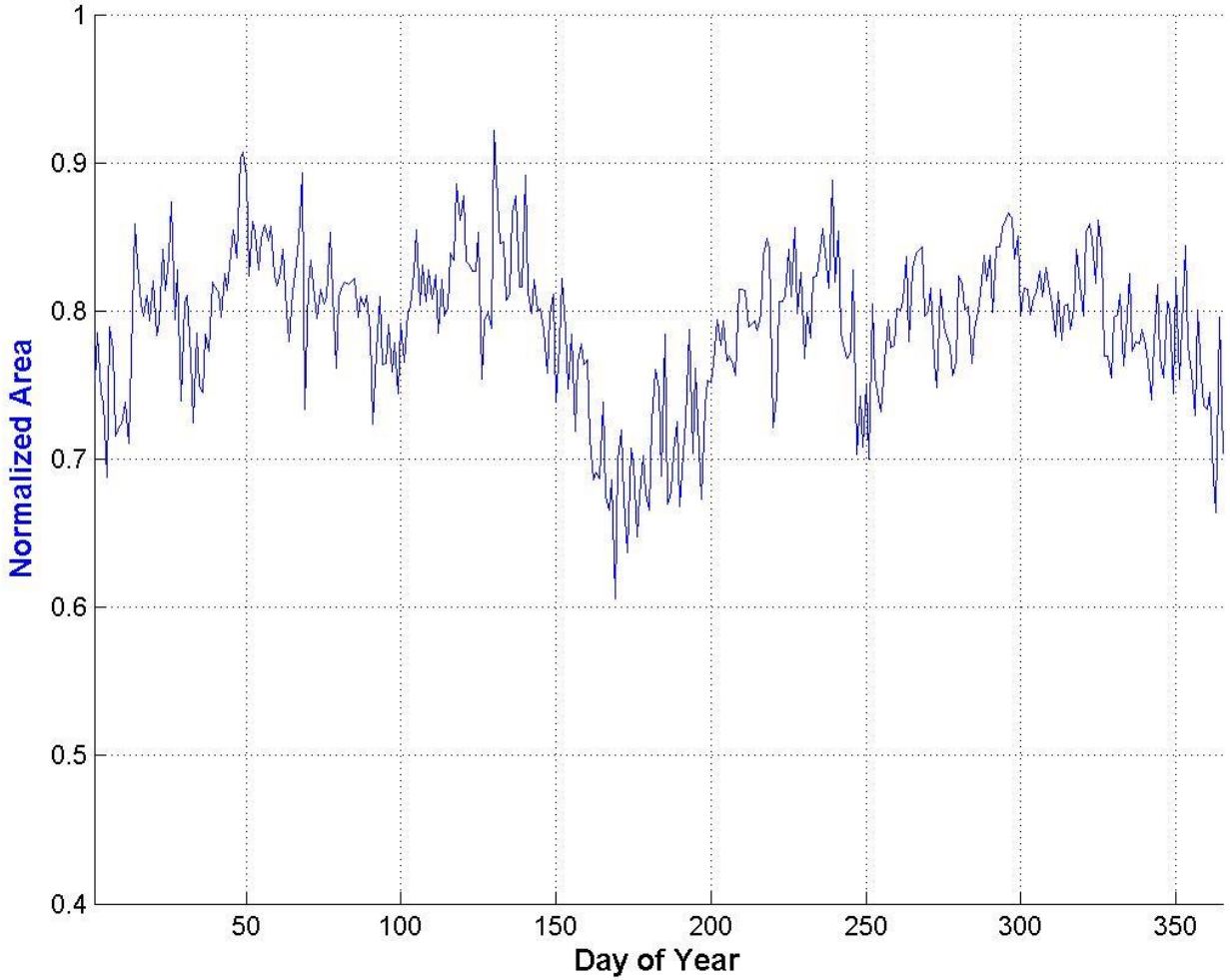

Figure 3.8. 2009 Normalized Area

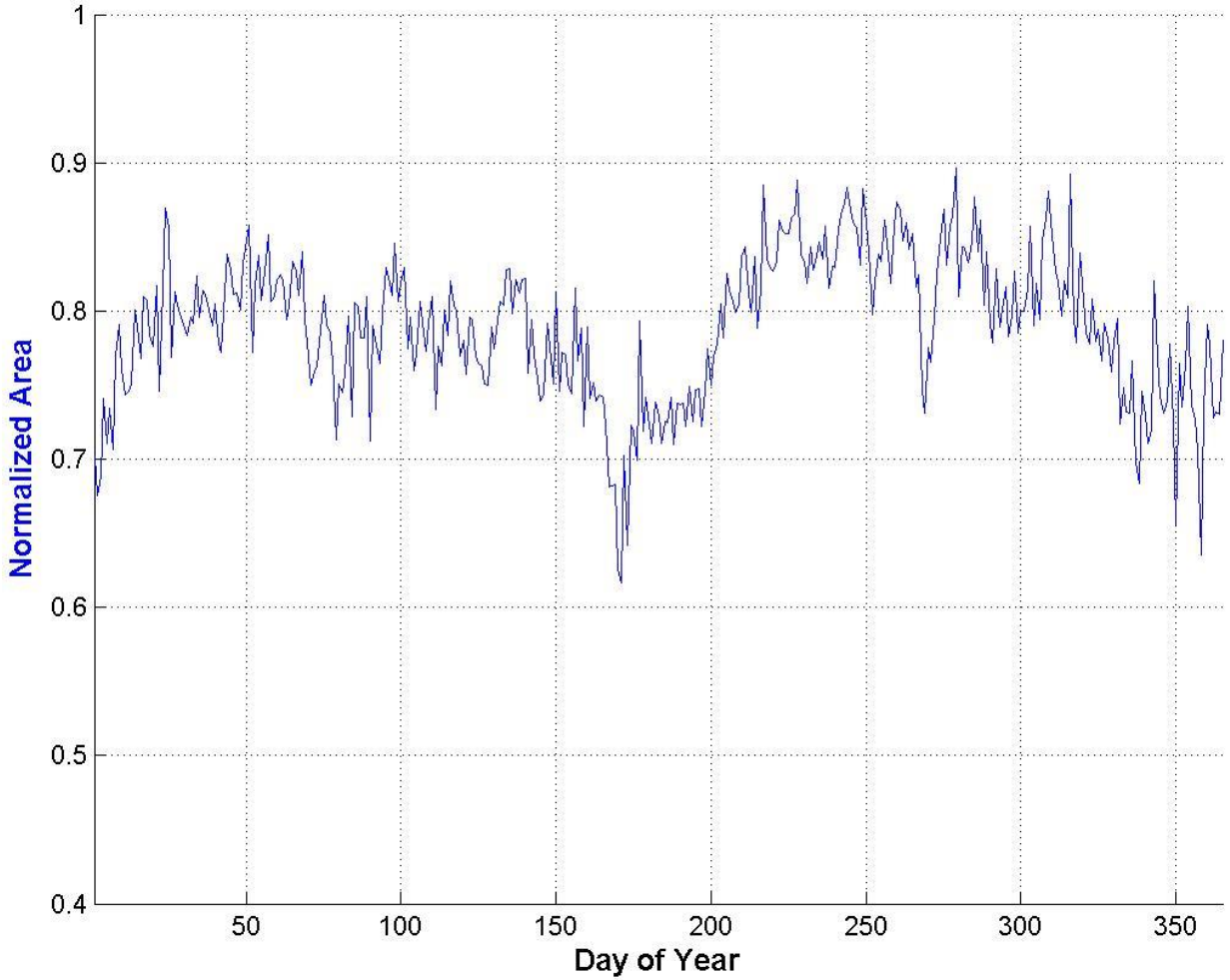

Figure 3.9. 2010 Normalized Area

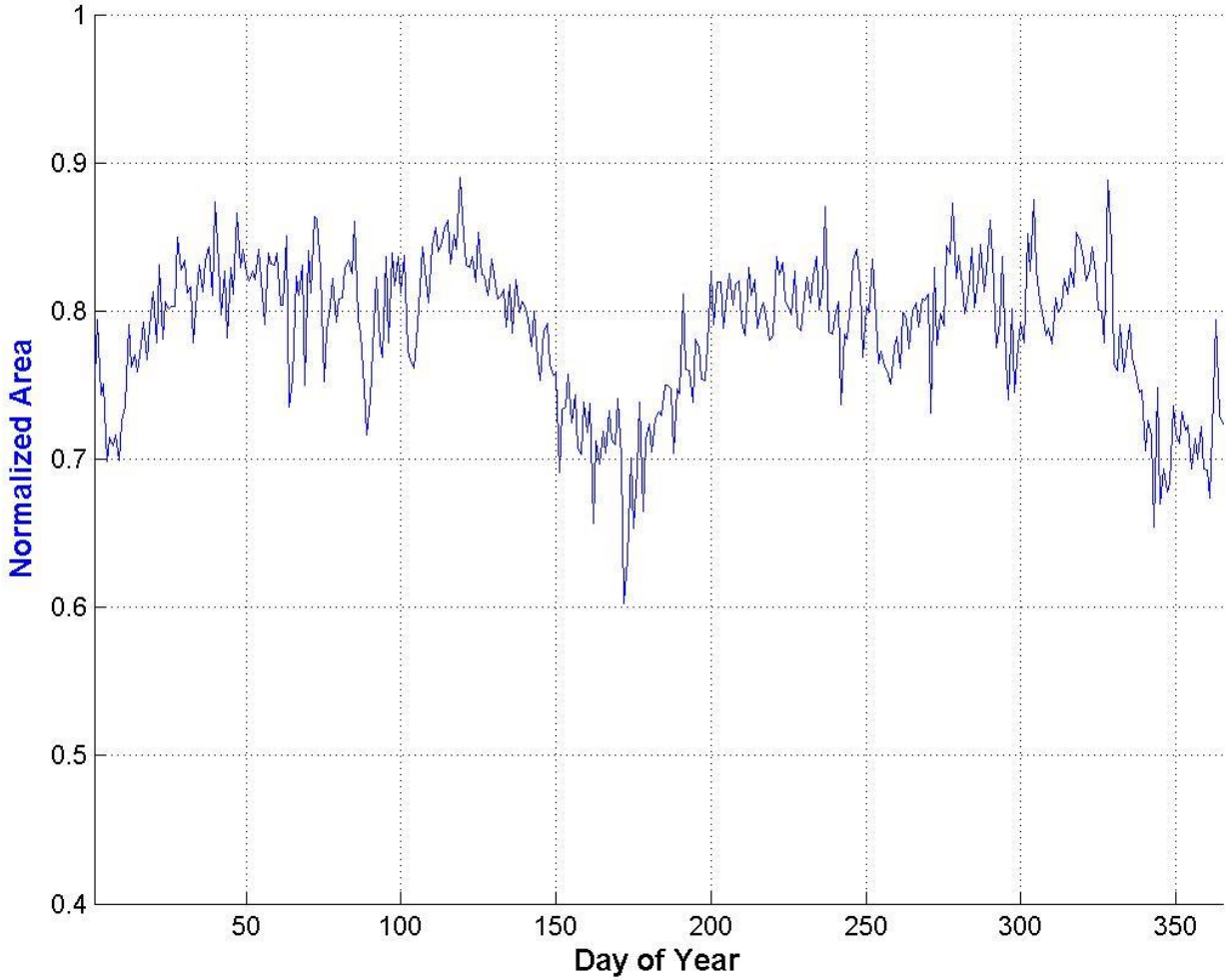

Figure 3.10. 2011 Normalized Area

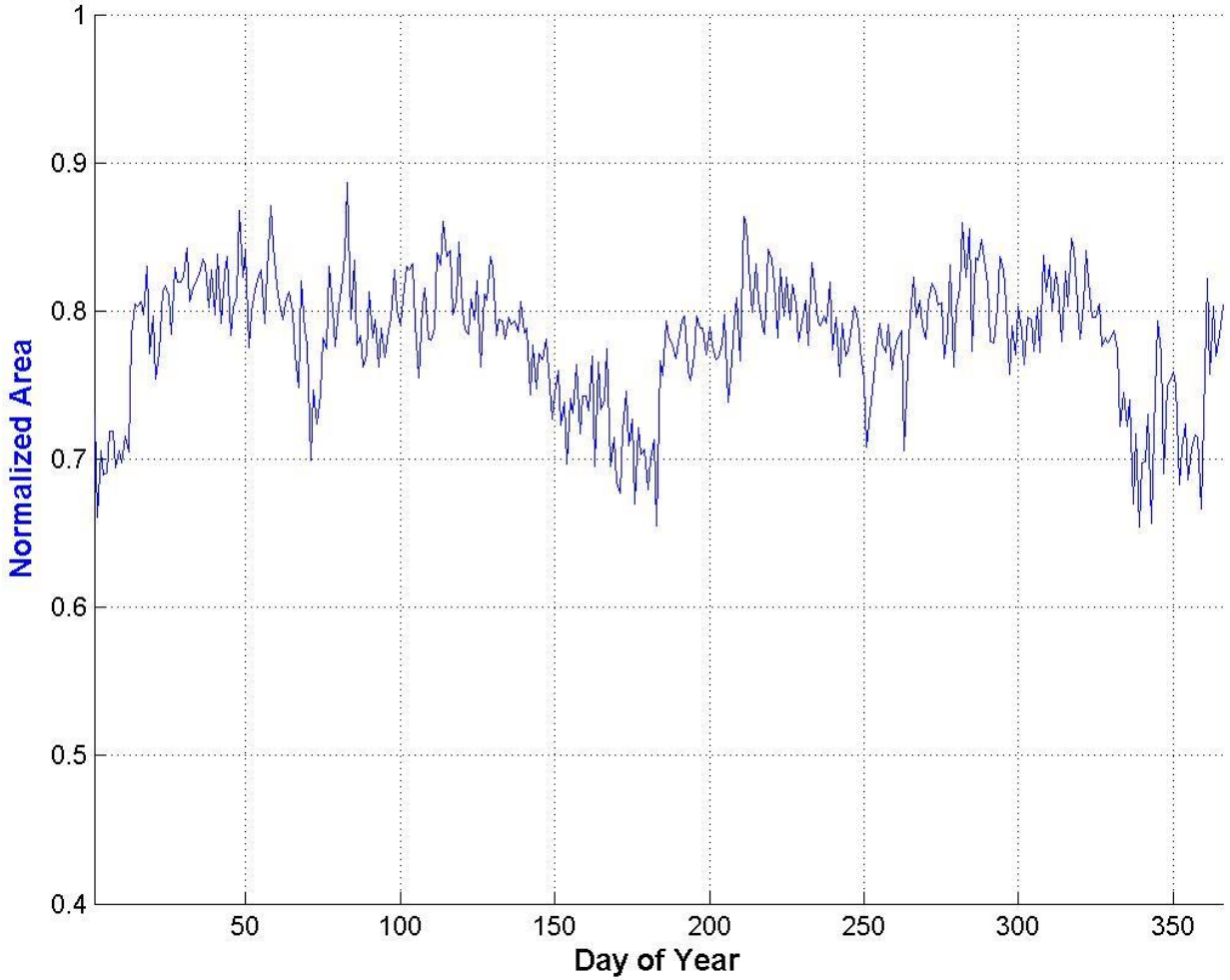

Figure 3.11. 2012 Normalized Area

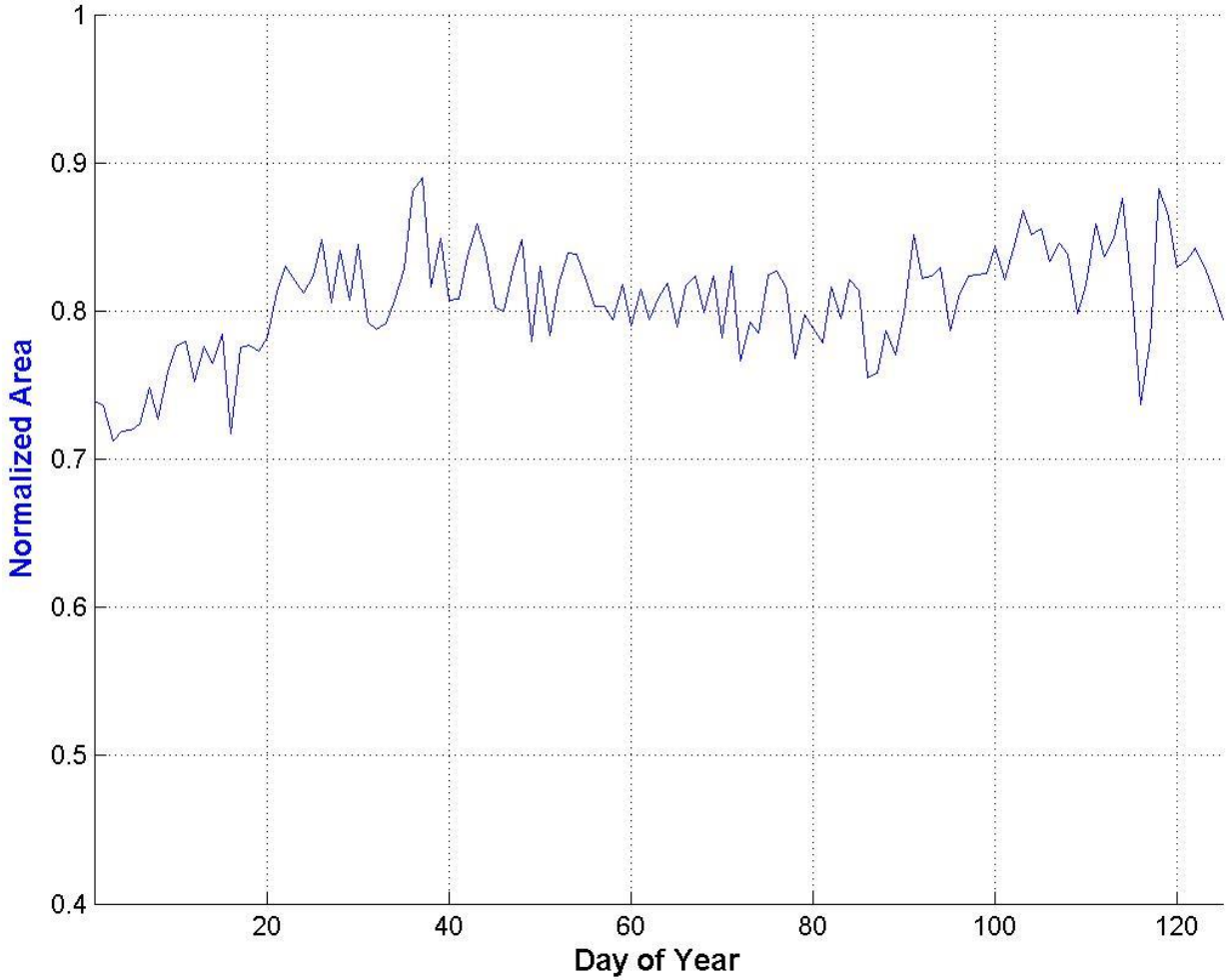

Figure 3.12. 2013 Normalized Area

3.2 Atmospheric Models

The main atmospheric model used for this analysis is the US Naval Research Laboratory's Mass Spectrometer and Incoherent Scatter Radar atmospheric model extending through the Exosphere, released in 2000 (NRLMSISE-00). The model is built upon data derived from incoherent scatter radar, mass spectrometers, solar ultraviolet occultation, pressure gauges, falling spheres, grenade detonations, drag measurements, and satellite-borne accelerometer measurements [Picone et al., 2002]. This particular model was chosen as it is the most current and widely accepted model available. The portion of the atmosphere being analyzed for *Swift* is based on a previous model, MSIS-86, which has been validated to be within an acceptable statistical deviation of the actual data gathered [Hedin, 1987].

Over the course of this analysis, some potential problems with the NRLMSISE-00 atmospheric model emerged. As a sanity check, an internally calculated density value was generated using a constant coefficient of drag value of 2.2. The density is then directly calculted and presented as a comparison to the values gathered from NRLMSISE-00. These two values are then divided to show the error between what the NRLMSISE-00 atmospheric model predicts and what values would have been generated if the coefficient of drag was a steady 2.2. Figures 3.13 through 3.32 show the yearly values used for the analysis.

Upon inspection, one notices that the two values are quite different, perhaps indicating that the assumption that the coefficient of drag is a steady value of 2.2 is not

valid, or that the density values at the altitude of *Swift* are not representative of reality. It is important to mention that these error plots incorporate all the error in the analysis, but even so, that does not account for such large differences.

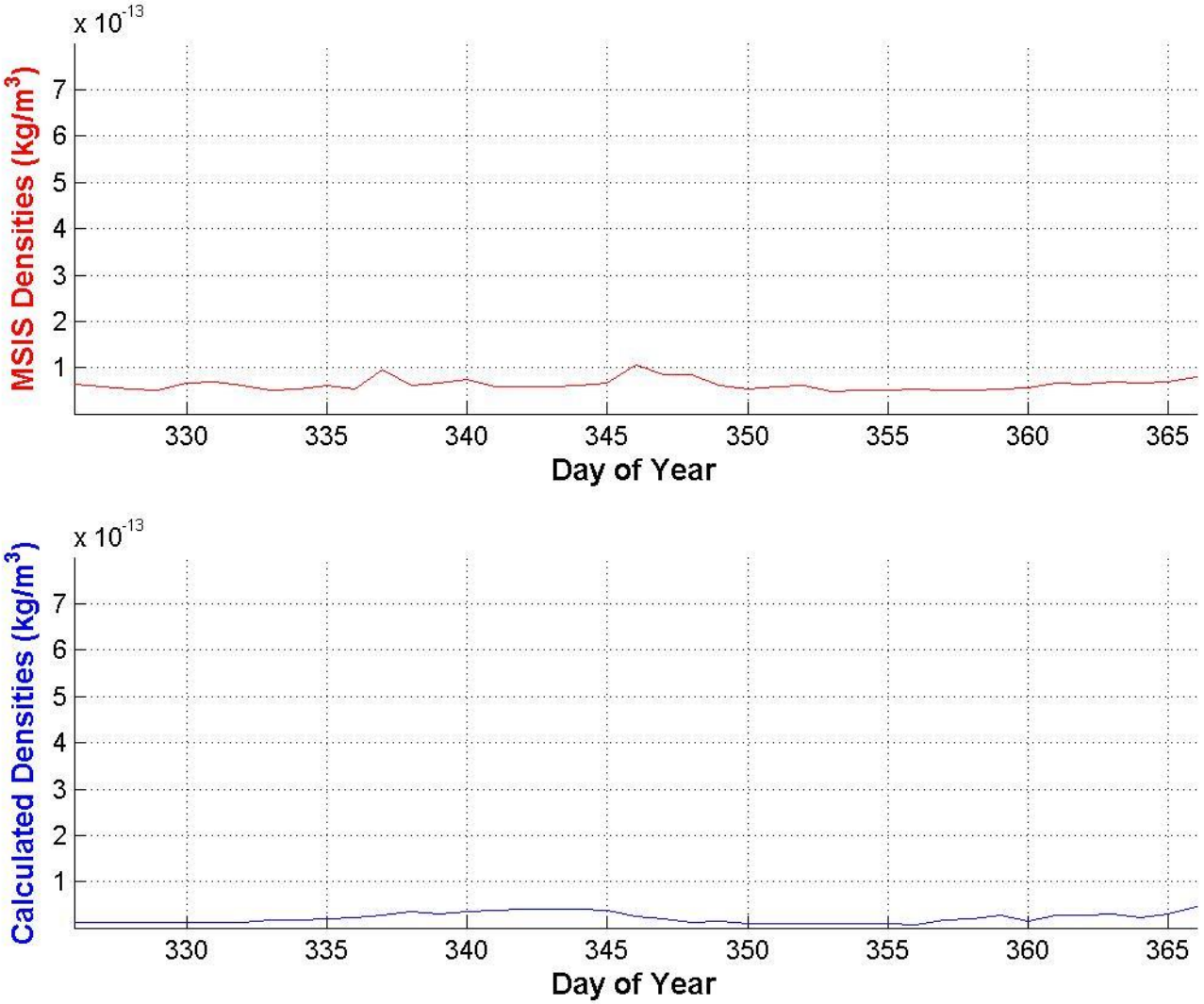

Figure 3.13. 2004 MSIS and Calculated Densities

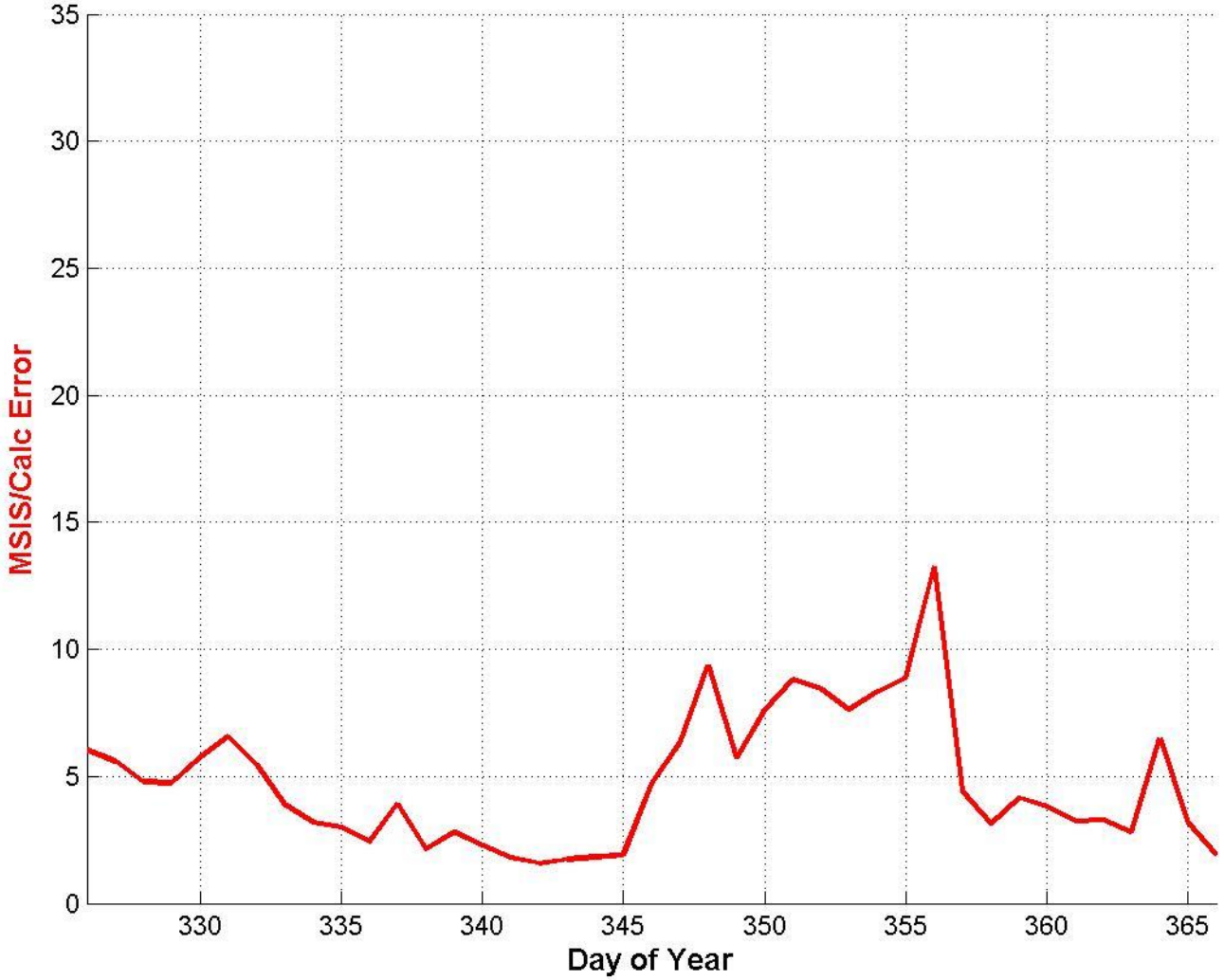

Figure 3.14. 2004 Density Error

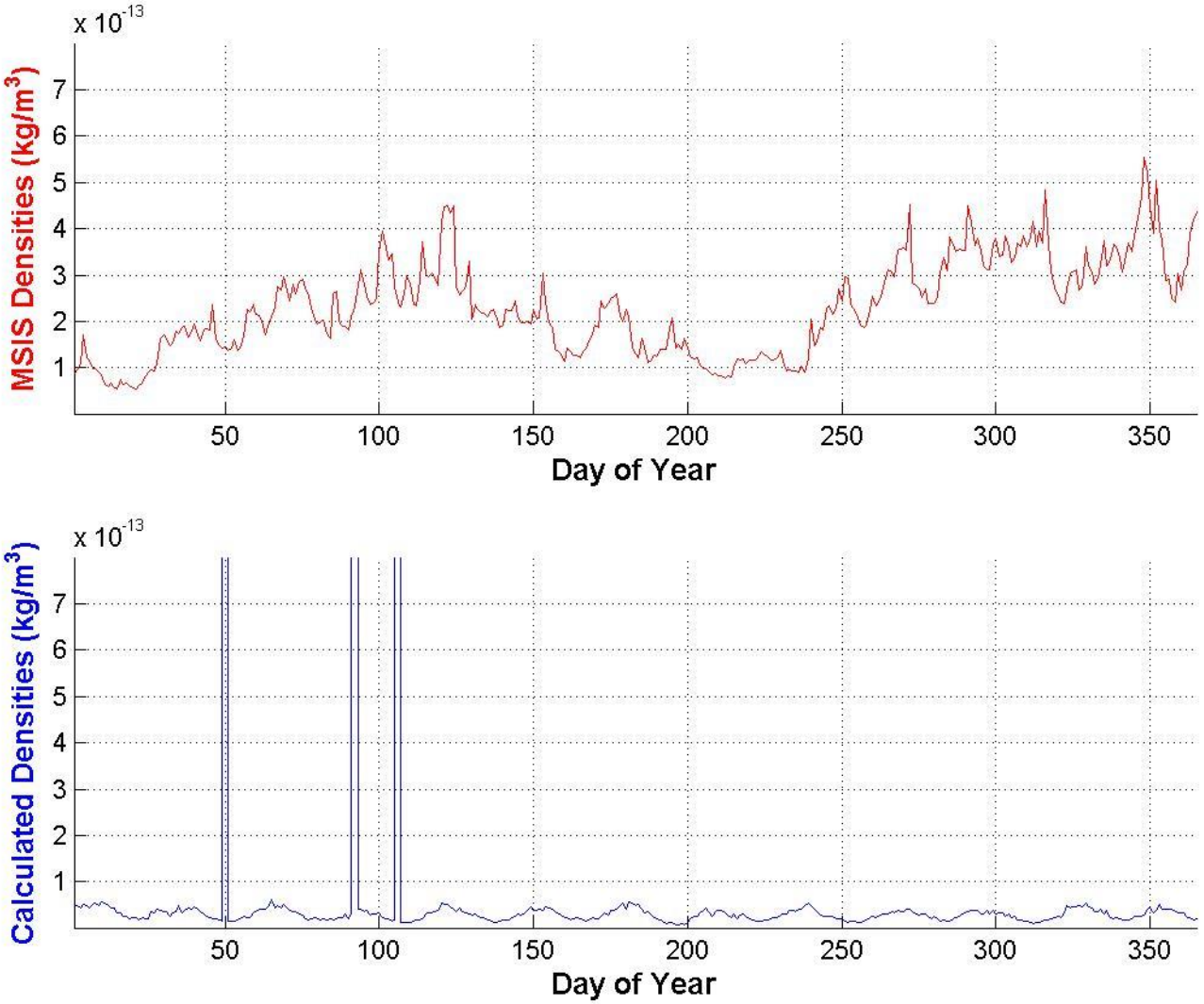

Figure 3.15. 2005 MSIS and Calculated Densities

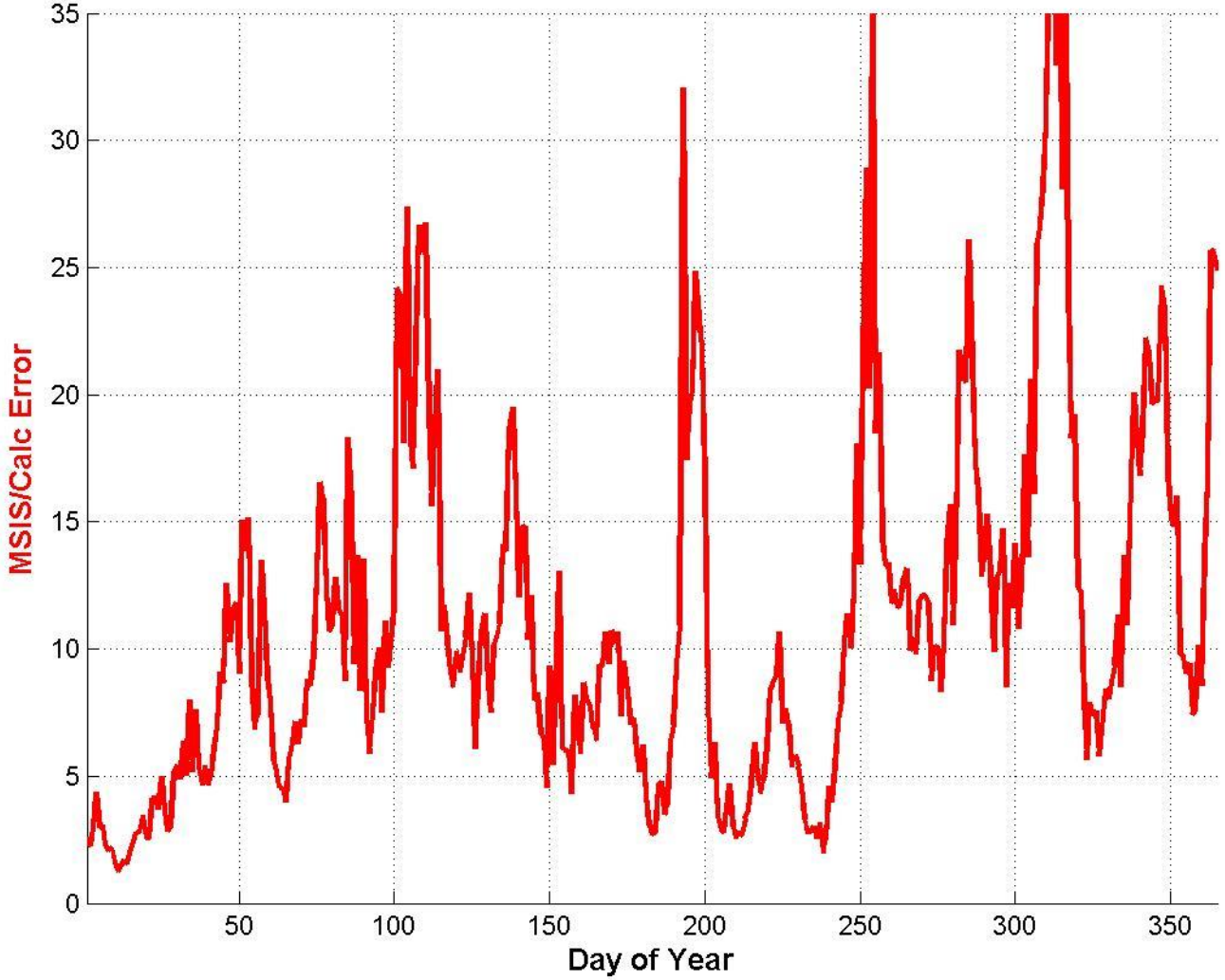

Figure 3.16. 2005 Density Error

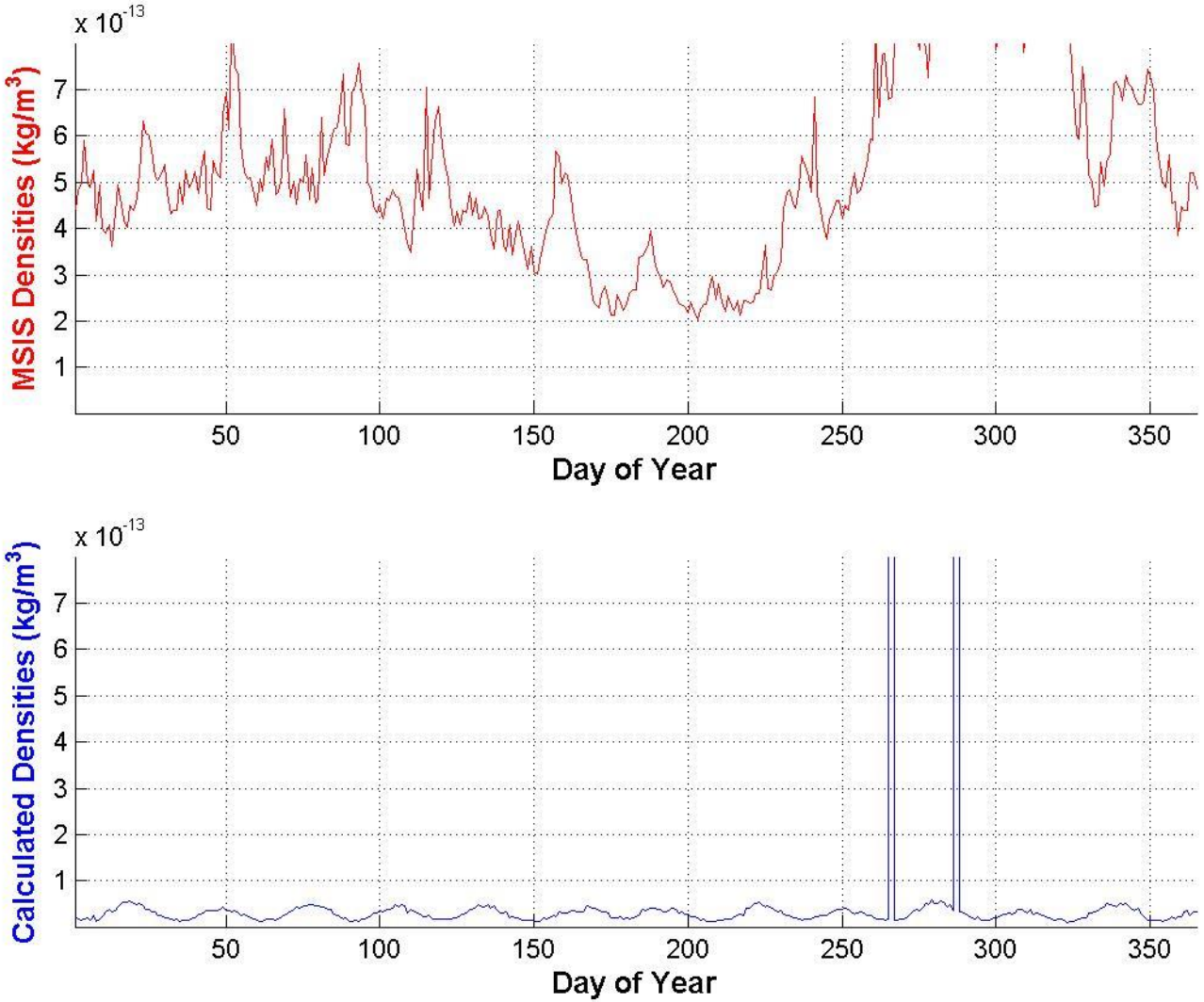

Figure 3.17. 2006 MSIS and Calculated Densities

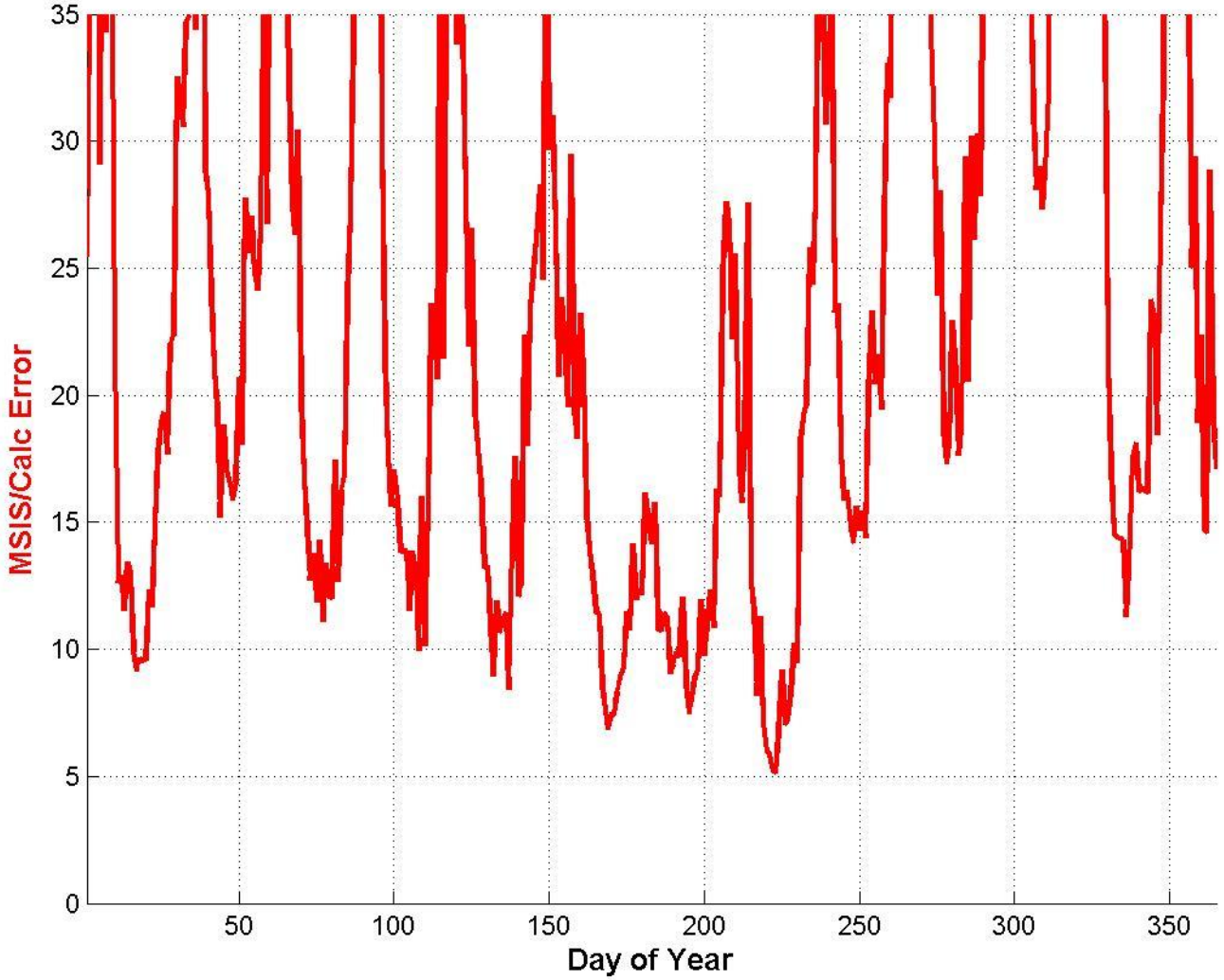

Figure 3.18. 2006 Density Error

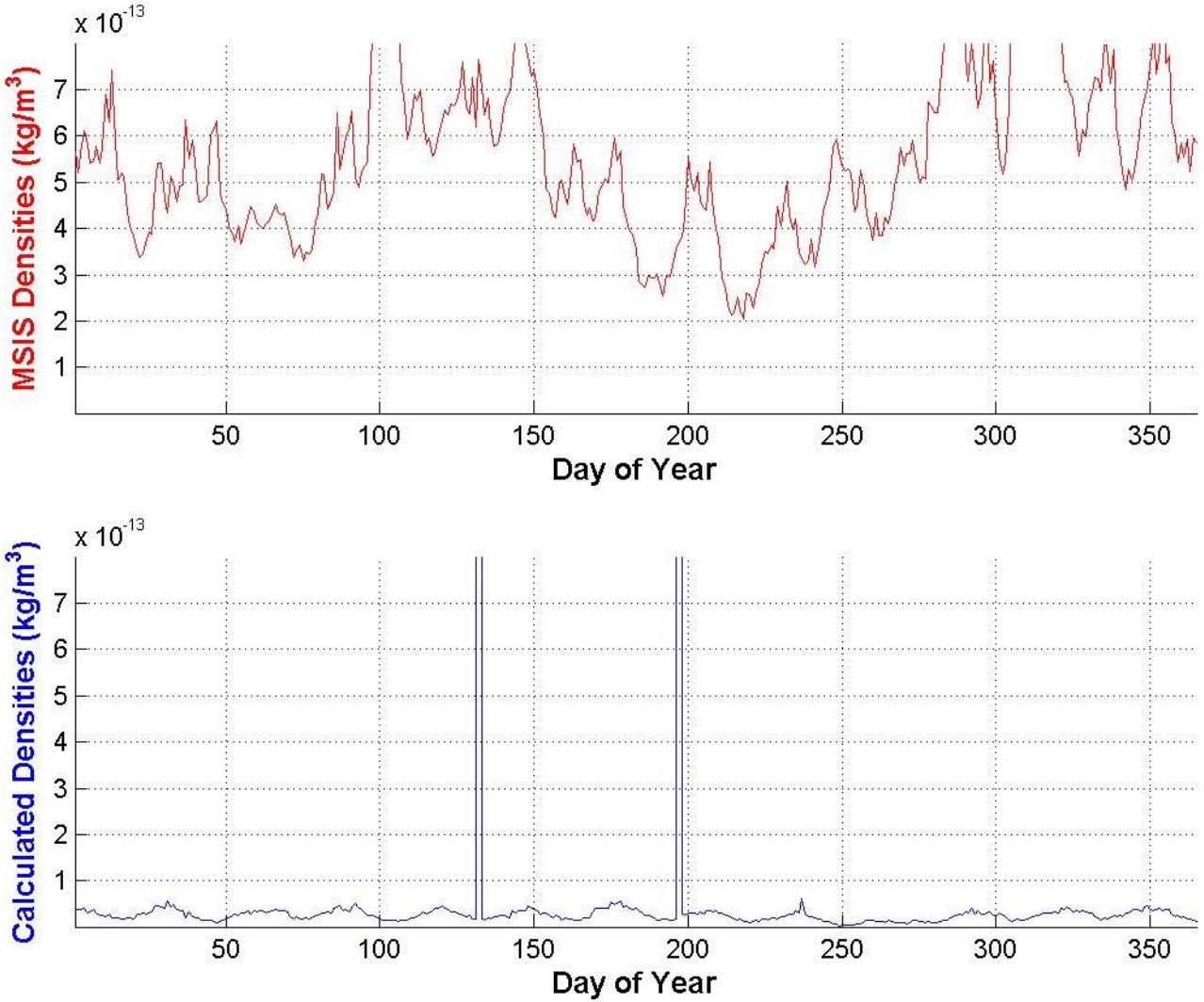

Figure 3.19. 2007 MSIS and Calculated Densities

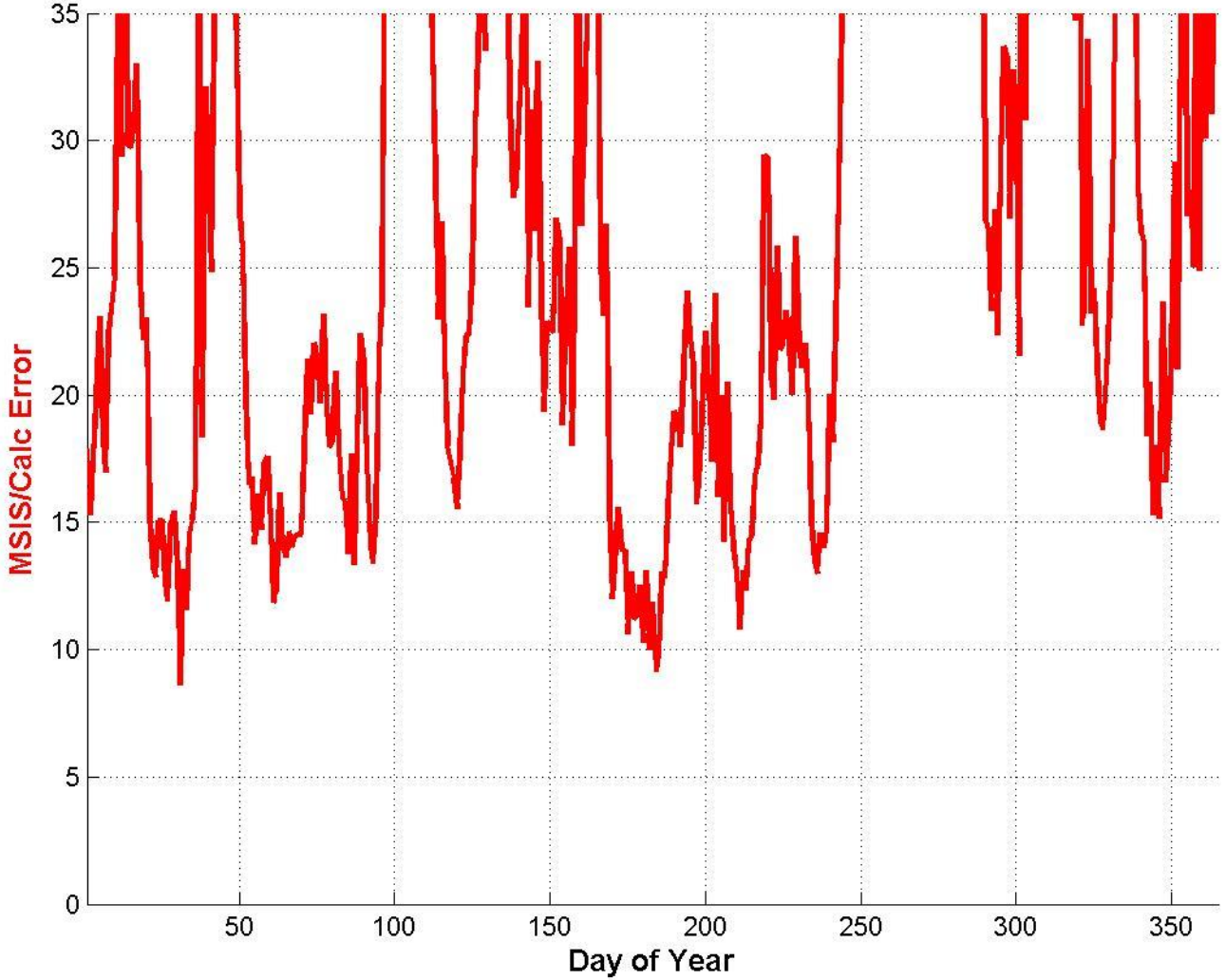

Figure 3.20. 2007 Density Error

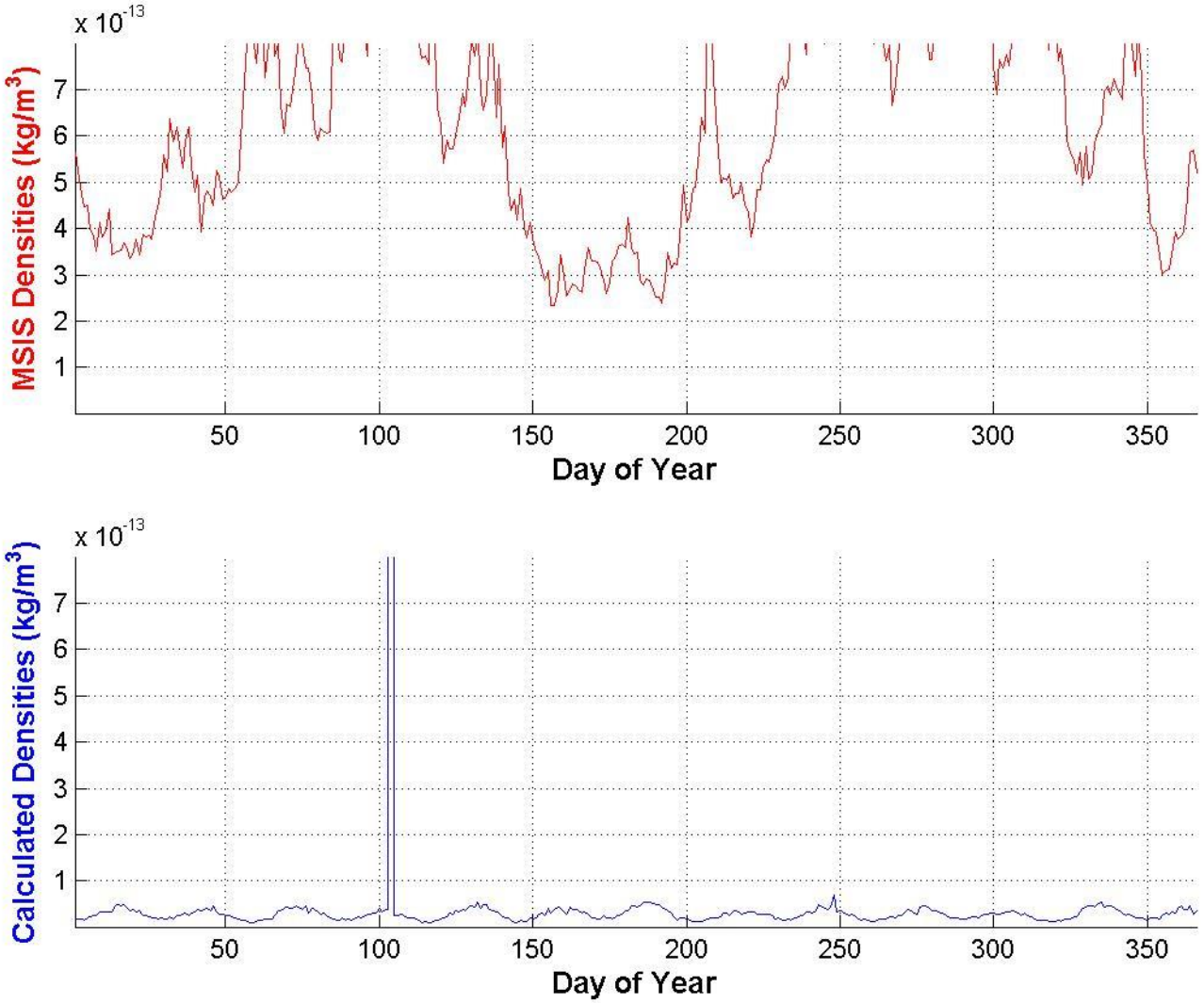

Figure 3.21. 2008 MSIS and Calculated Densities

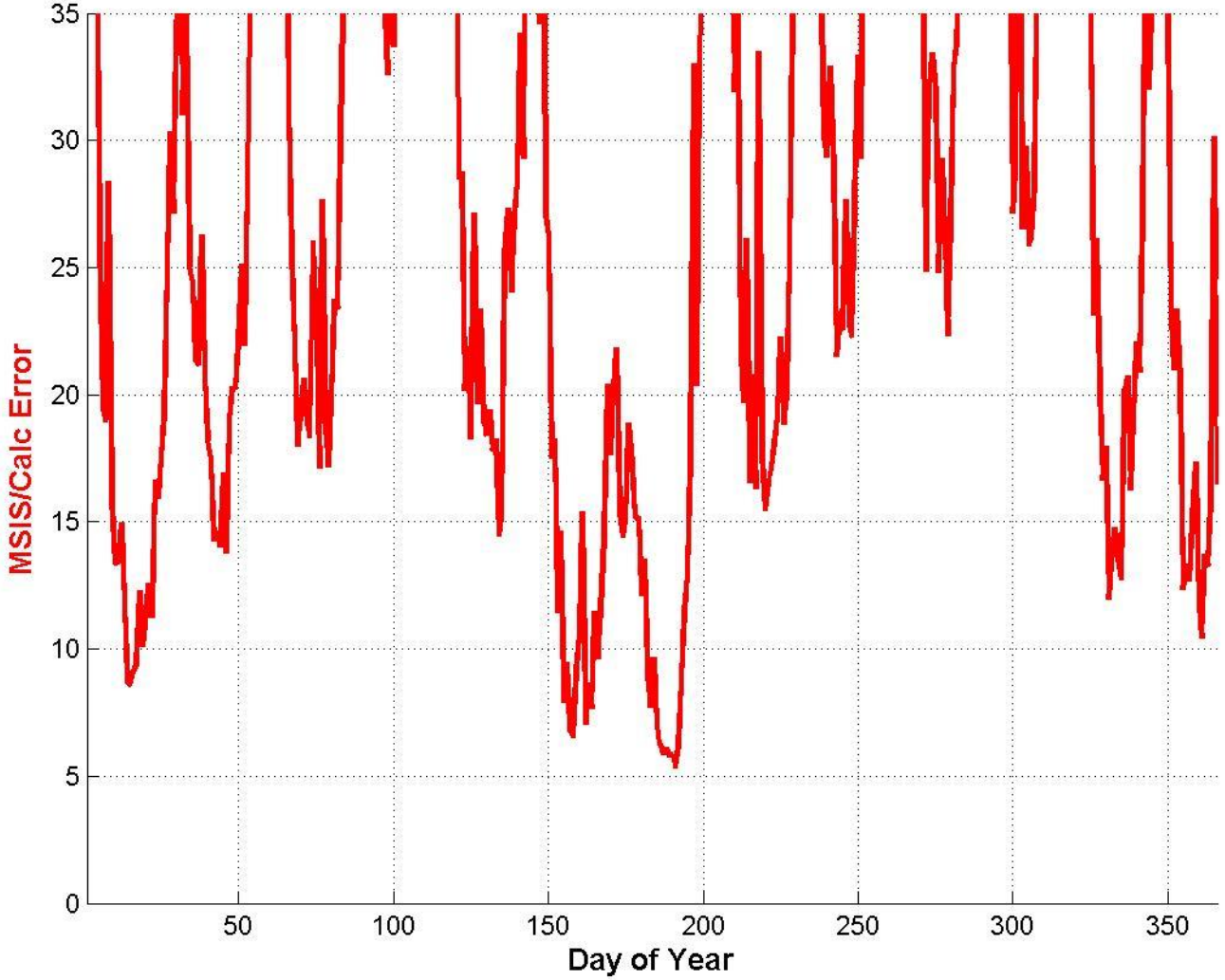

Figure 3.22. 2008 Density Error

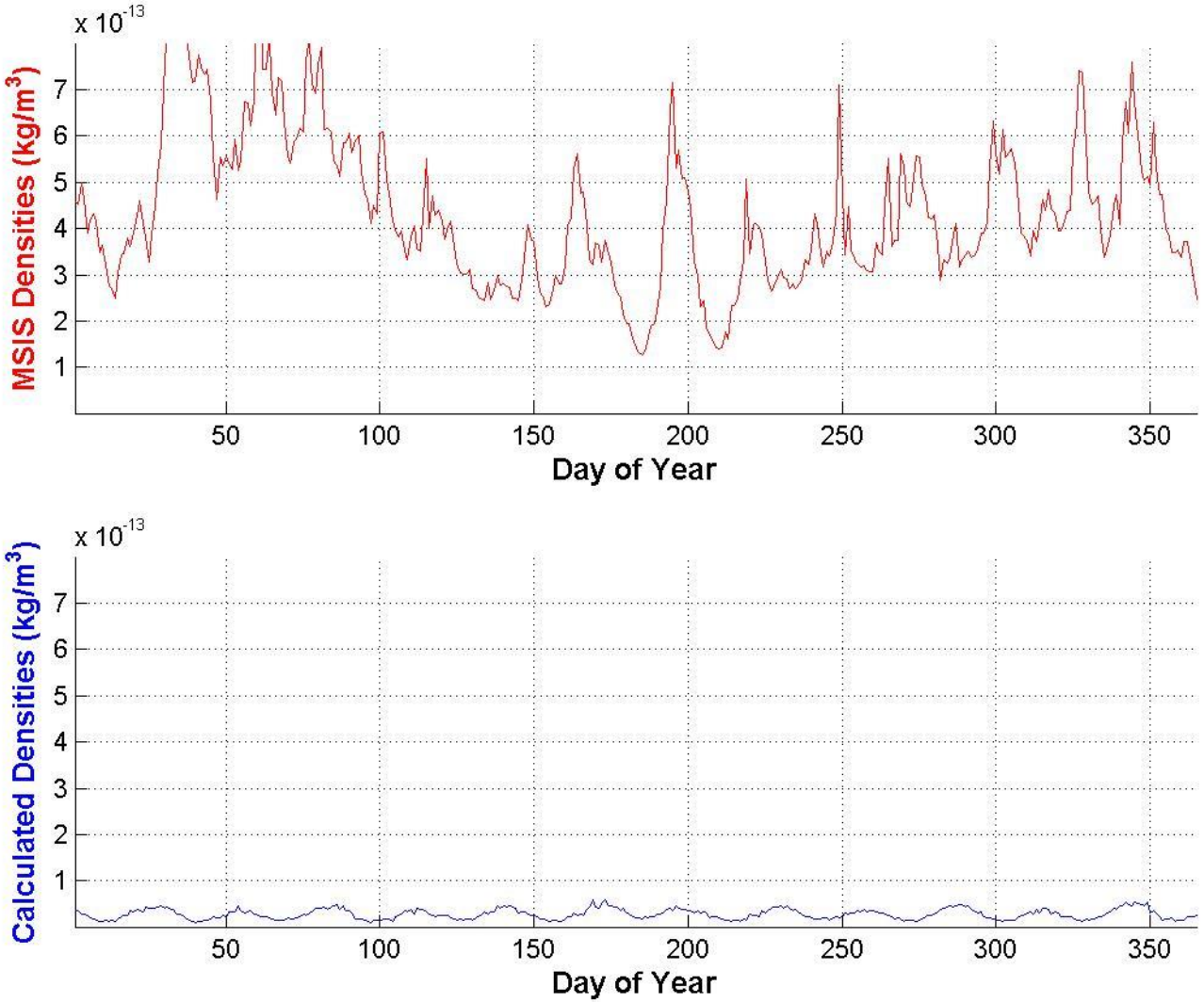

Figure 3.23. 2009 MSIS and Calculated Densities

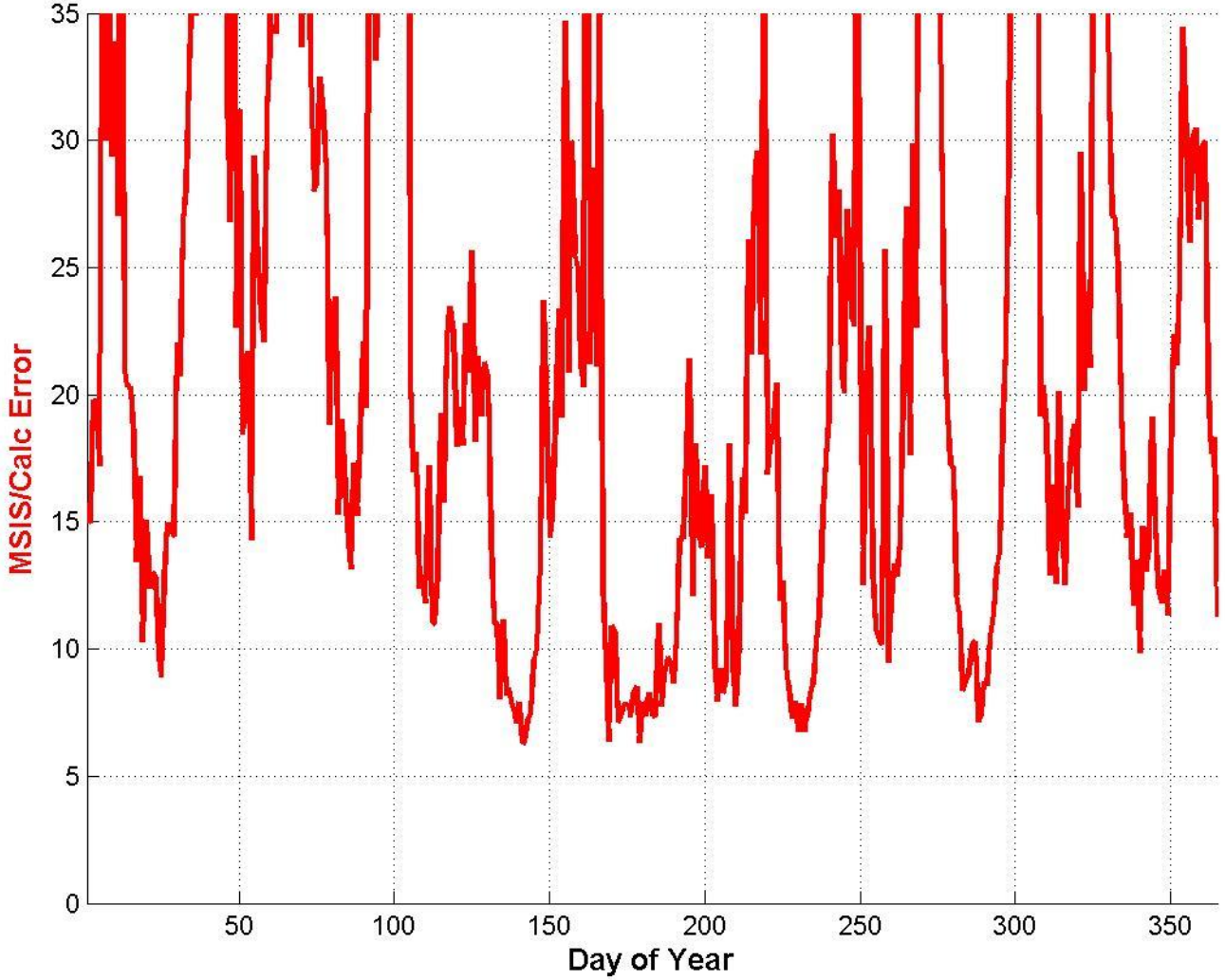

Figure 3.24. 2009 Density Error

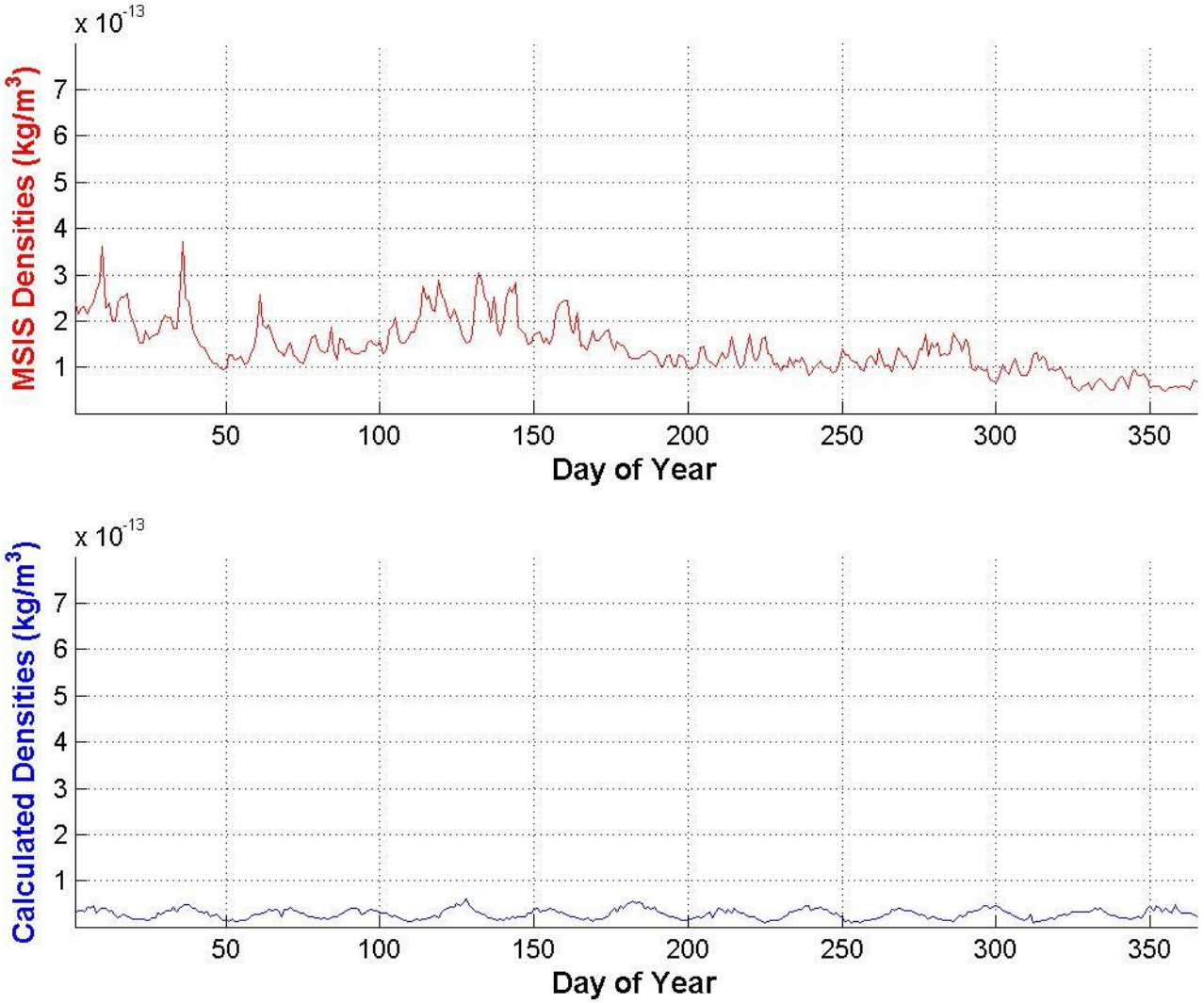

Figure 3.25. 2010 MSIS and Calculated Densities

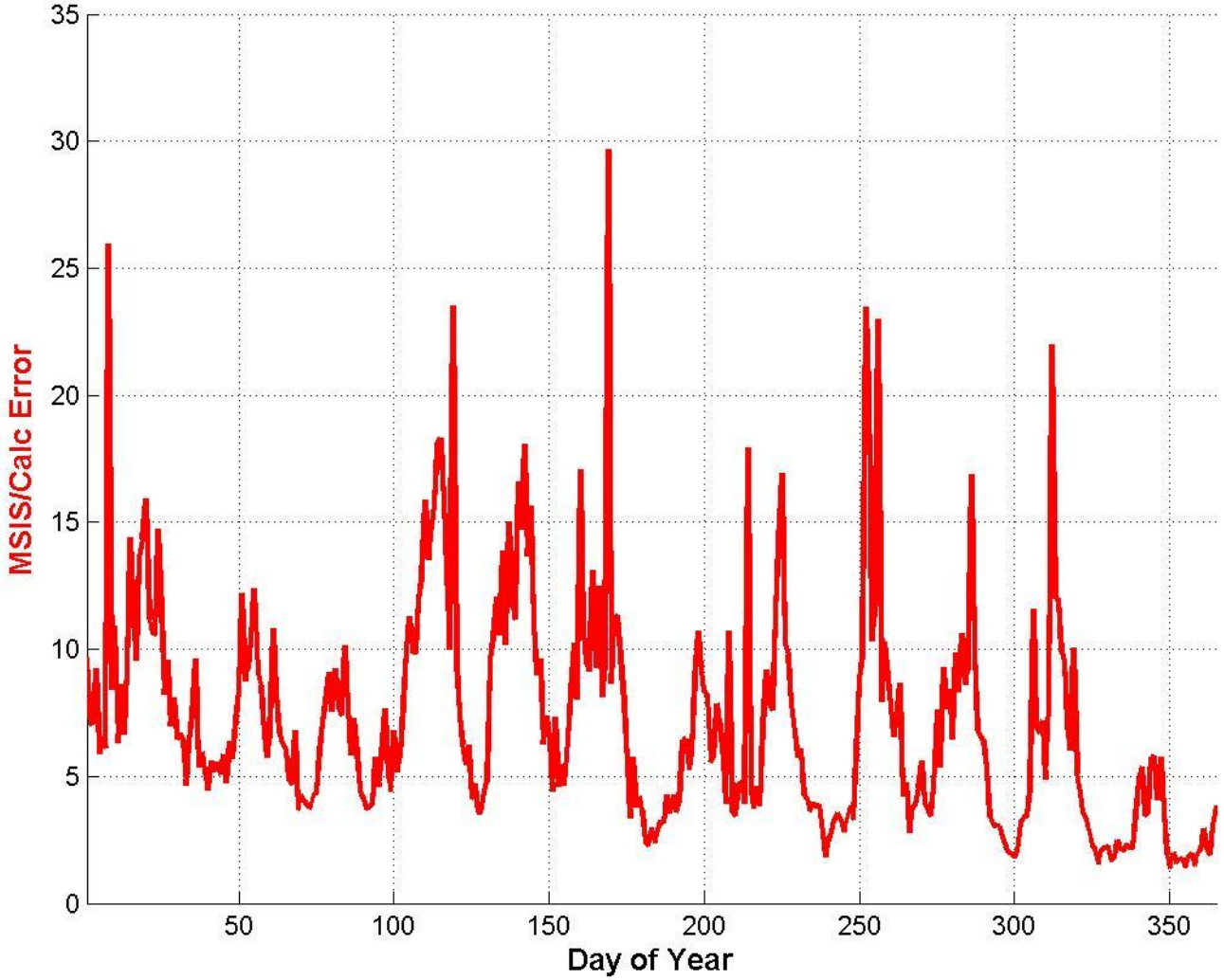

Figure 3.26. 2010 Density Error

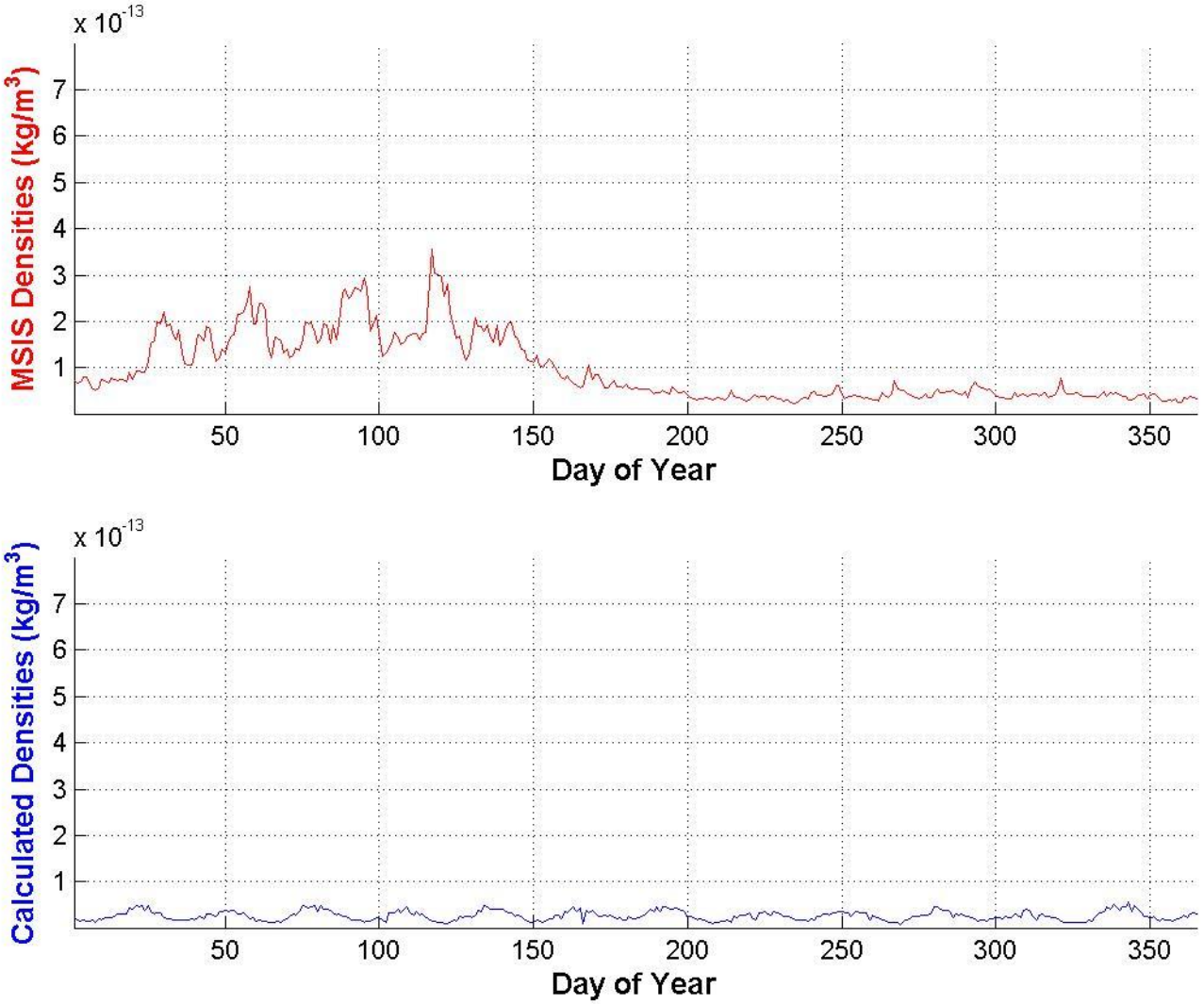

Figure 3.27. 2011 MSIS and Calculated Densities

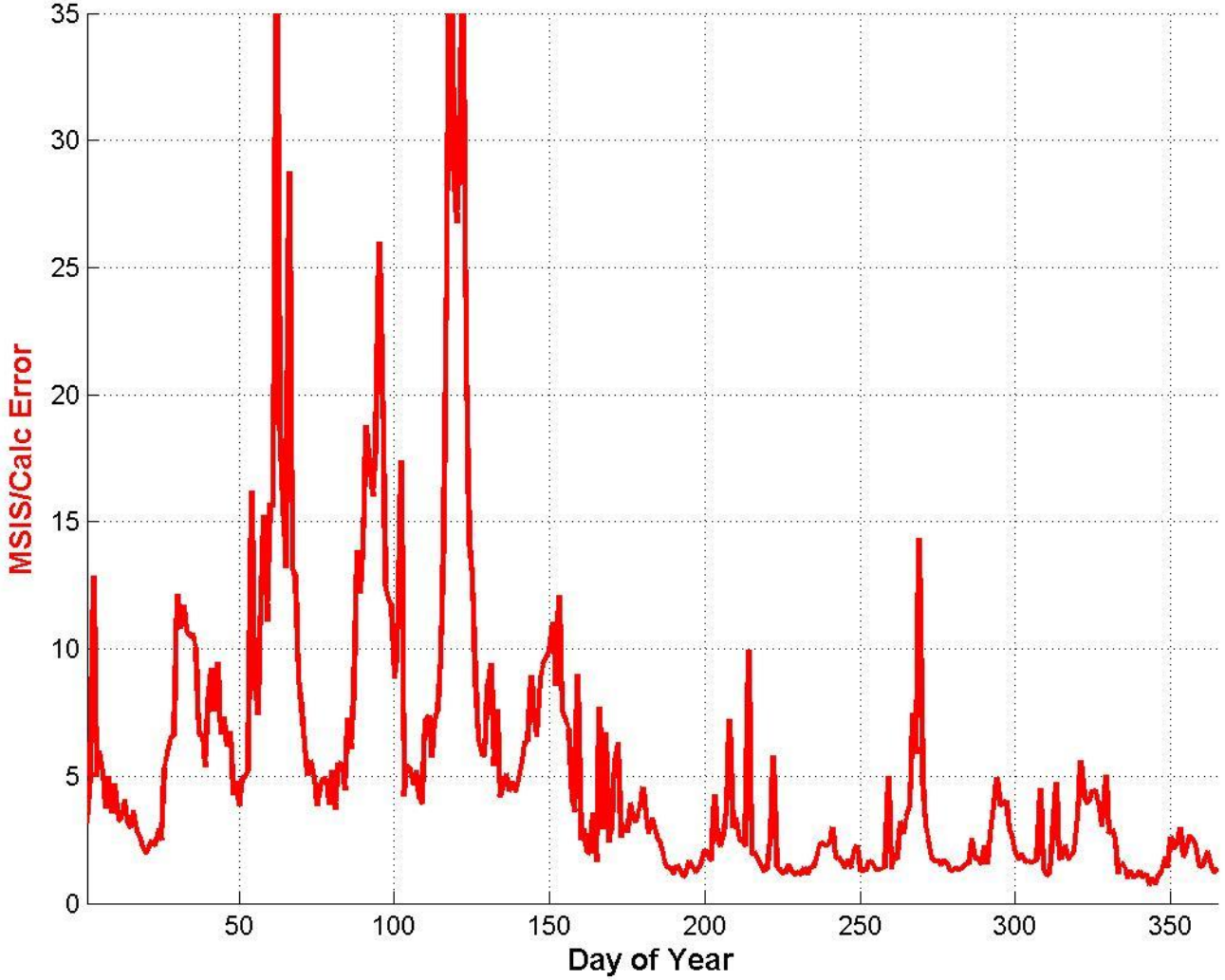

Figure 3.28. 2011 Density Error

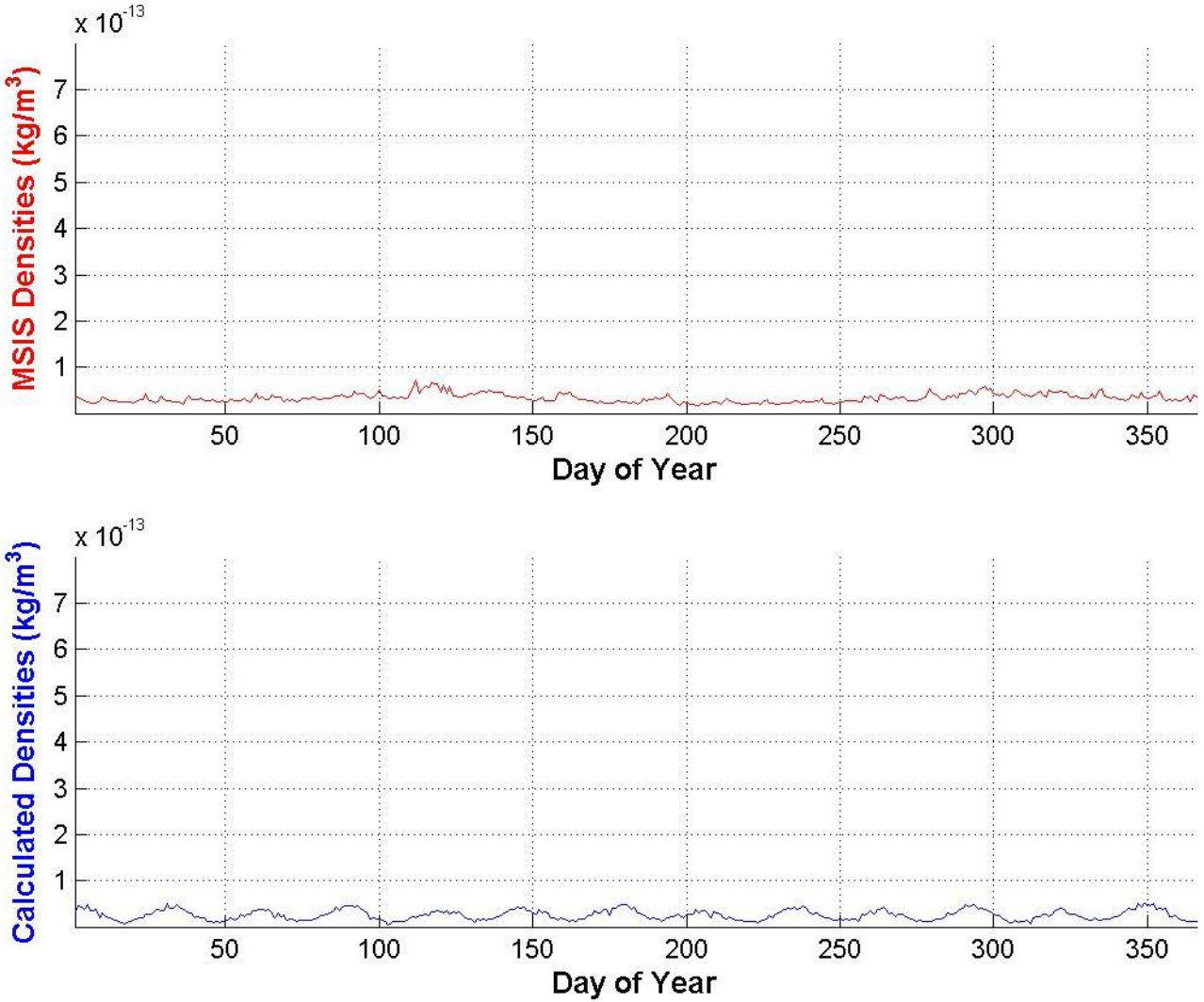

Figure 3.29. 2012 MSIS and Calculated Densities

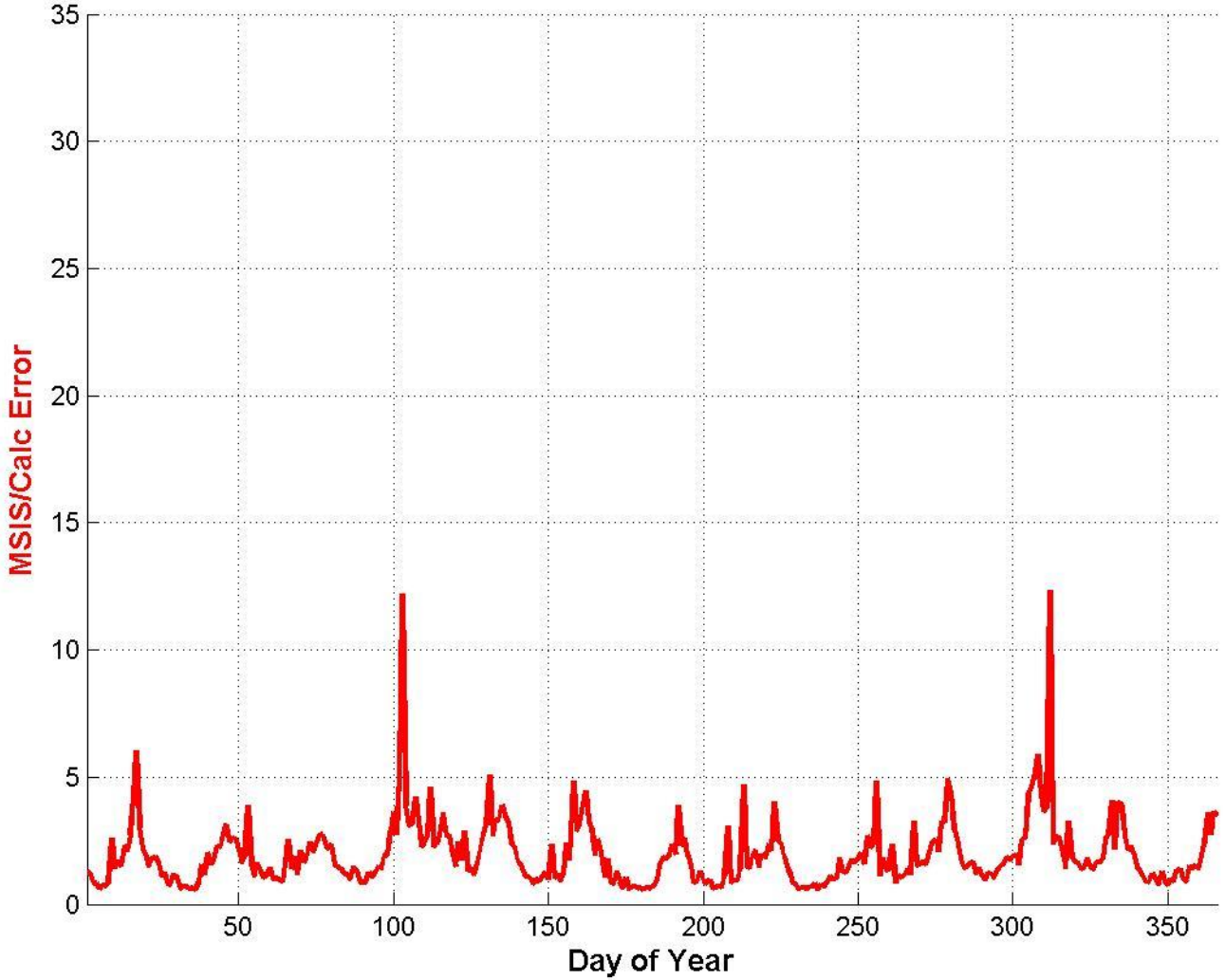

Figure 3.30. 2012 Density Error

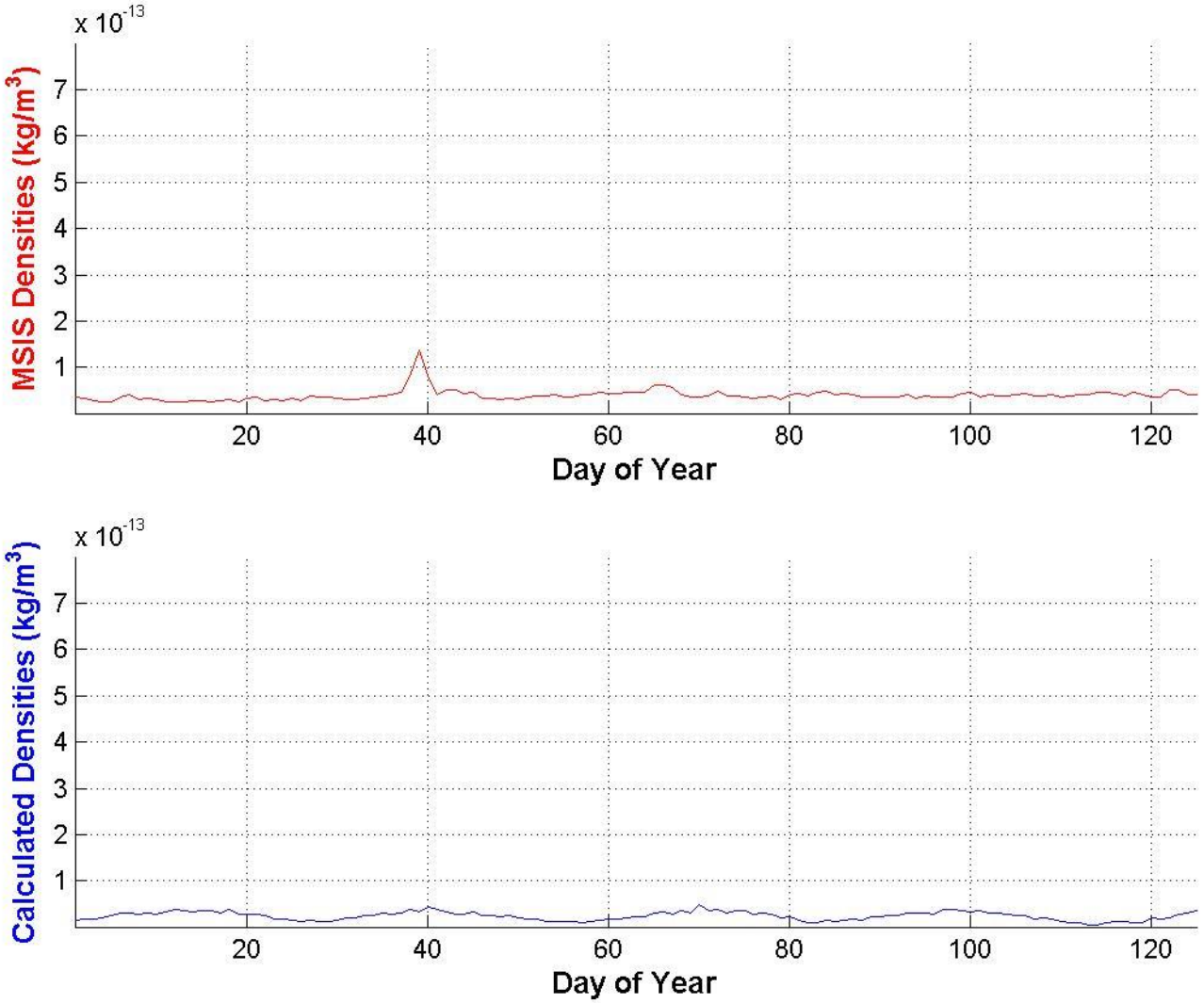

Figure 3.31. 2013 MSIS and Calculated Densities

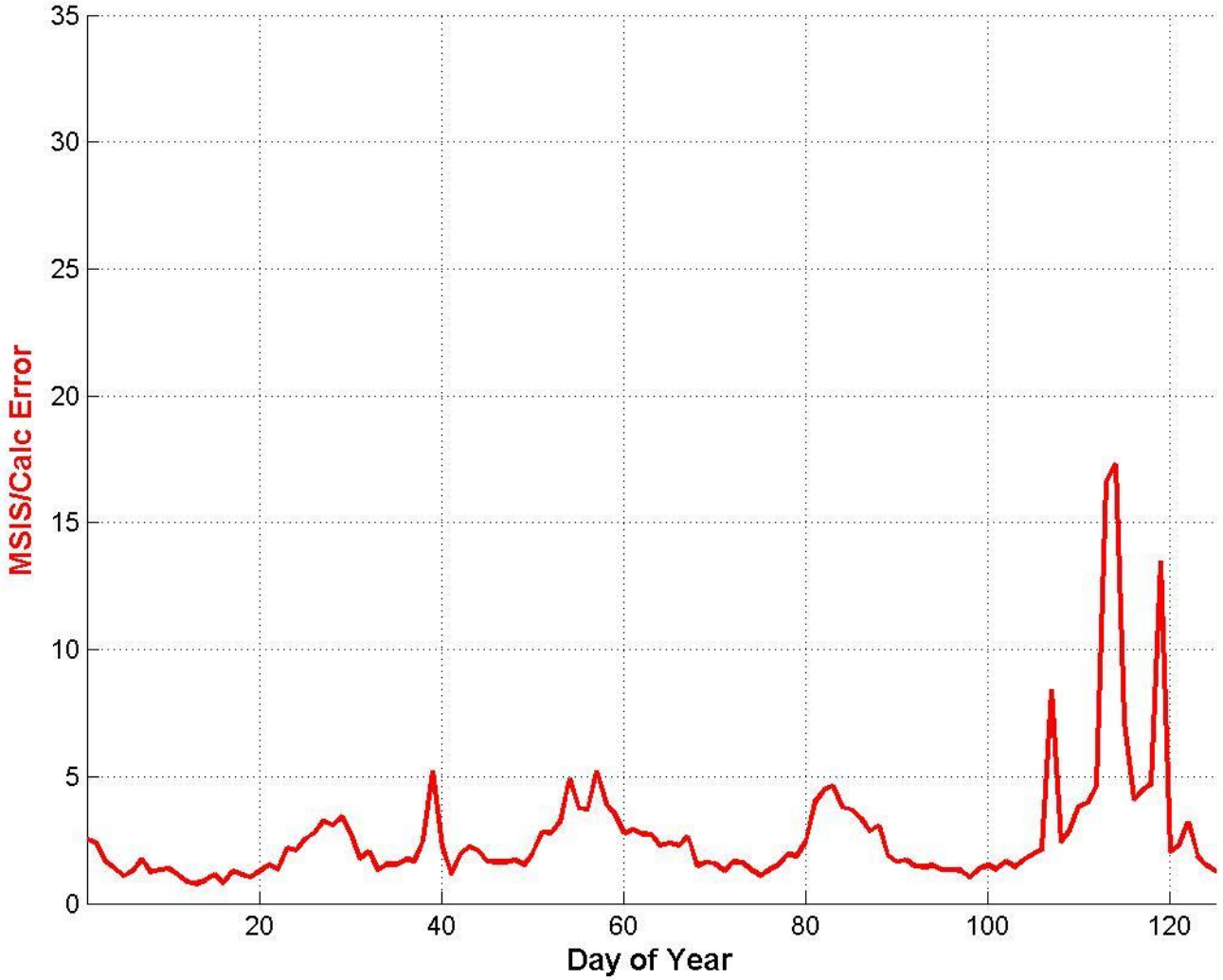

Figure 3.32. 2013 Density Error

3.3 Integrating On-Orbit Data into a Drag Analysis

Swift keeps state-of-health data for its entire mission duration. These data are sampled at approximately 5–30 Hz, depending on the source of the data. The clock on *Swift* is kept to within ± 100 μs, so it can be reasonably assumed that all data is accurately time stamped. *Swift* uses Two Line Element (TLE) sets to generate position and velocity vectors via AGI's Satellite Toolkit program and synchronizes to them three times per day. Unfortunately, the error in the velocity vector is driven by the accuracy of the TLEs, which have been shown to be quite inaccurate the greater the time that has elapsed between measurements [Legendre et al., 2006]. In order to reduce error caused by TLEs, *Swift* only processes a new TLE that is within an acceptable fluctuation of the previous TLE.[2]

Once these vectors have been uplinked and synchronized, *Swift* maintains information on its altitude, velocity, and attitude. These data are then easily used in the various portions of this research. It is the source of the measured altitude data that can then be binned into hour-long segments that are then fed into the NRLMSISE-00 atmospheric model in order to determine the proper density value to use. Binning this data into hourly segments is an acceptable approximation because the altitude of *Swift* does not change by a measurable amount in an hour. Figures 3.13 through 3.22 show *Swift*'s mean semimajor axis over each year and the figures clearly show the validity of this assumption. This validates the assumption that the density is a constant for the given hour that is analyzed, which becomes an especially important when looking at the big

[2] *Swift* procedures, program manuals, and script documentation.

picture of trying to develop an up-to-date prediction of the deorbit estimate for *Swift*, a topic that is discussed in Chapter 4.2.

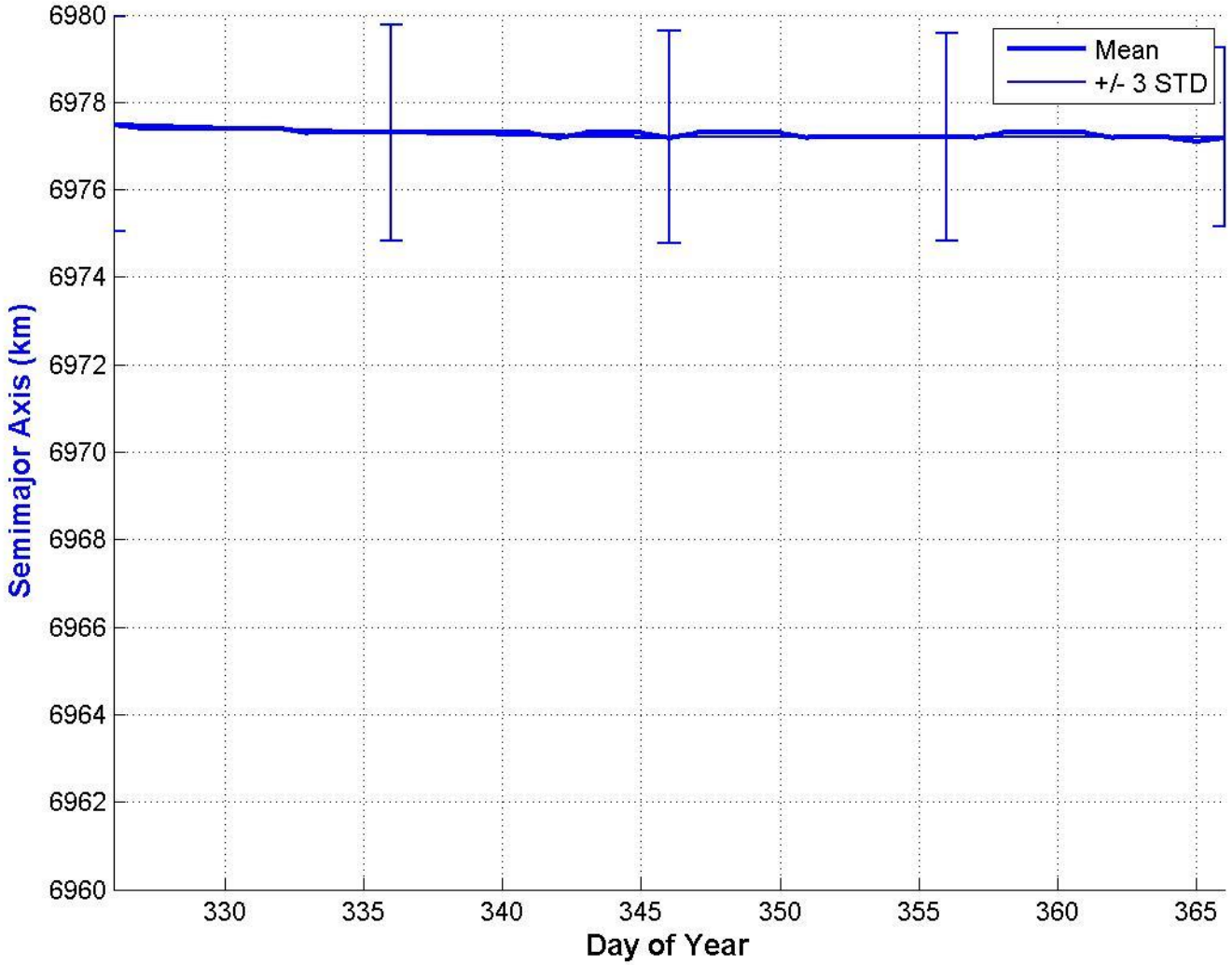

Figure 3.33. 2004 Semimajor Axis

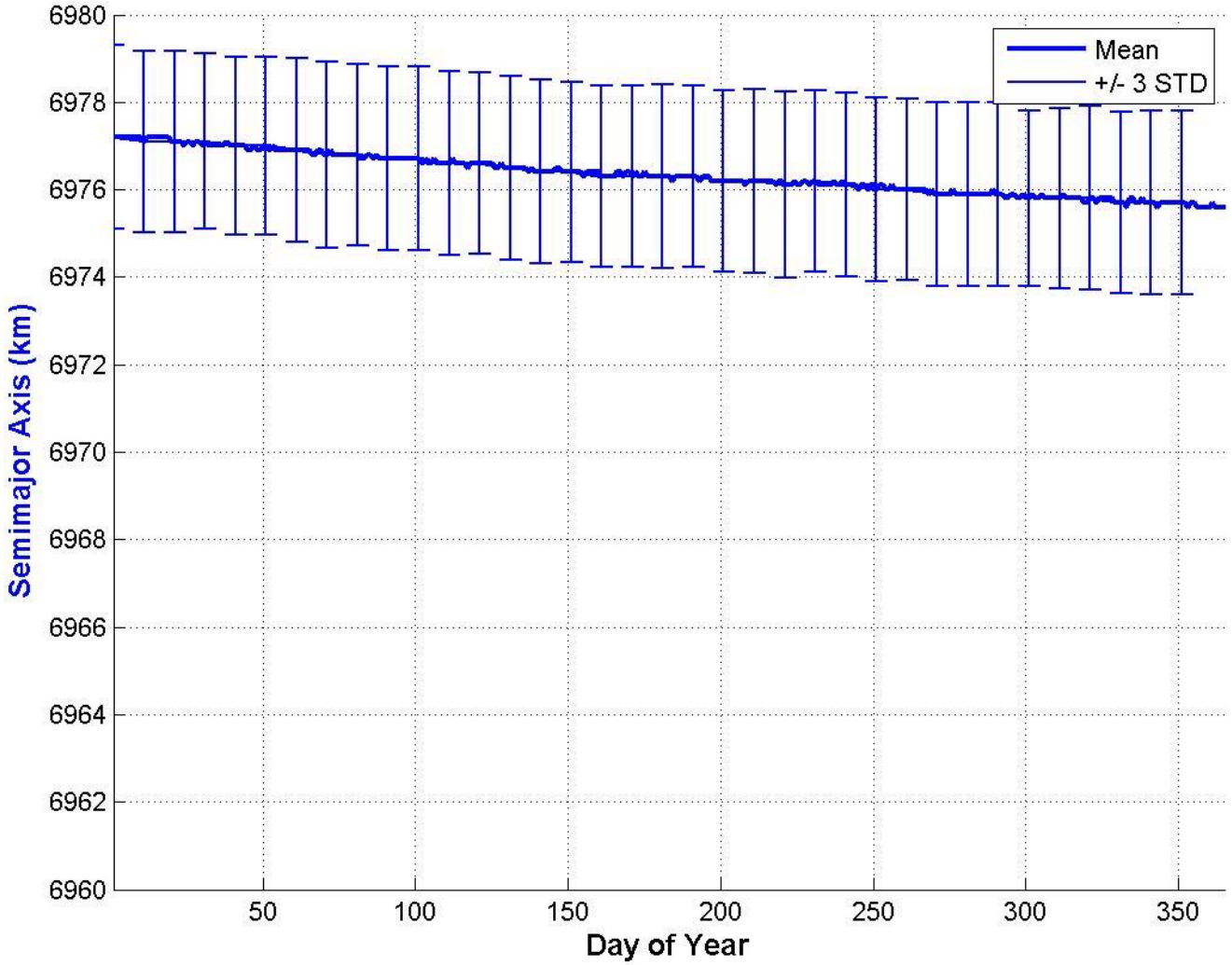

Figure 3.34. 2005 Semimajor Axis

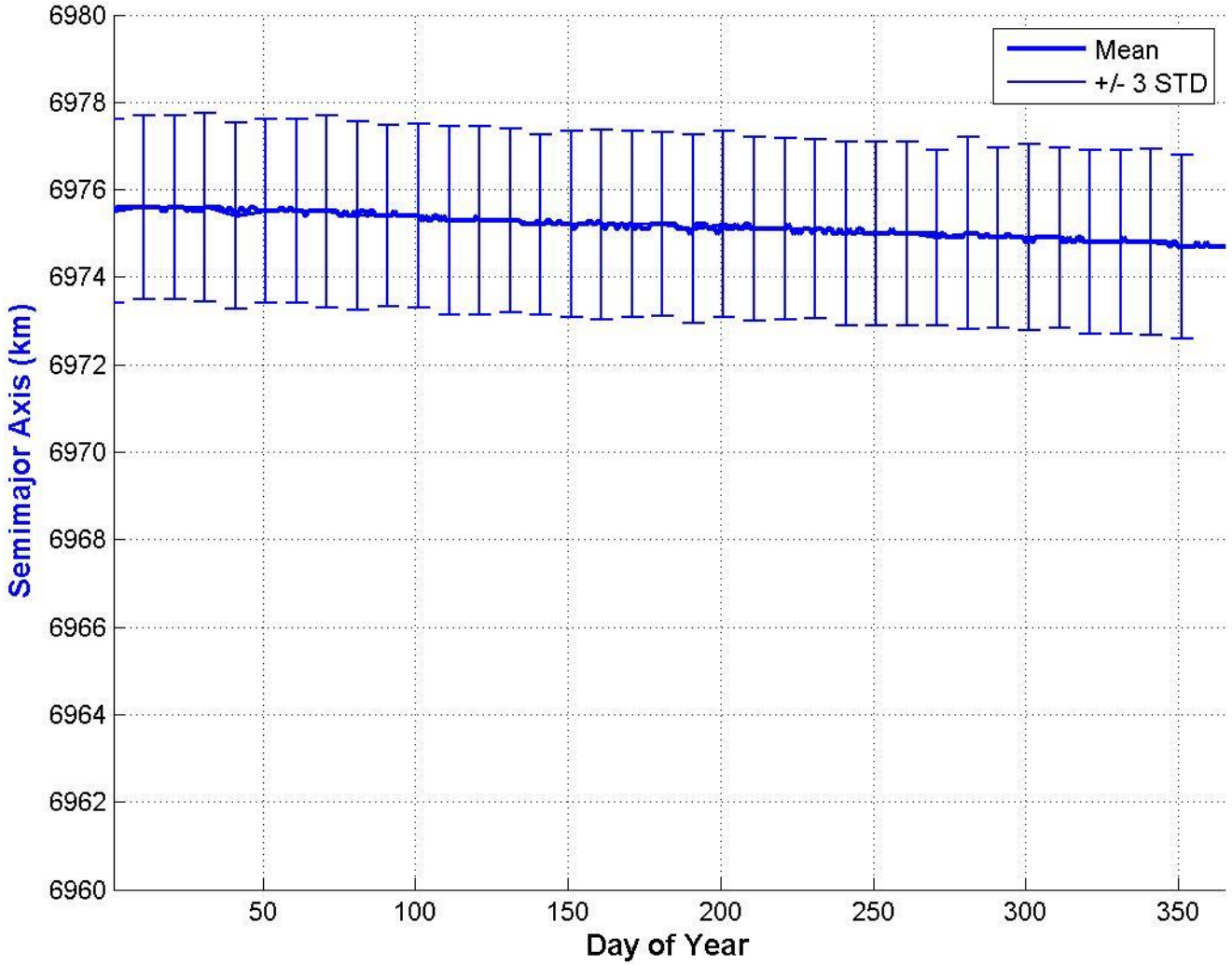

Figure 3.35. 2006 Semimajor Axis

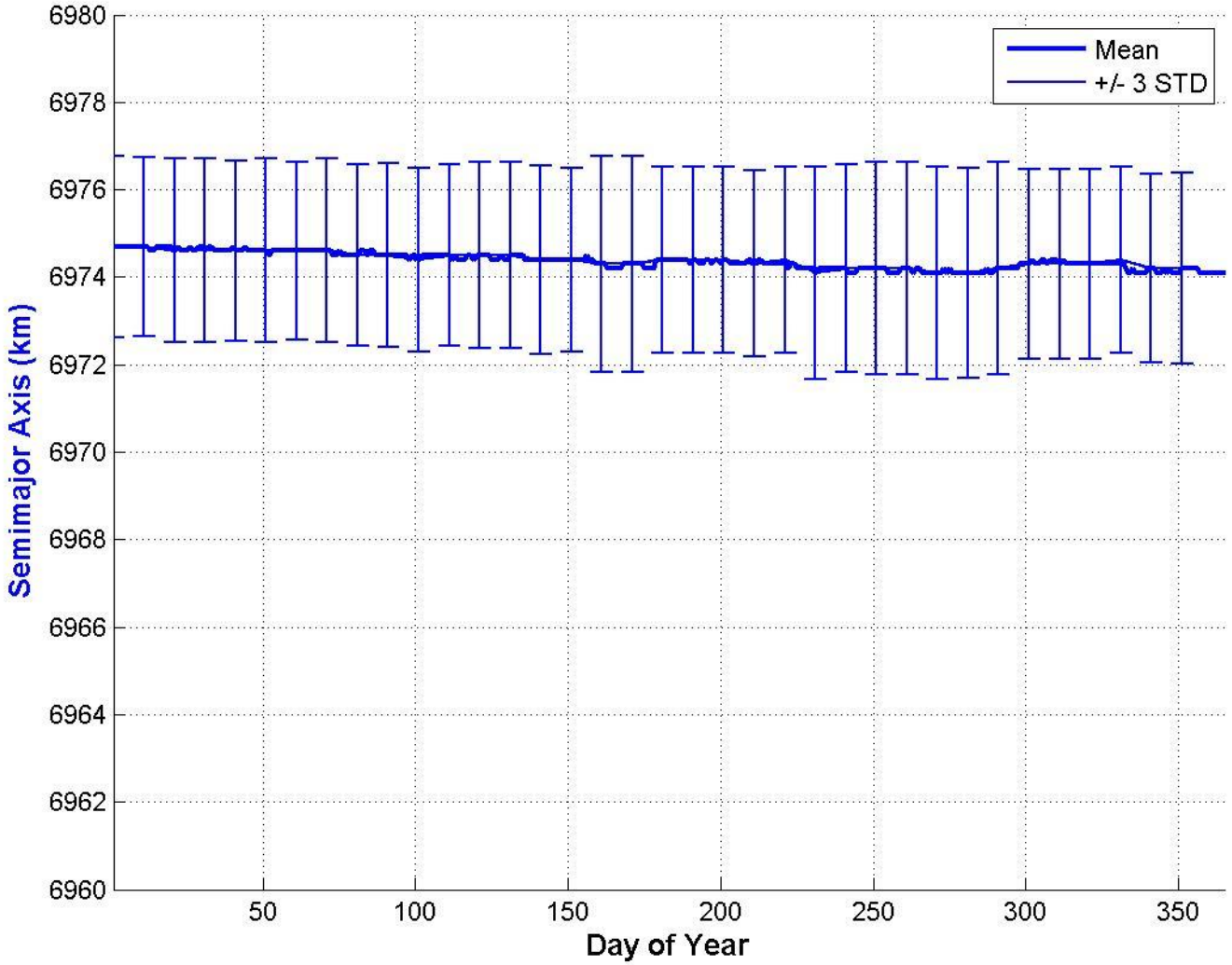

Figure 3.36. 2007 Semimajor Axis

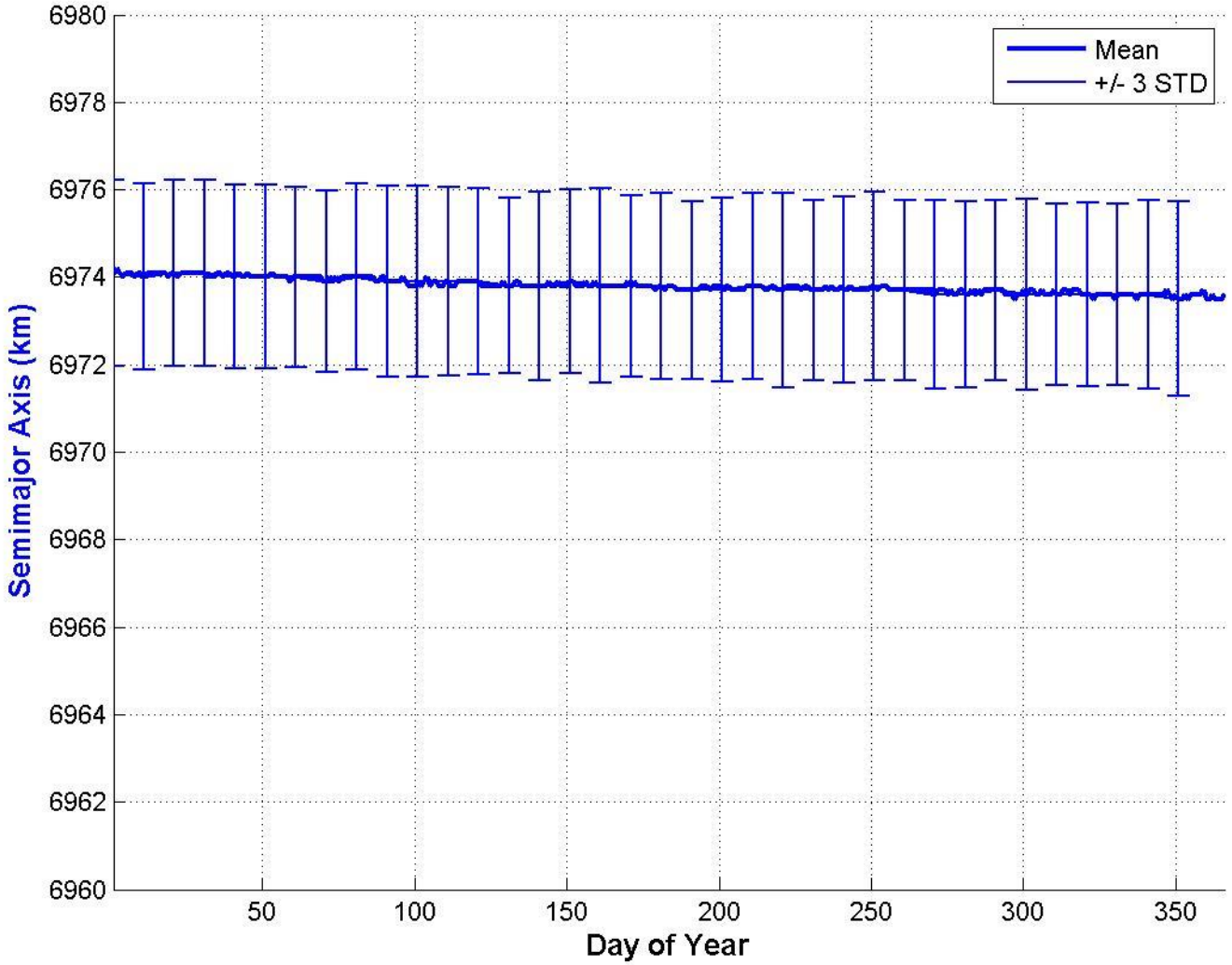

Figure 3.37. 2008 Semimajor Axis

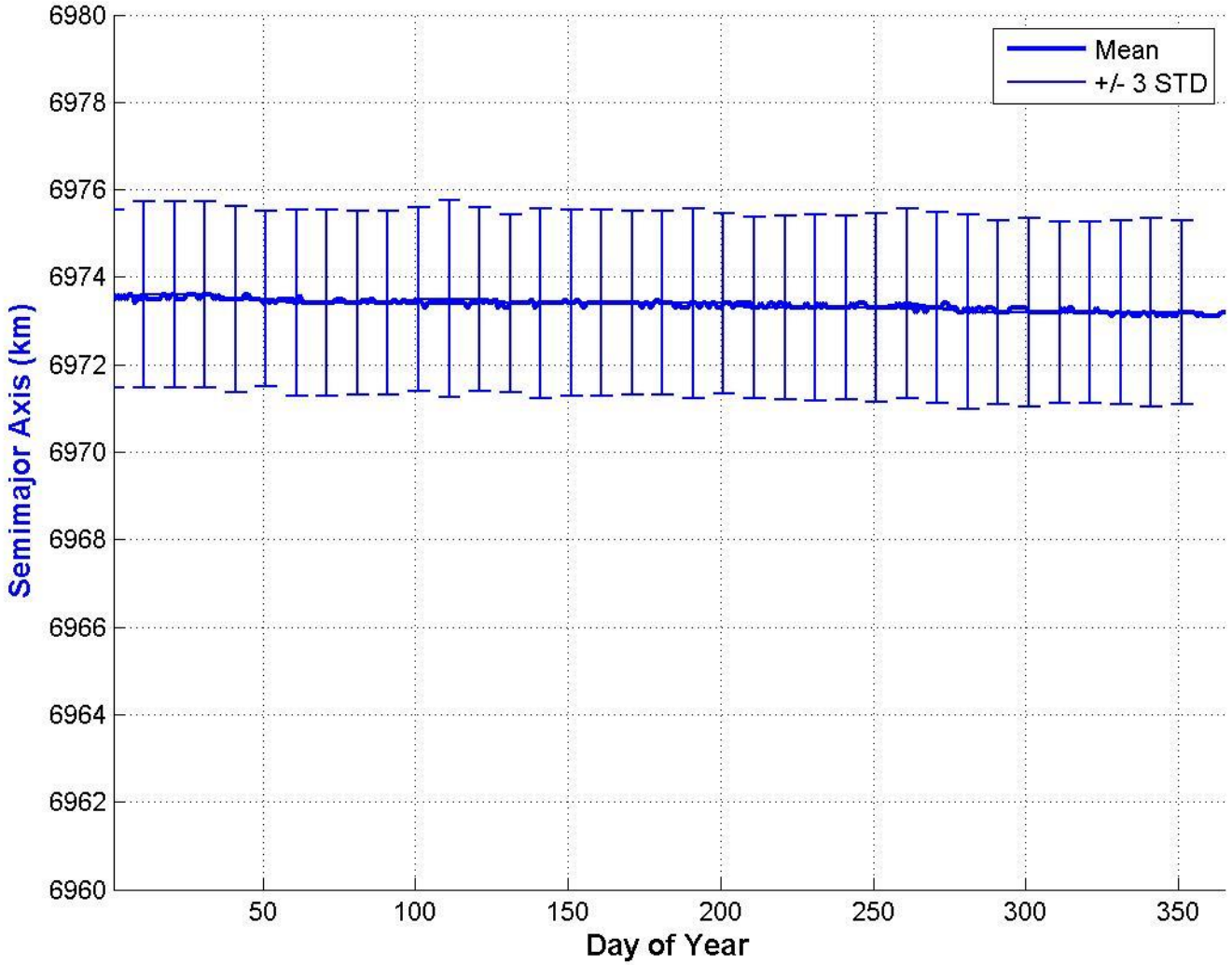

Figure 3.38. 2009 Semimajor Axis

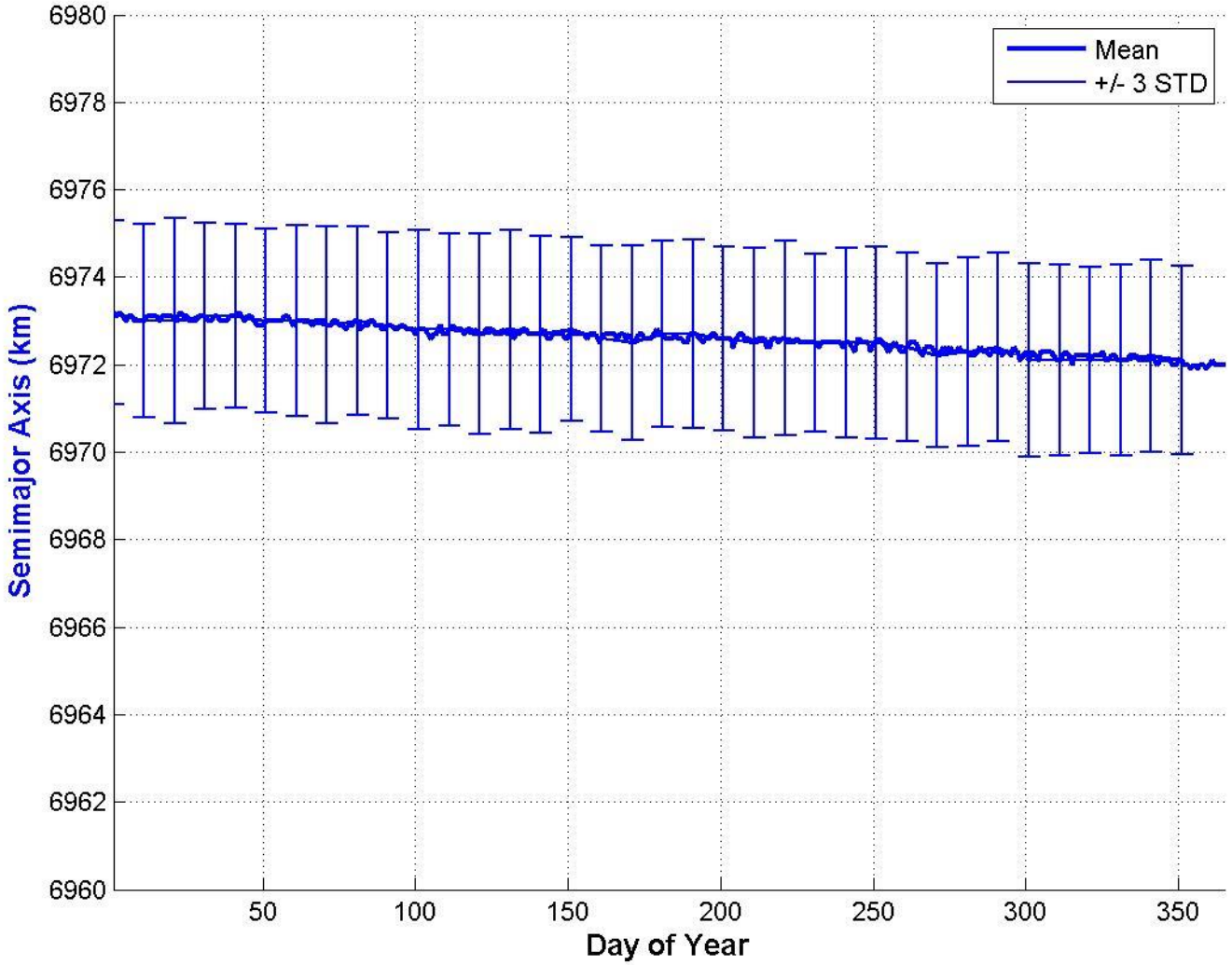

Figure 3.39. 2010 Semimajor Axis

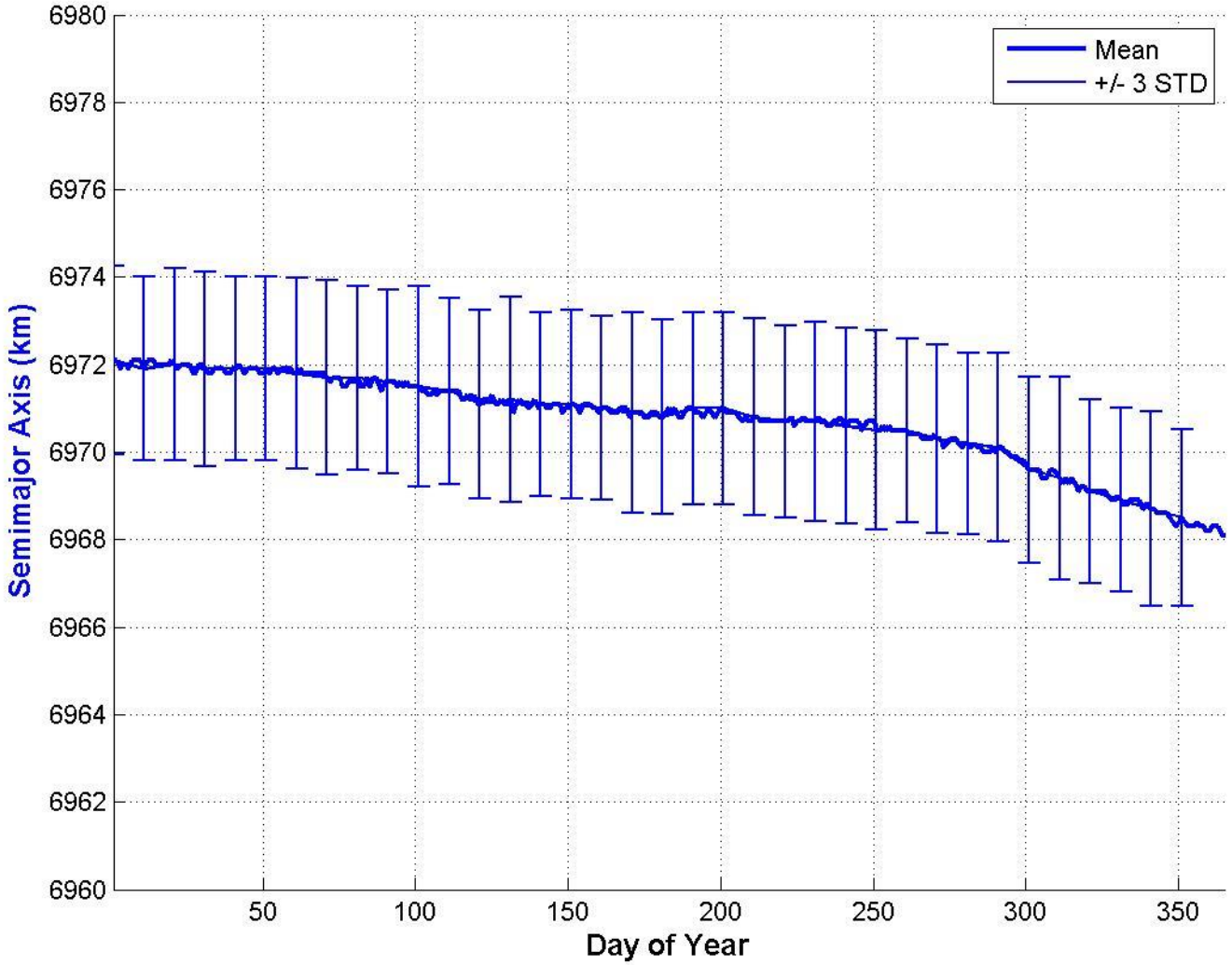

Figure 3.40. 2011 Semimajor Axis

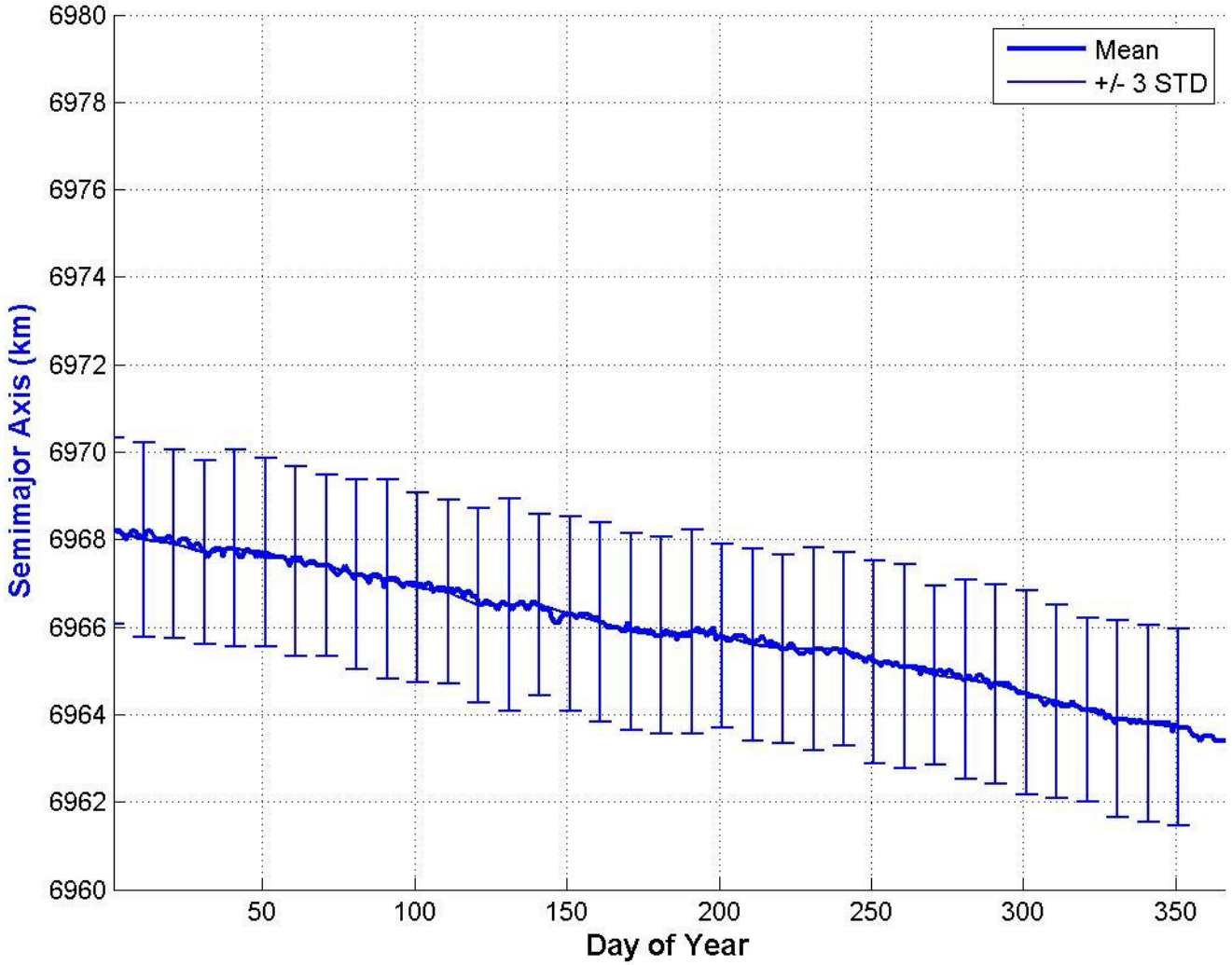

Figure 3.41. 2012 Semimajor Axis

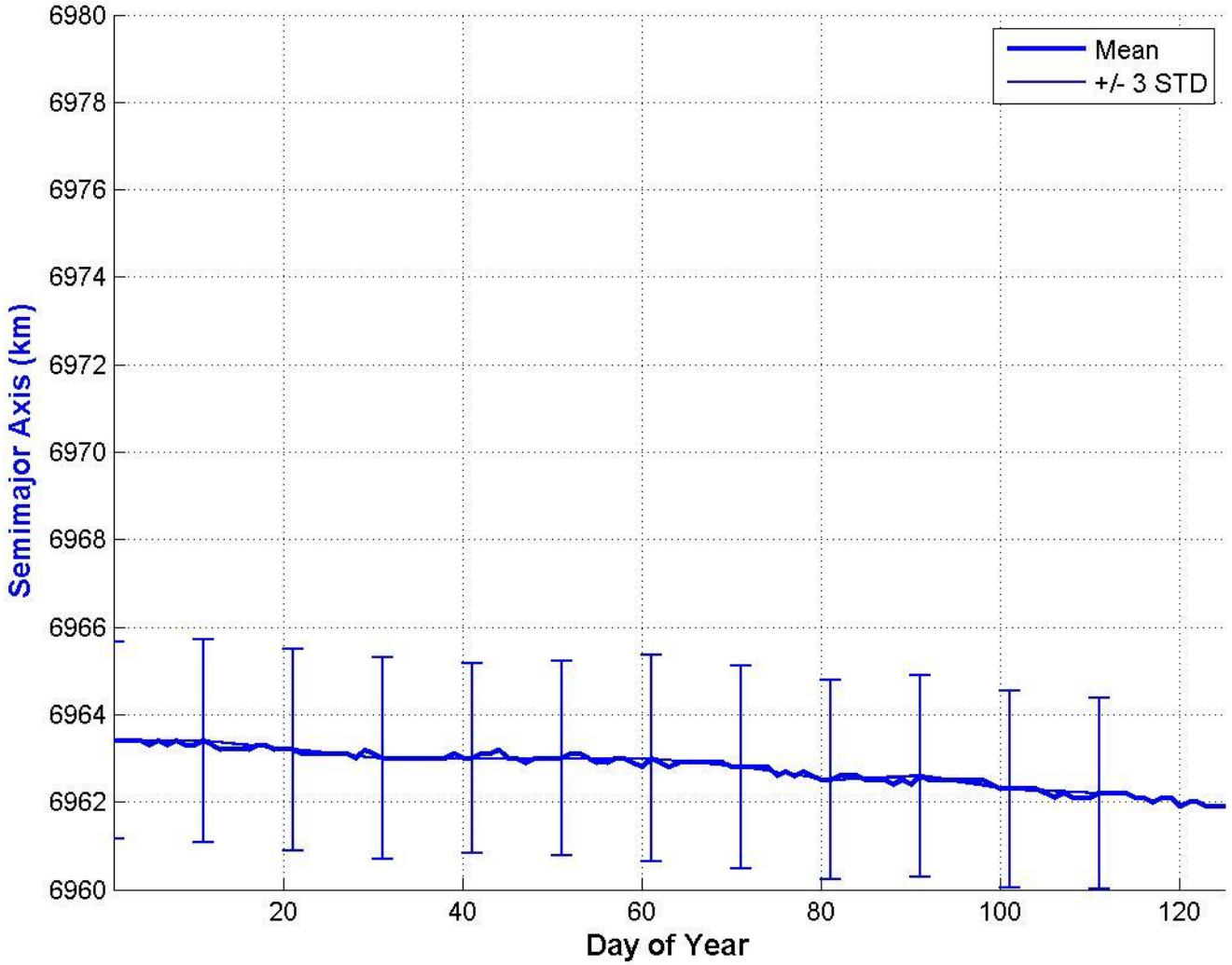

Figure 3.42. 2013 Semimajor Axis

3.4 Predicting the Orbital Lifetime of *Swift*

Predicting the lifetime of a spacecraft has many applications including determining how long resources must be allocated to monitoring its decent, how long operational resources must be dedicated to maintaining the spacecraft, and how long useful science data can be collected from its payloads. Previous estimates for *Swift* show a deorbit date of approximately 2040.[3] However, this research took a slightly different approach and generated a method to determine altitude based on a yearly average of atmospheric density, a yearly average of relative velocity, and varying yearly selections of cross sectional area and coefficient of drag. These calculations were performed with both the NRLMSISE-00 and internally calculated density values. Finally, these are compared to the actual altitude loss and shown in Figures 3.33 through 3.42.

Each of these figures shows a certain section where the predicted and actual altitudes match, but no one model truly follows the decay. For example, Figure 3.47 shows that the model with a coefficient of drag of 3 using the internally calculated density data follows the actual decay of *Swift* quite closely from 2004–2010, but then only generally follows the true decay. Figure 3.43 shows that the model with a coefficient of drag of 2 using internally calculated density data closely predicts the altitude in years 2011 and 2012. Finally, Figure 3.49 shows that the model with a coefficient of drag of 4 using internally calculated density data closely predicts the altitude in 2013.

[3] *Swift* end of mission documentation

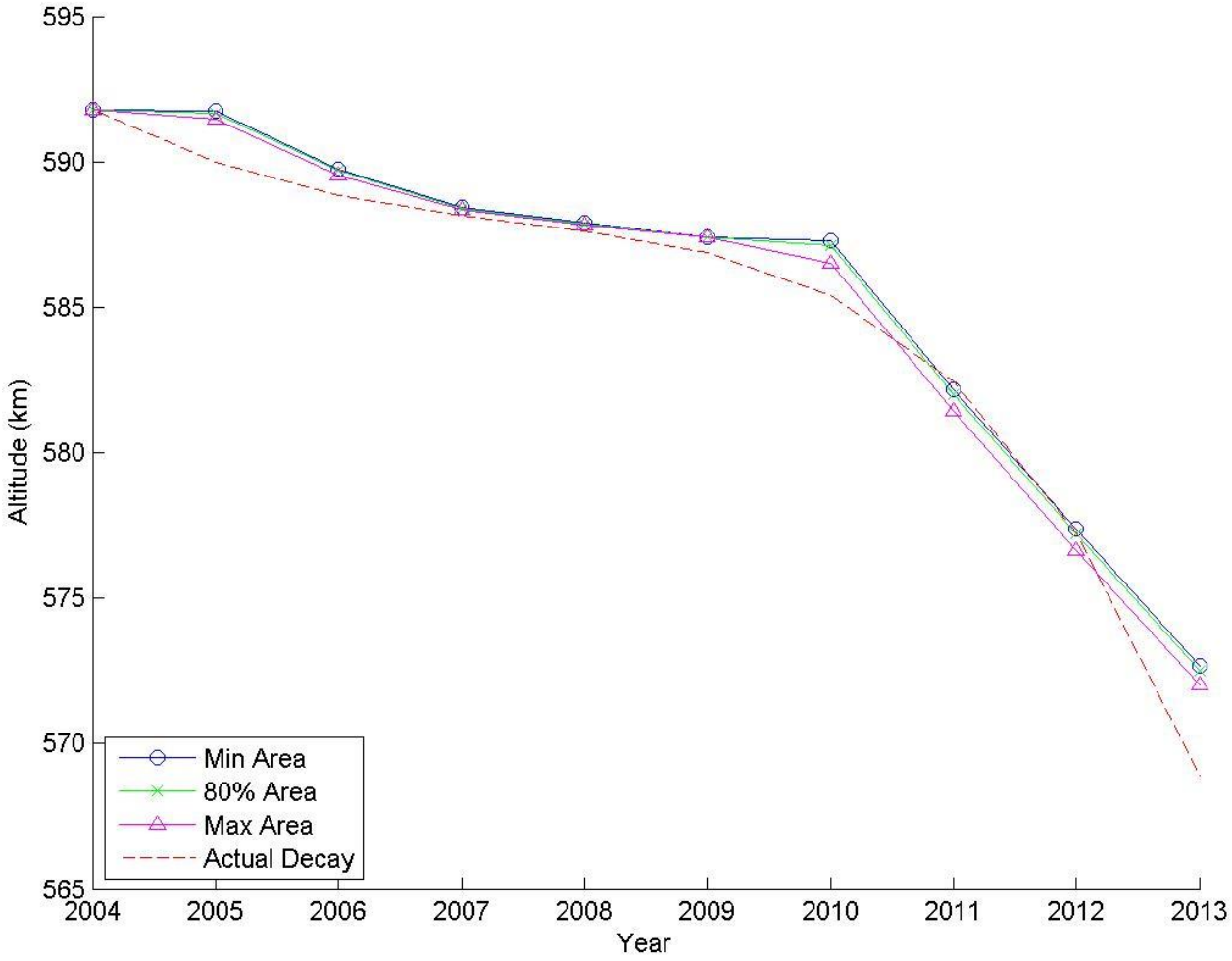

Figure 3.43. Orbit Decay $c_D = 2$, Calculated Data

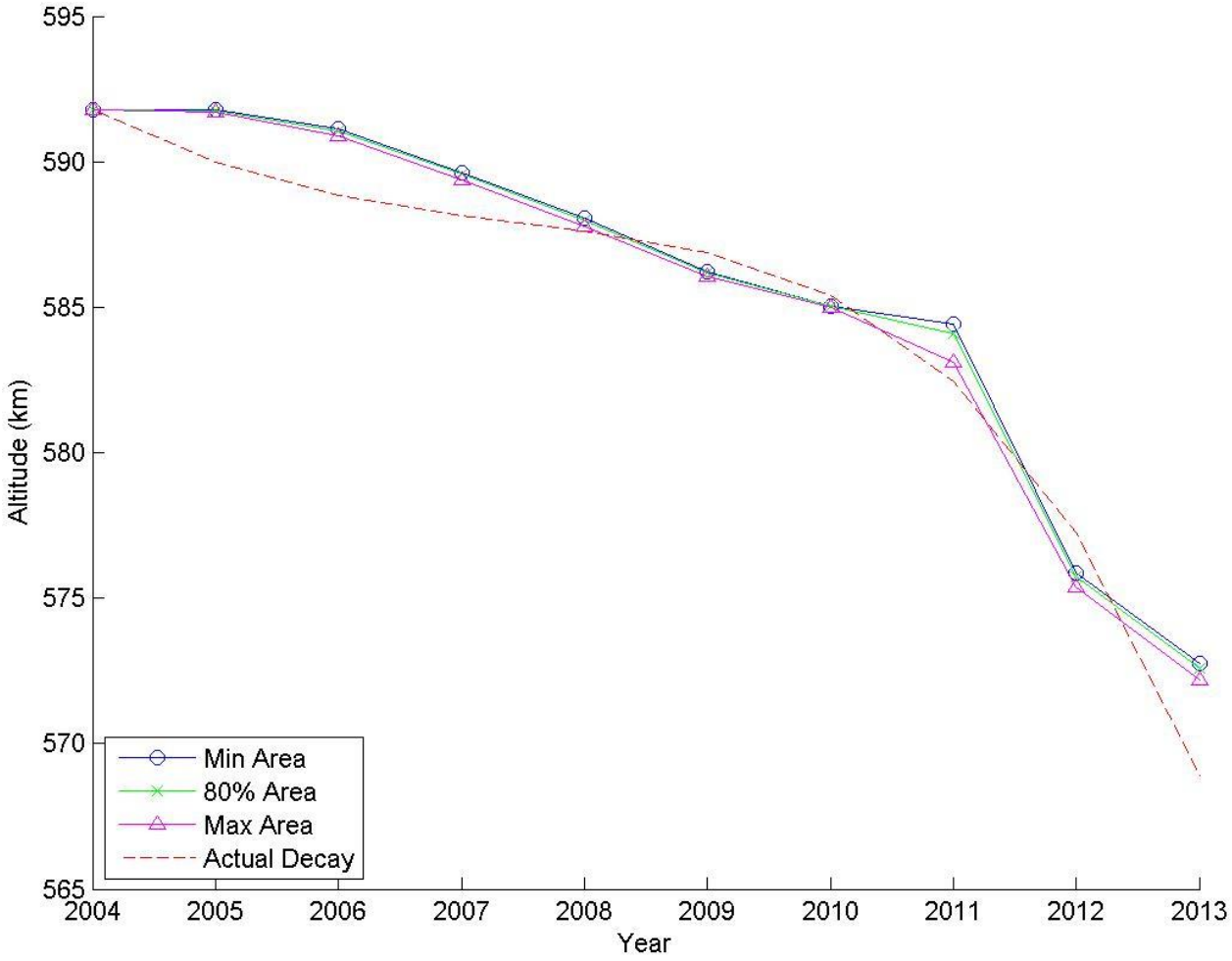

Figure 3.44. Orbit Decay $c_D = 2$, MSIS Data

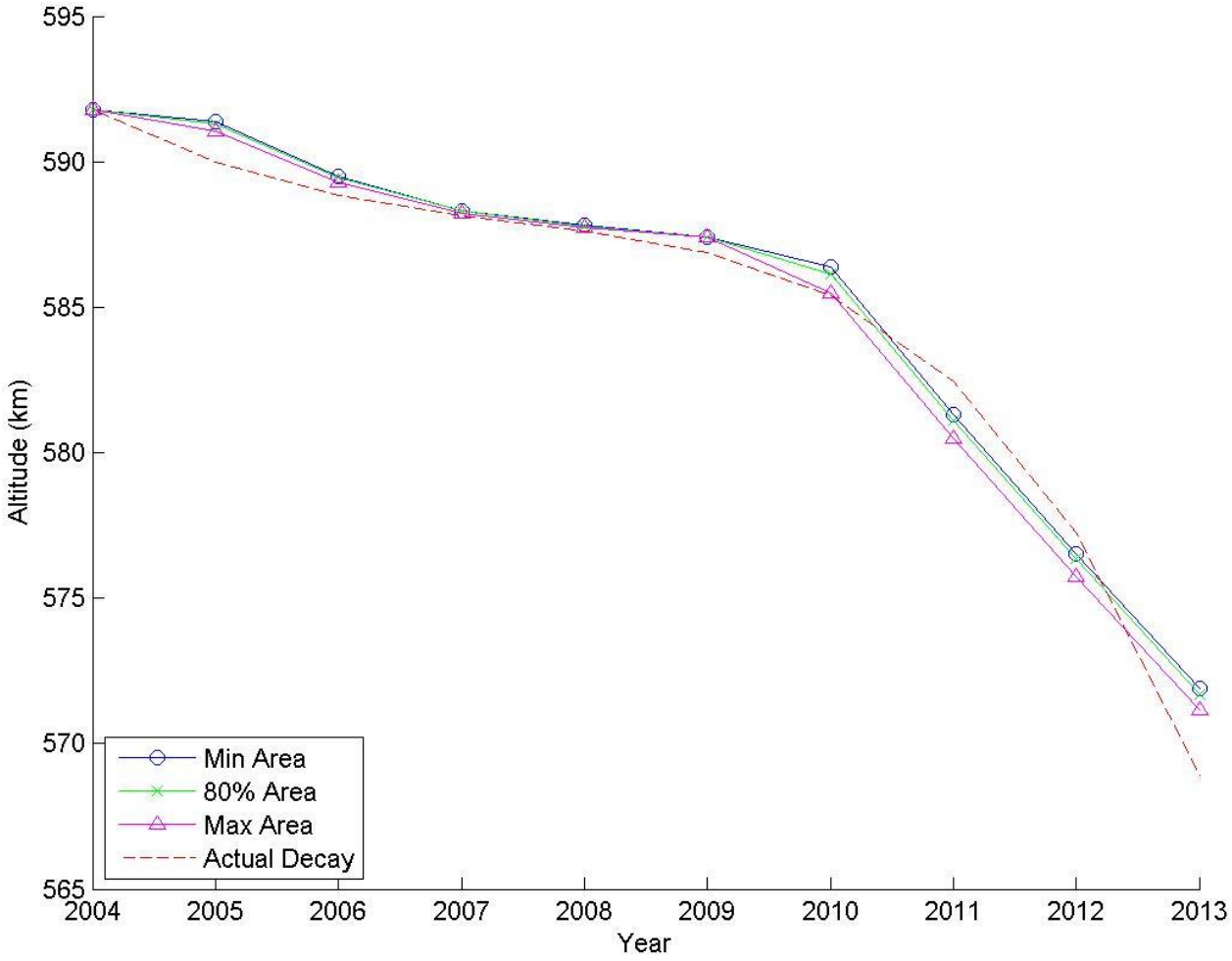

Figure 3.45. Orbit Decay $c_D = 2.2$, Calculated Data

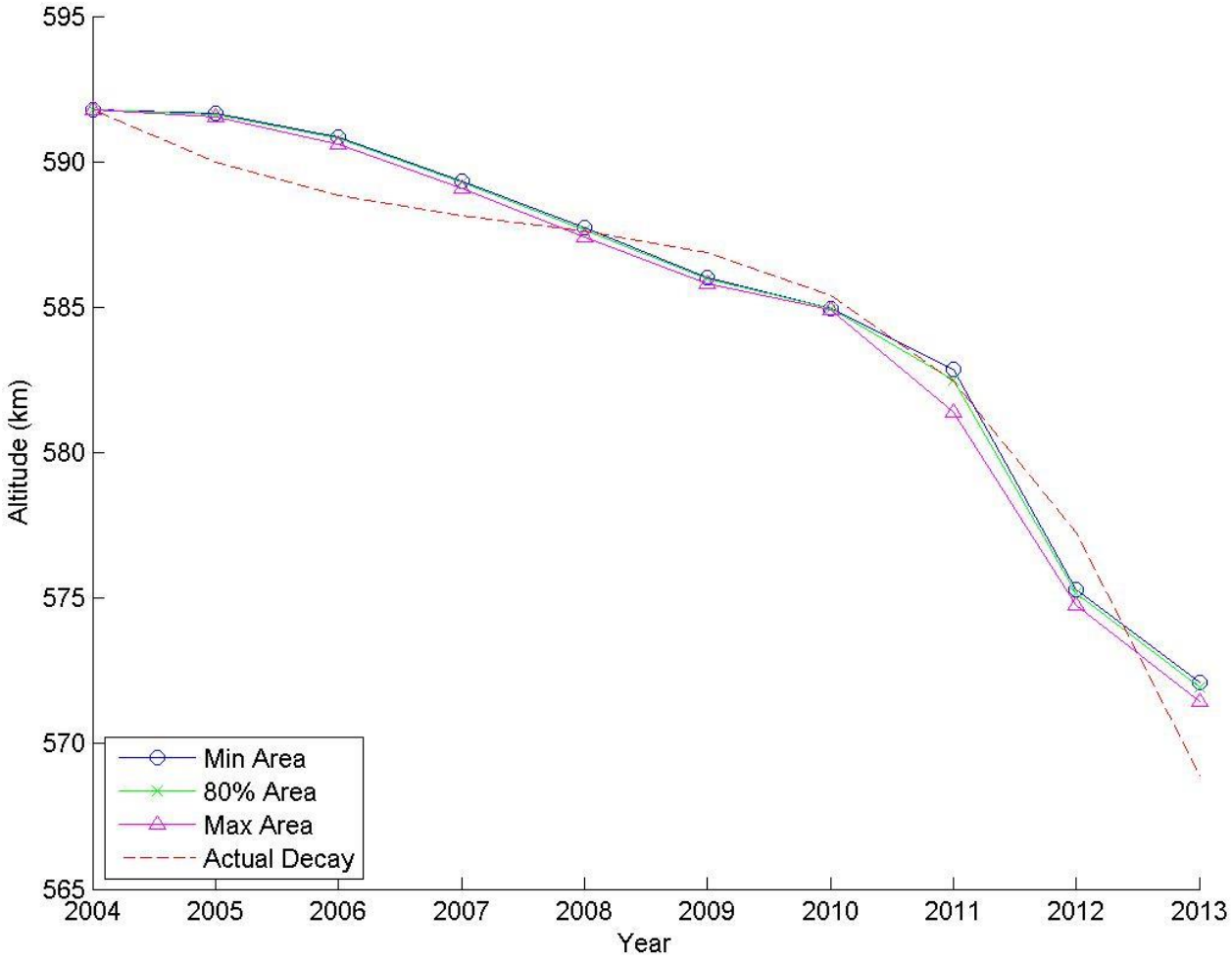

Figure 3.46. Orbit Decay $c_D = 2.2$, MSIS Data

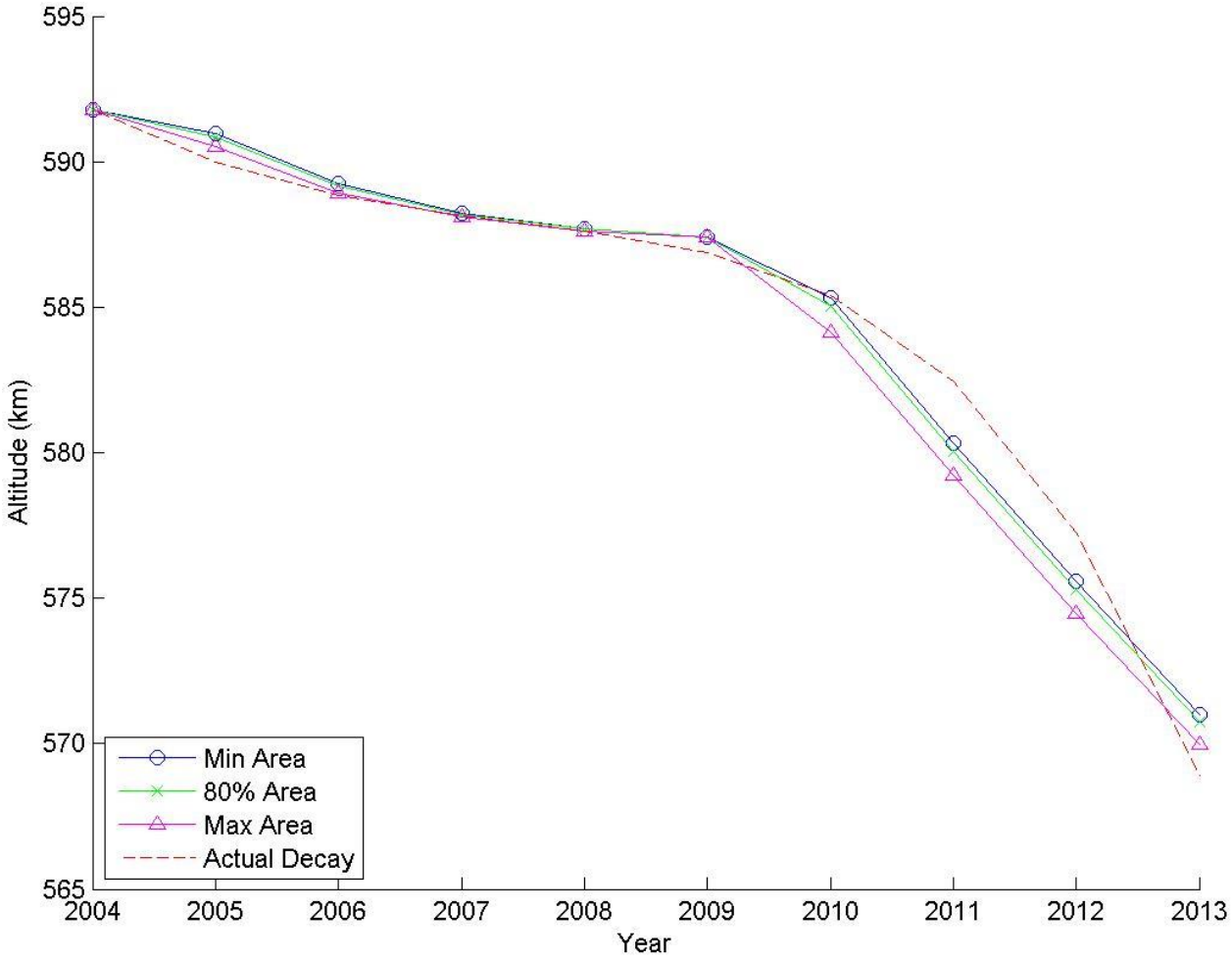

Figure 3.47. Orbit Decay $c_D = 3$, Calculated Data

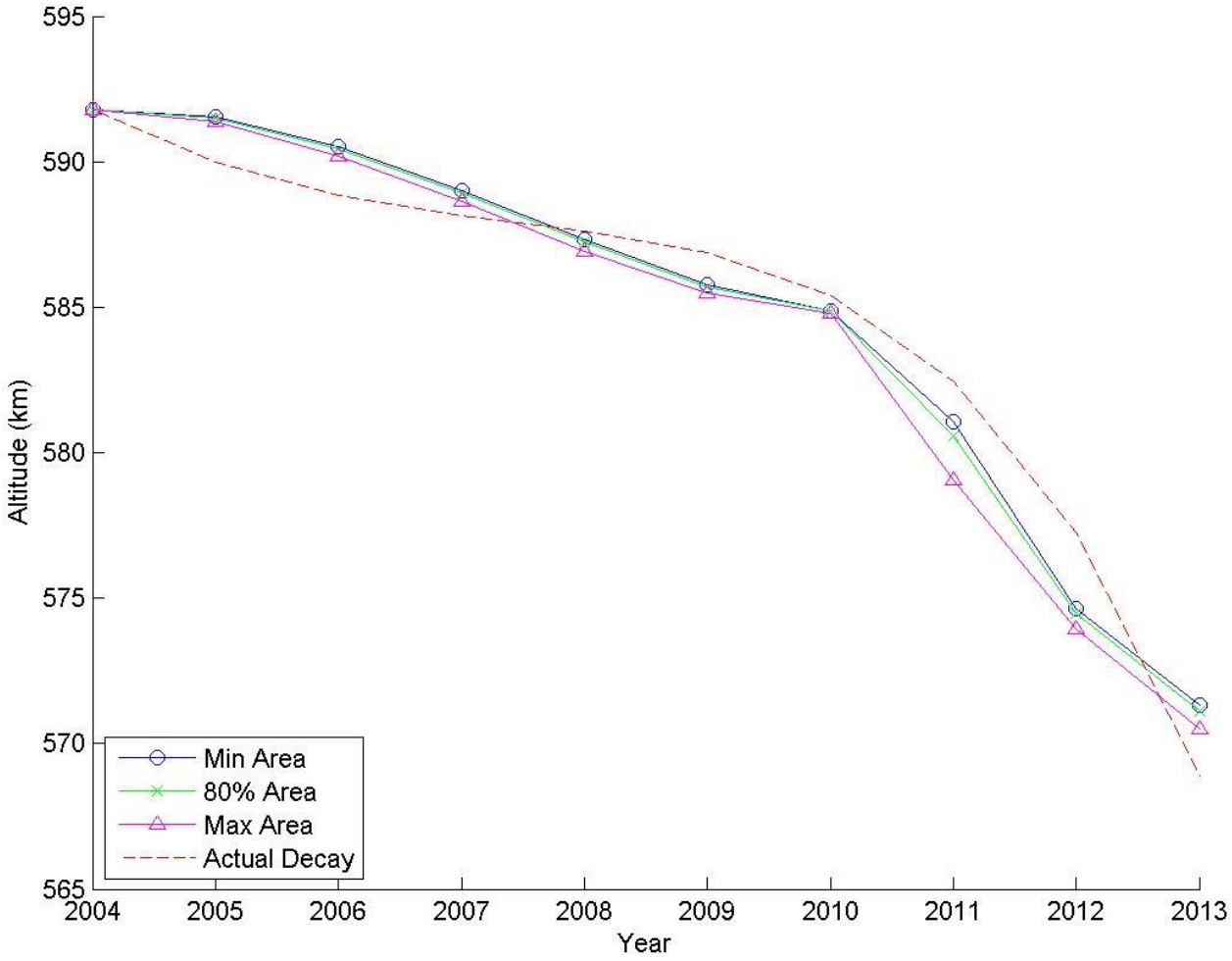

Figure 3.48. Orbit Decay $c_D = 3$, MSIS Data

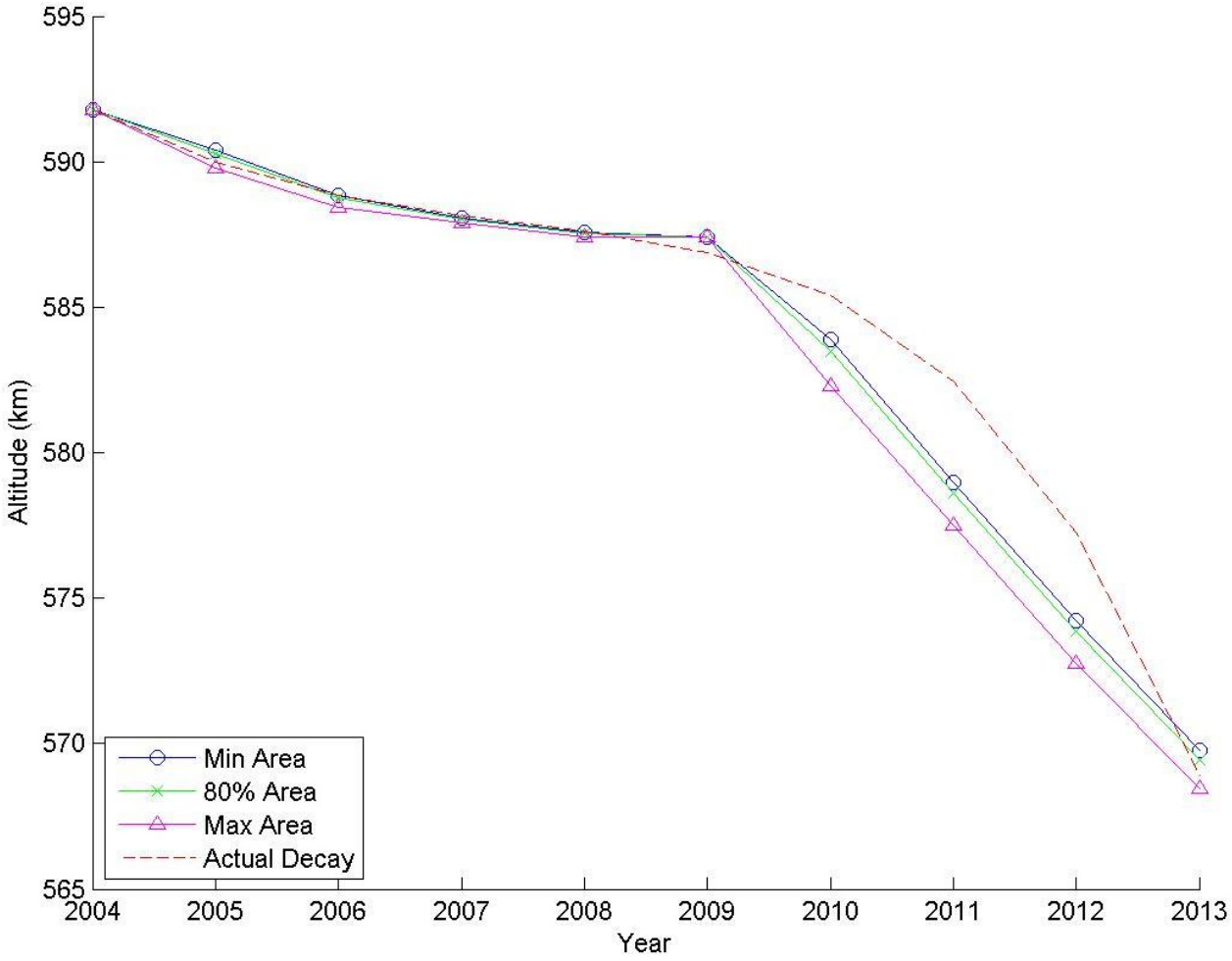

Figure 3.49. Orbit Decay $c_D = 4$, Calculated Data

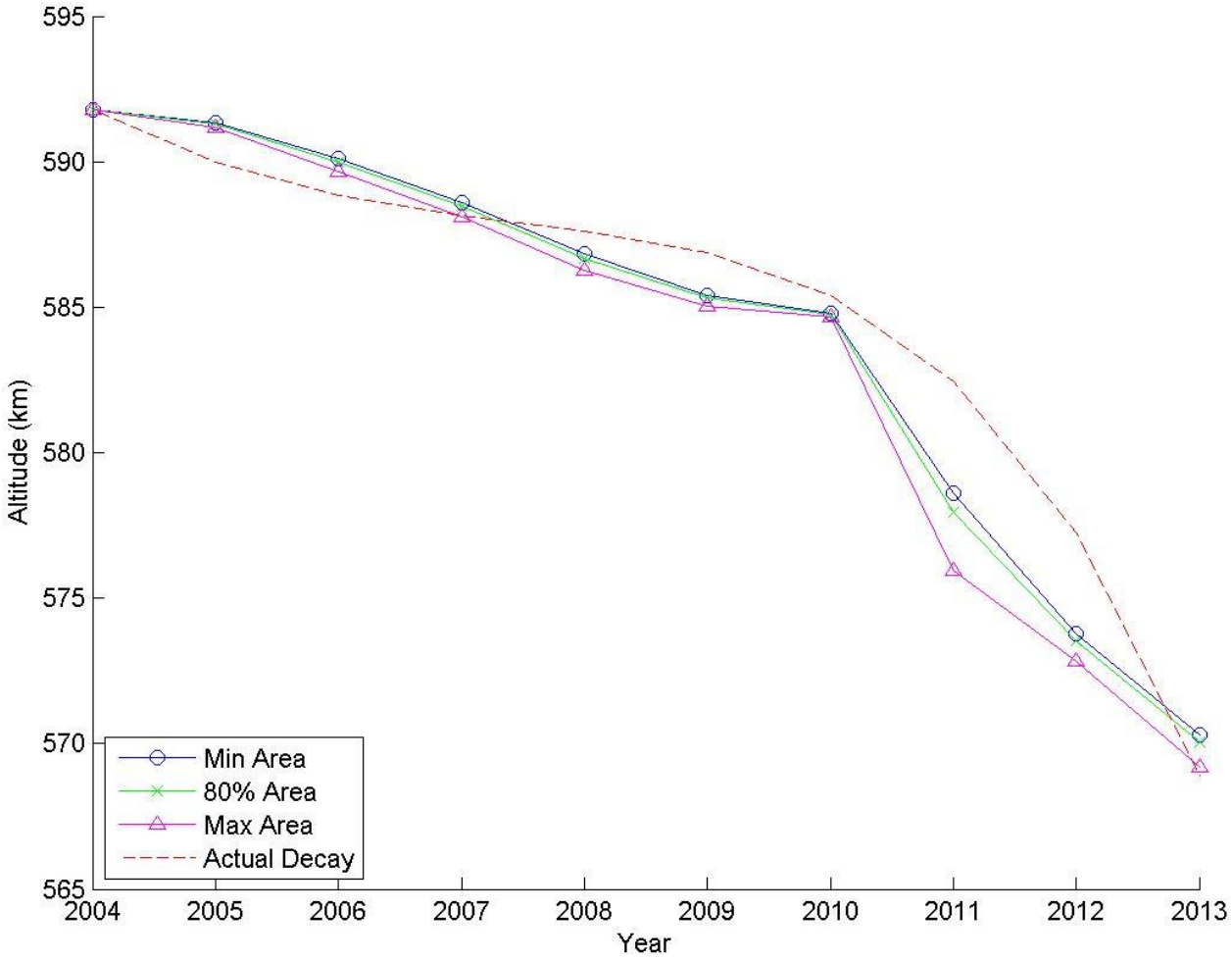

Figure 3.50. Orbit Decay $c_D = 4$, MSIS Data

No single model tracks the actual decay profile. This could imply several things, including the possibility that the coefficient of drag changes throughout the mission duration. Unfortunately, this would make predicting the day of deorbit of any spacecraft much more difficult. This uncertainty let to one final analysis being performed using strictly past altitude data and developing a fit equation. Because none of the above analyses decay as rapidly as the fourth-order fit developed for the curve shown in Figure 3.31, this fit is used as the earliest deorbit date, of approximately mid-2022 (200 km altitude) to early 2023 (120 km altitude). It is important to realize that the decay rate is highly dependent on the thickness of the atmosphere, which can vary greatly. These dates are to be considered "not earlier than" dates.

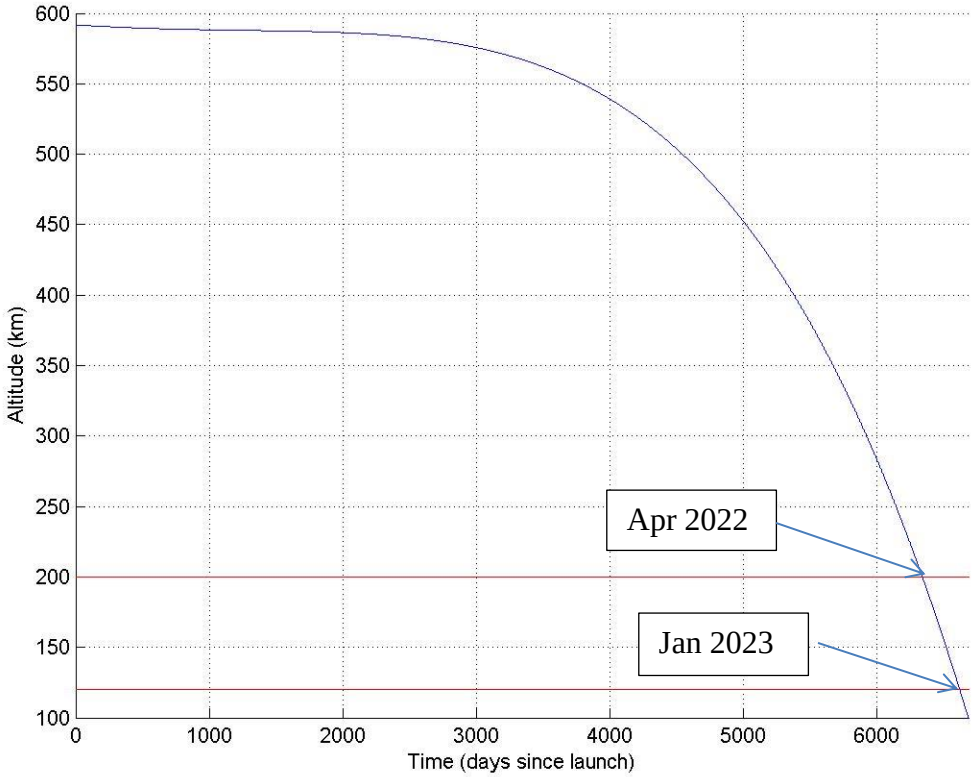

Figure 3.51. Expected Decay of *Swift*

3.5 Calculating the Coefficient of Drag

The previous sections discuss the individual elements required in order to begin calculating the coefficient of drag. The primary equation used for this calculation is Equation 2.9.

Figures 3.52 through 3.61 show the yearly mean and ±1 and ±3 standard deviations of the calculated coefficient of drag. The negative values of the coefficient of drag associated with the negative standard deviations are presented only to show the approximate confidence in the mean. The most important features are that, for 2004, the coefficient of drag is around 1, in years 2005–2010 it is much lower than that, and in years 2011–2013 it is in the more-expected range of 2–3. This directly implies that the assumption that the coefficient of drag is not a static value of 2.2, but can in fact vary over a mission's lifetime. It is important to note that during the middle of *Swift*'s mission duration, the coefficient of drag seems to stay close to 0. This is a curious result, as it was previously mentioned that the coefficient of drag is loosely bounded between 2 and 4. This may indicate that additional variables must be considered when determining the coefficient of drag for a spacecraft in this region of the atmosphere, or that the density value from the atmospheric density model is inaccurate.

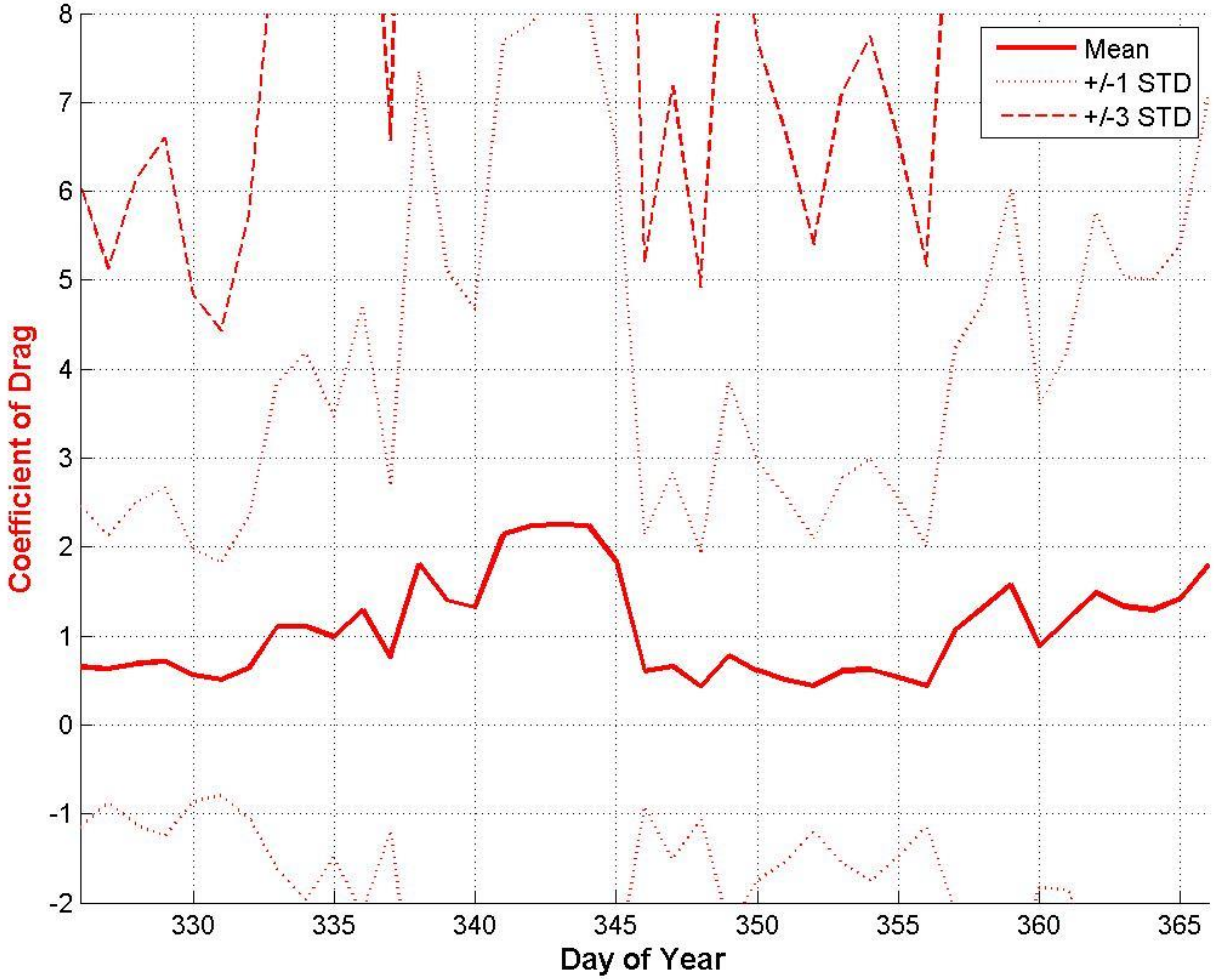

Figure 3.52. 2004 Mean Coefficient of Drag

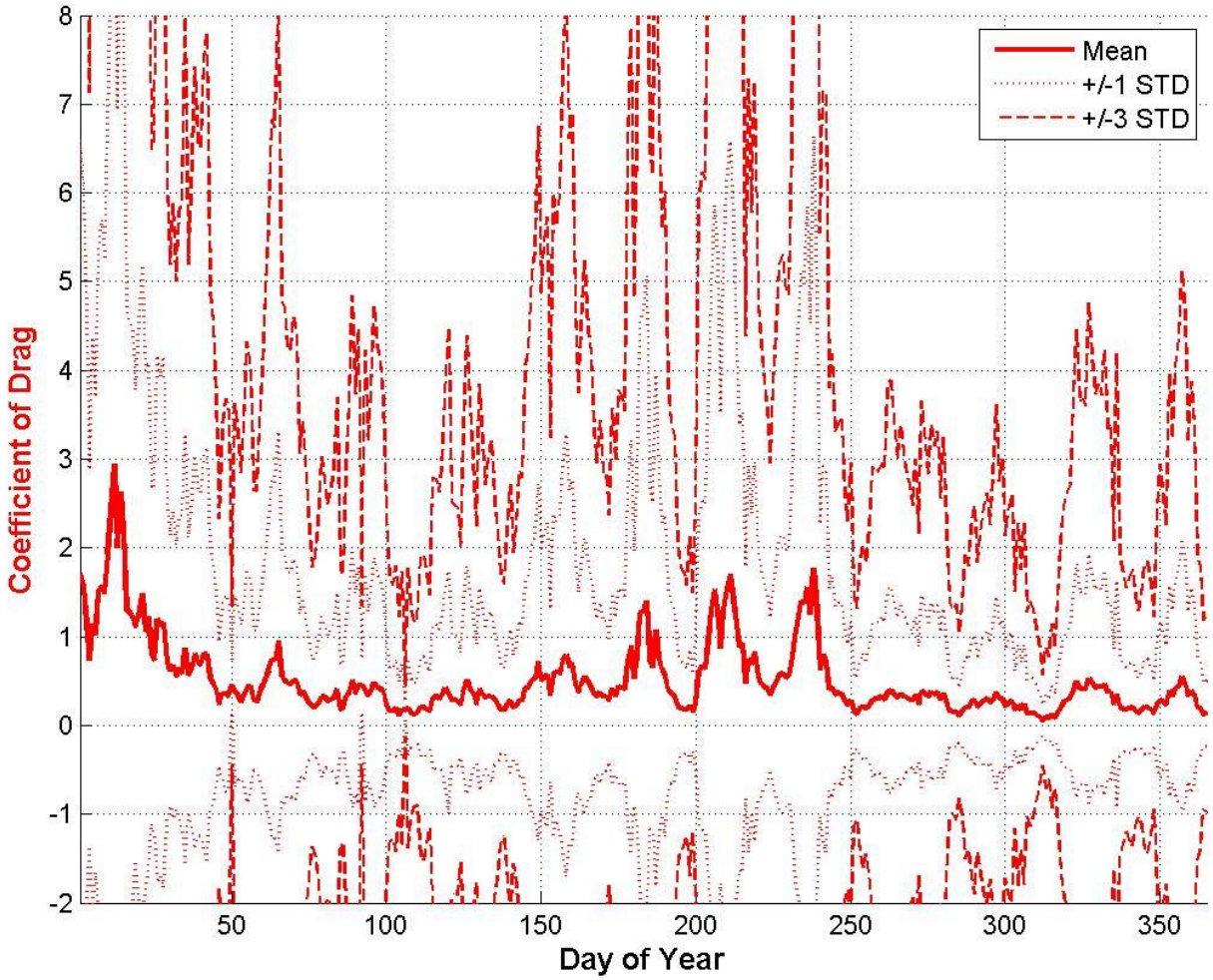

Figure 3.53. 2005 Mean Coefficient of Drag

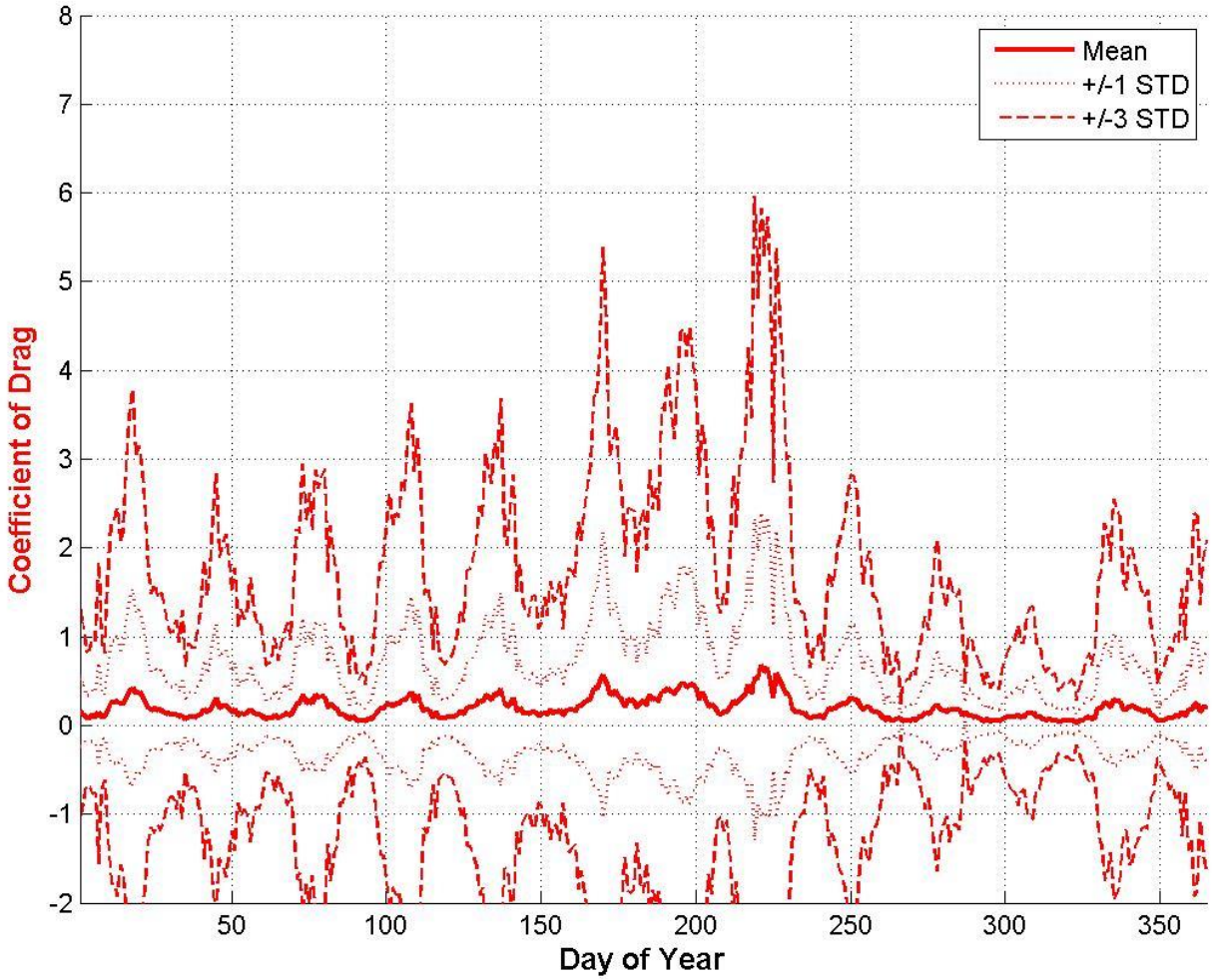

Figure 3.54. 2006 Mean Coefficient of Drag

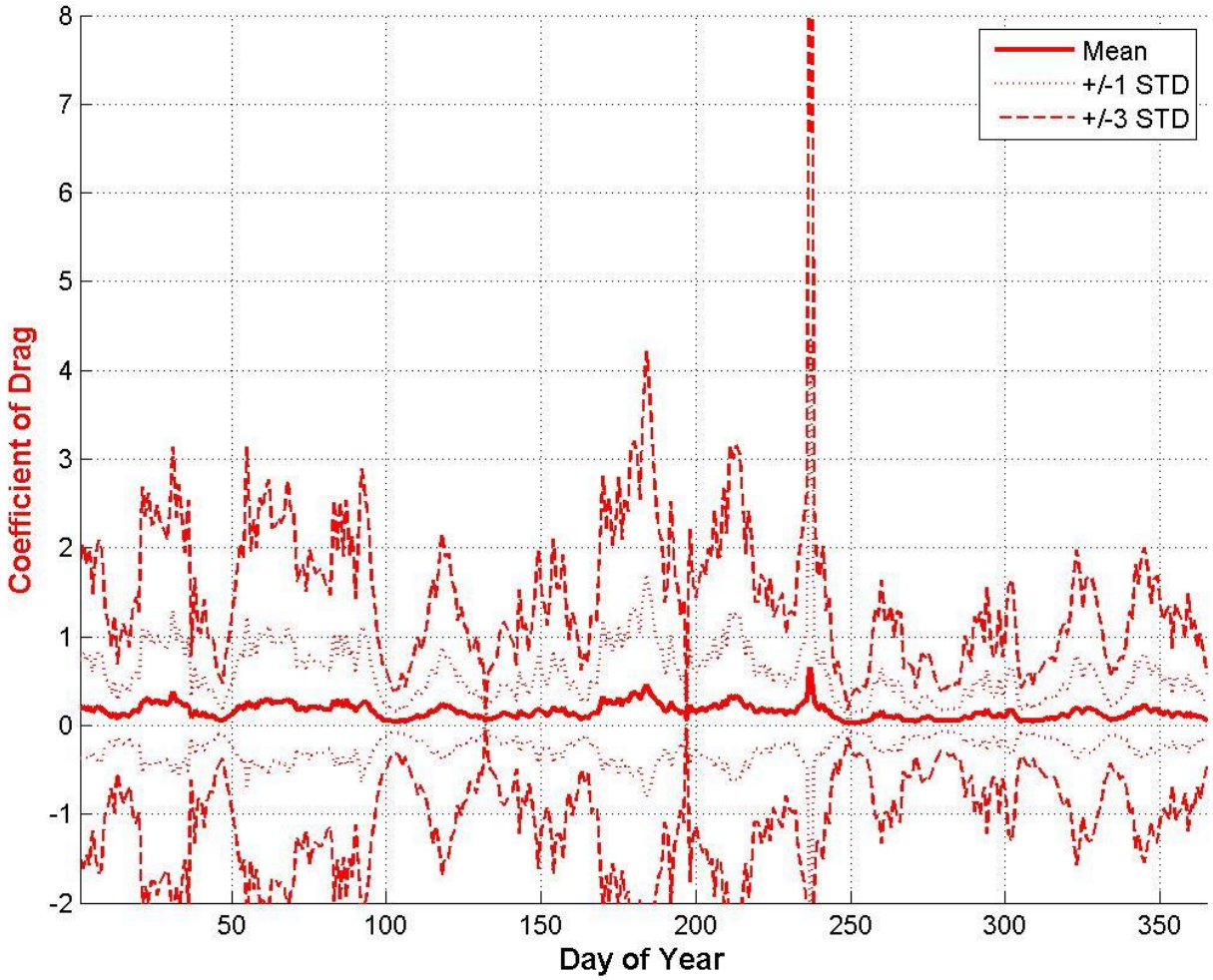

Figure 3.55. 2007 Mean Coefficient of Drag

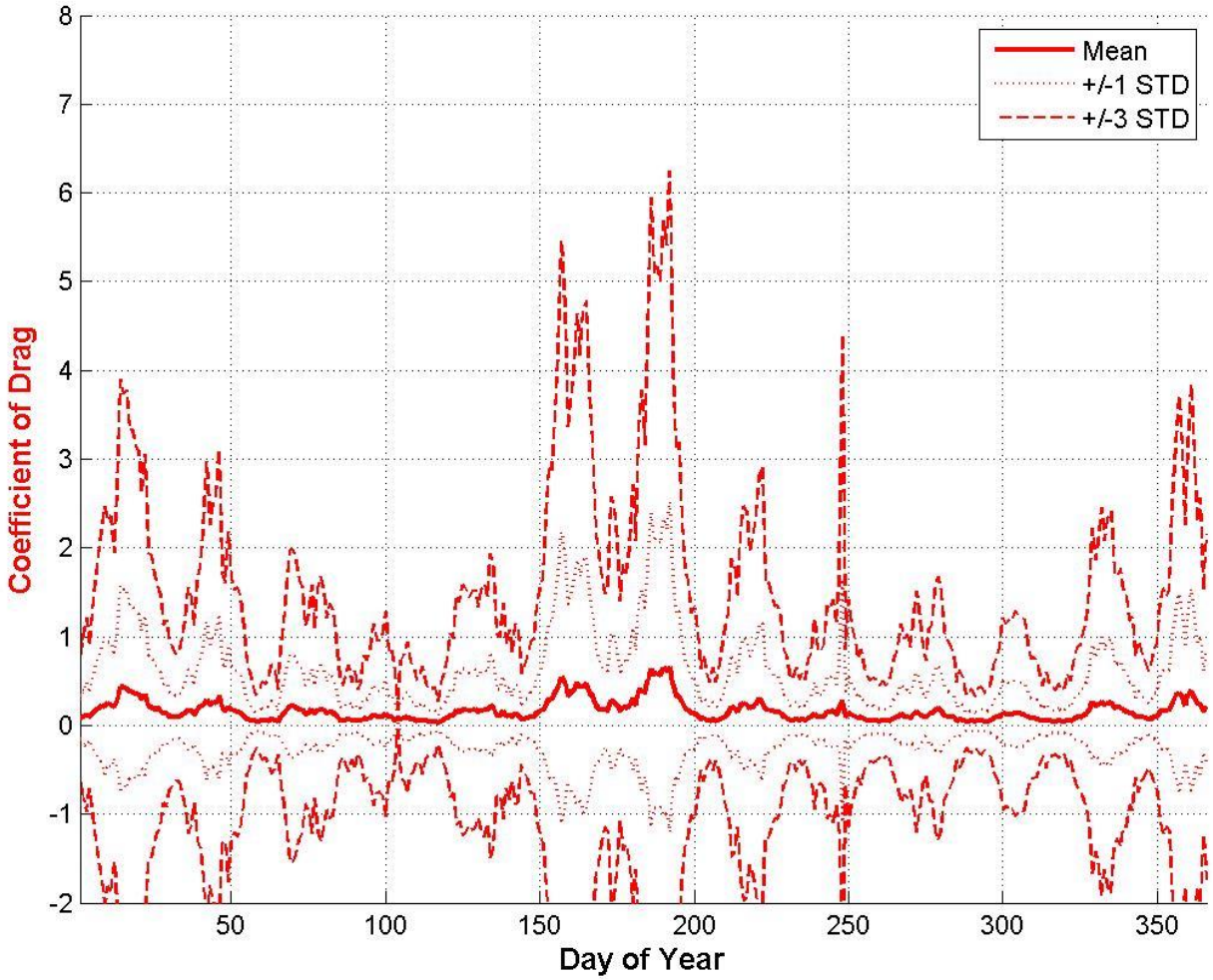

Figure 3.56. 2008 Mean Coefficient of Drag

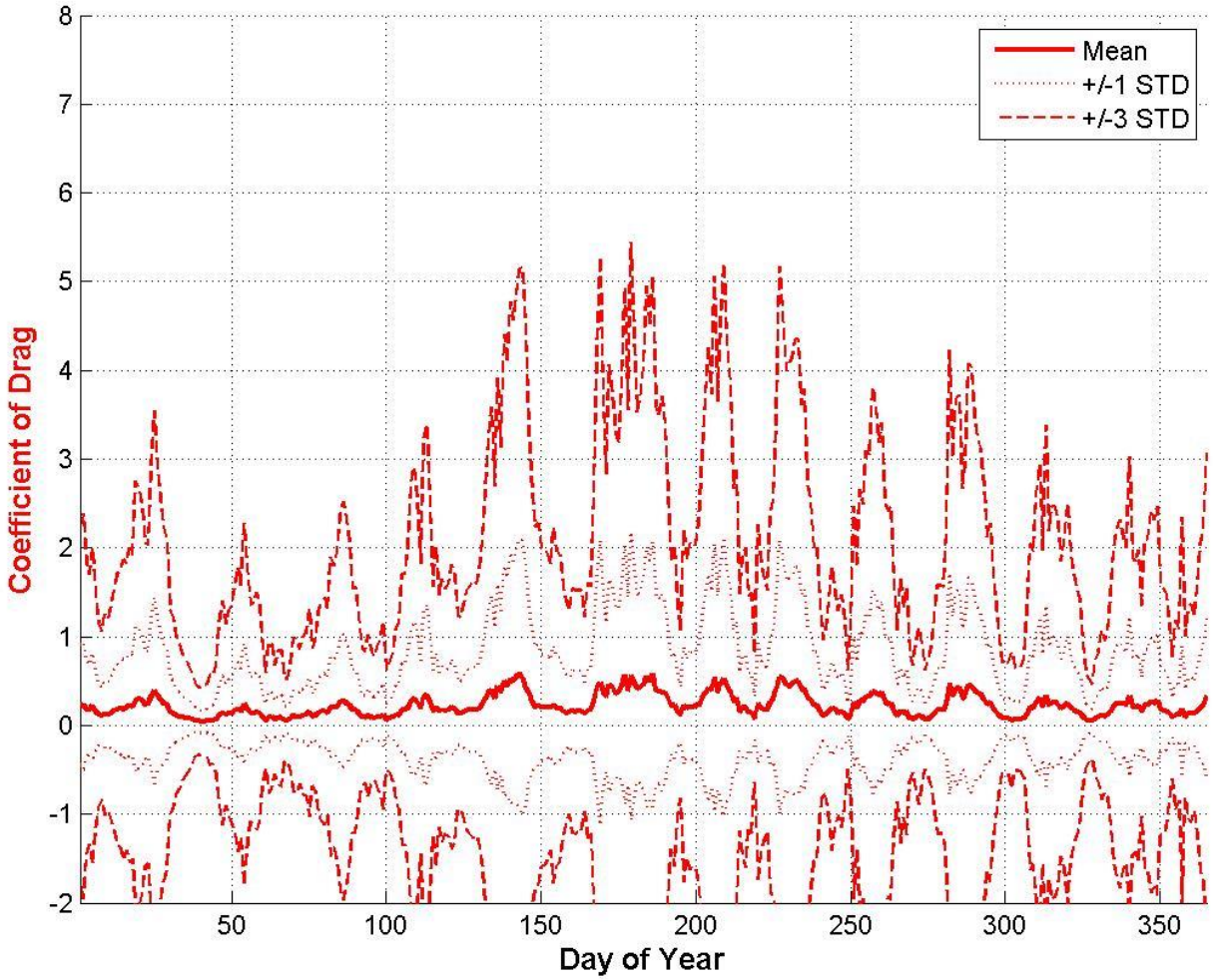

Figure 3.57. 2009 Mean Coefficient of Drag

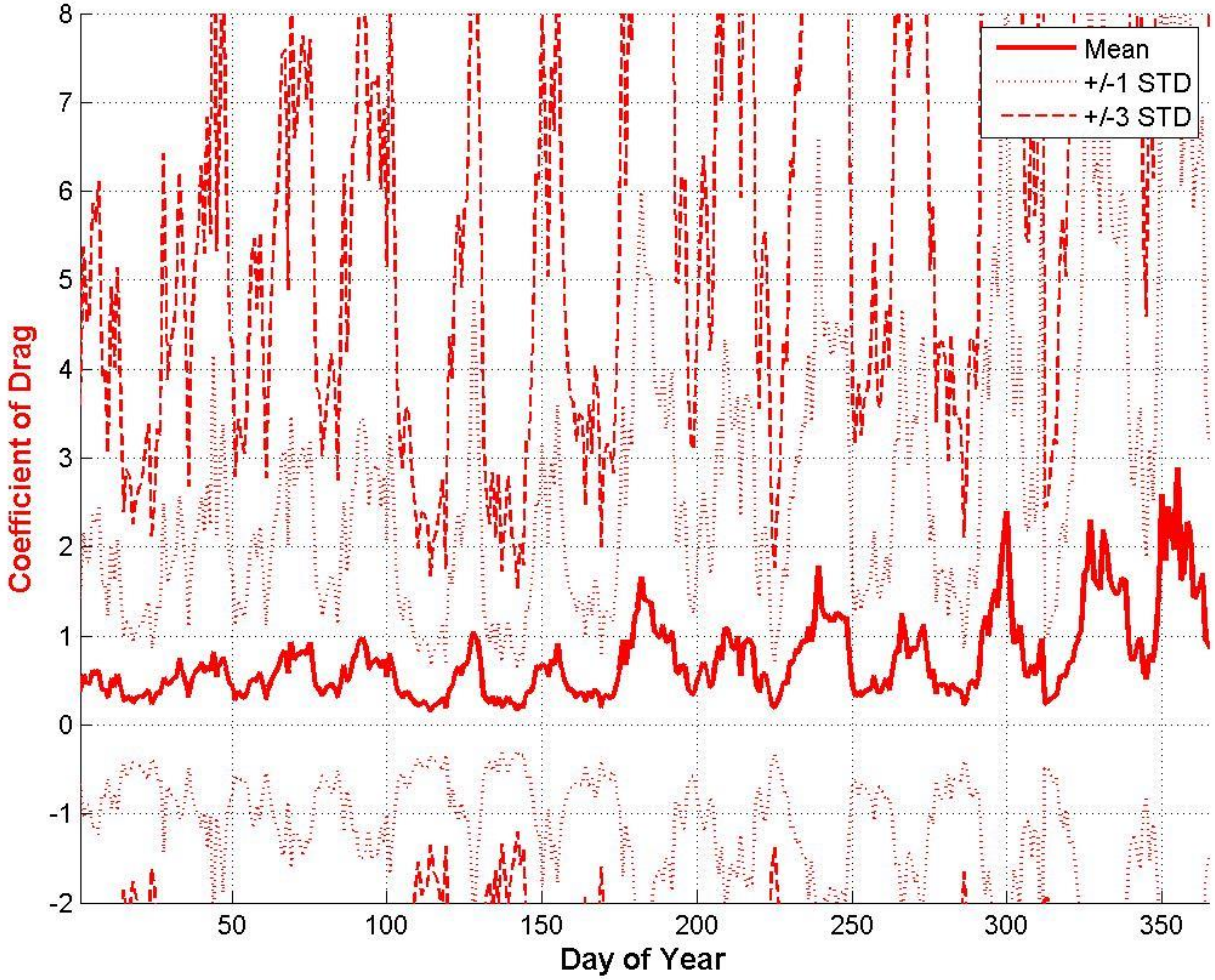

Figure 3.58. 2010 Mean Coefficient of Drag

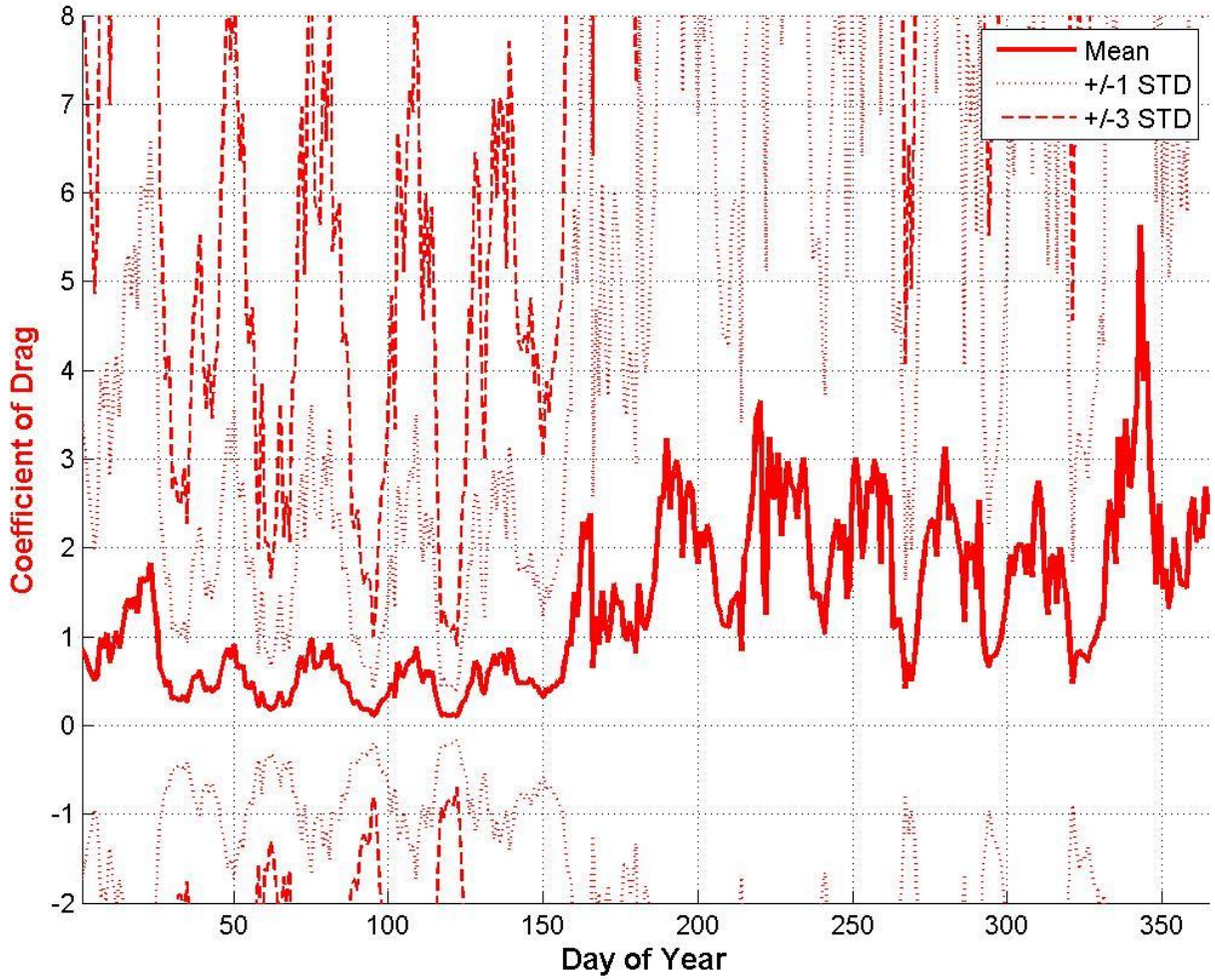

Figure 3.59. 2011 Mean Coefficient of Drag

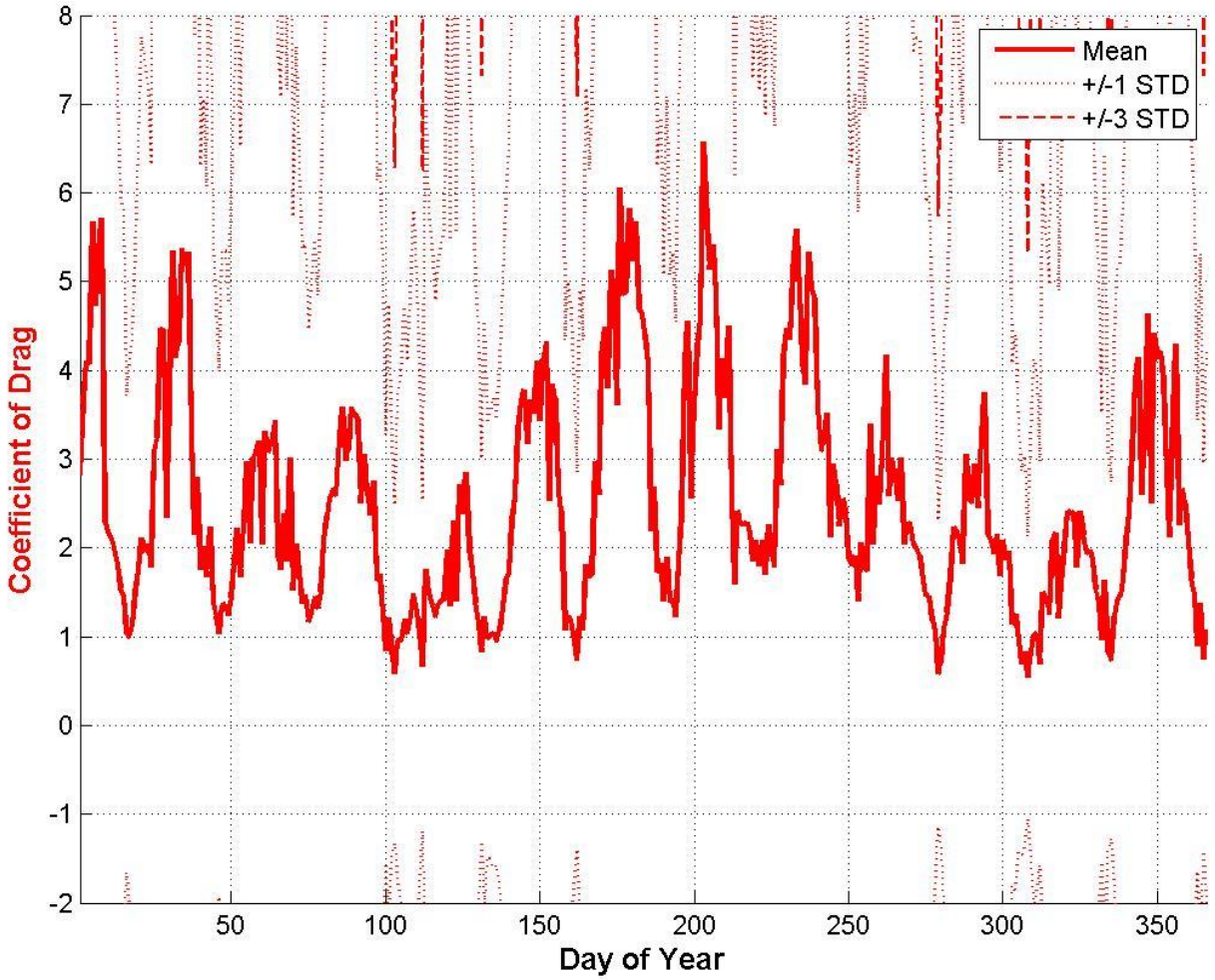

Figure 3.60. 2012 Mean Coefficient of Drag

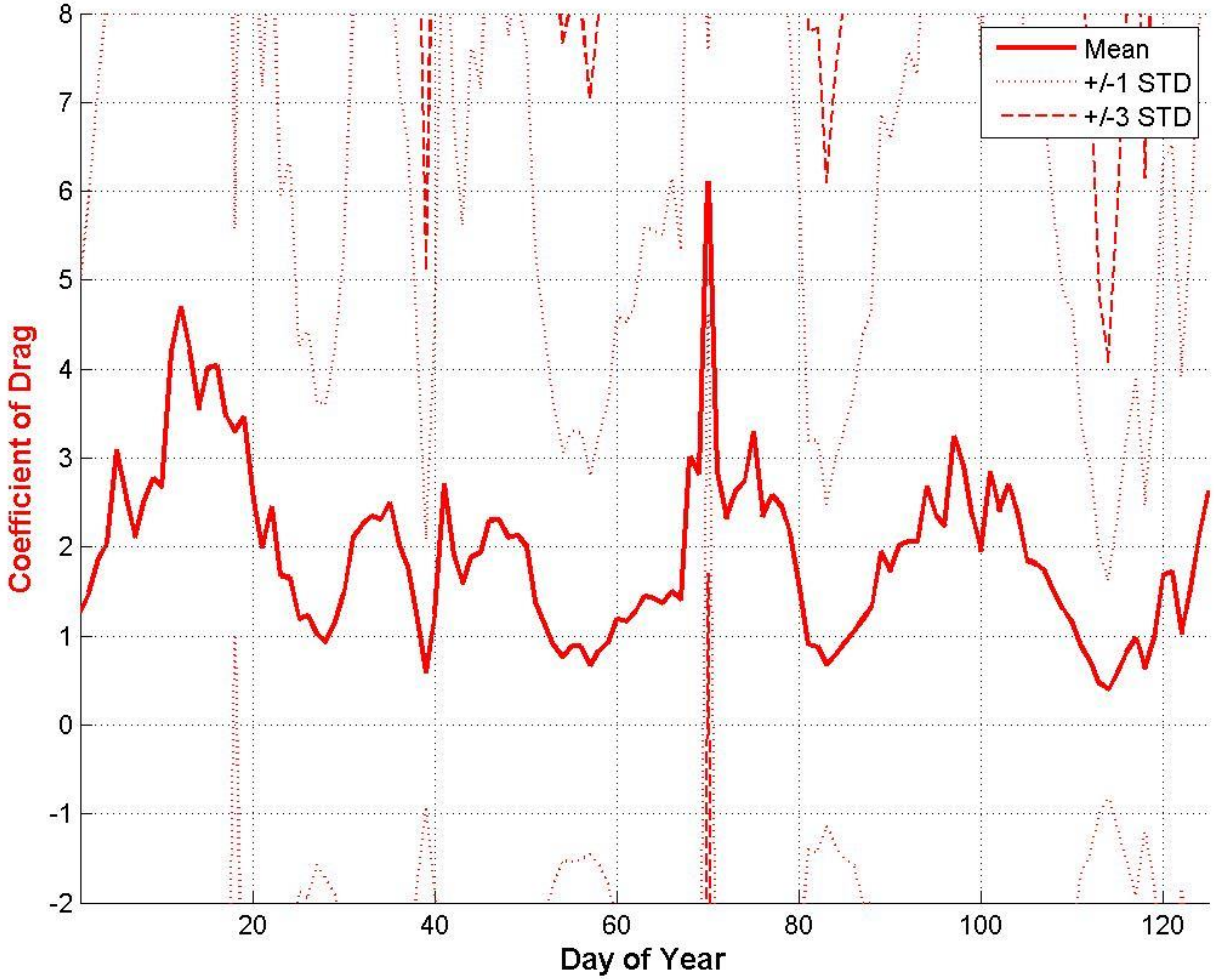

Figure 3.61. 2013 Mean Coefficient of Drag

Chapter 4

4.1 Conclusions

This research set out to accomplish four goals, including generating a functional area determination algorithm that accurately predicts the cross-sectional area of NASA's *Swift* spacecraft in any orientation; developing a method to incorporate state-of-health data including attitude and altitude measurements into a drag analysis; predicting the orbital lifetime of *Swift*; and discussing the validity of current assumptions regarding the coefficient of drag.

The algorithm to accurately predict the operating area of *Swift* was generated and provided results implying that the spacecraft typically orients itself with approximately 75–80% of the maximum operating area. The operating area is understood to be the center body of *Swift* with a minute-based average of the independently-maneuvering solar arrays. Figure 4.1 shows the mission duration normalized area of *Swift*, which is simply a combination of the yearly results in Figures 3.3 through 3.12.

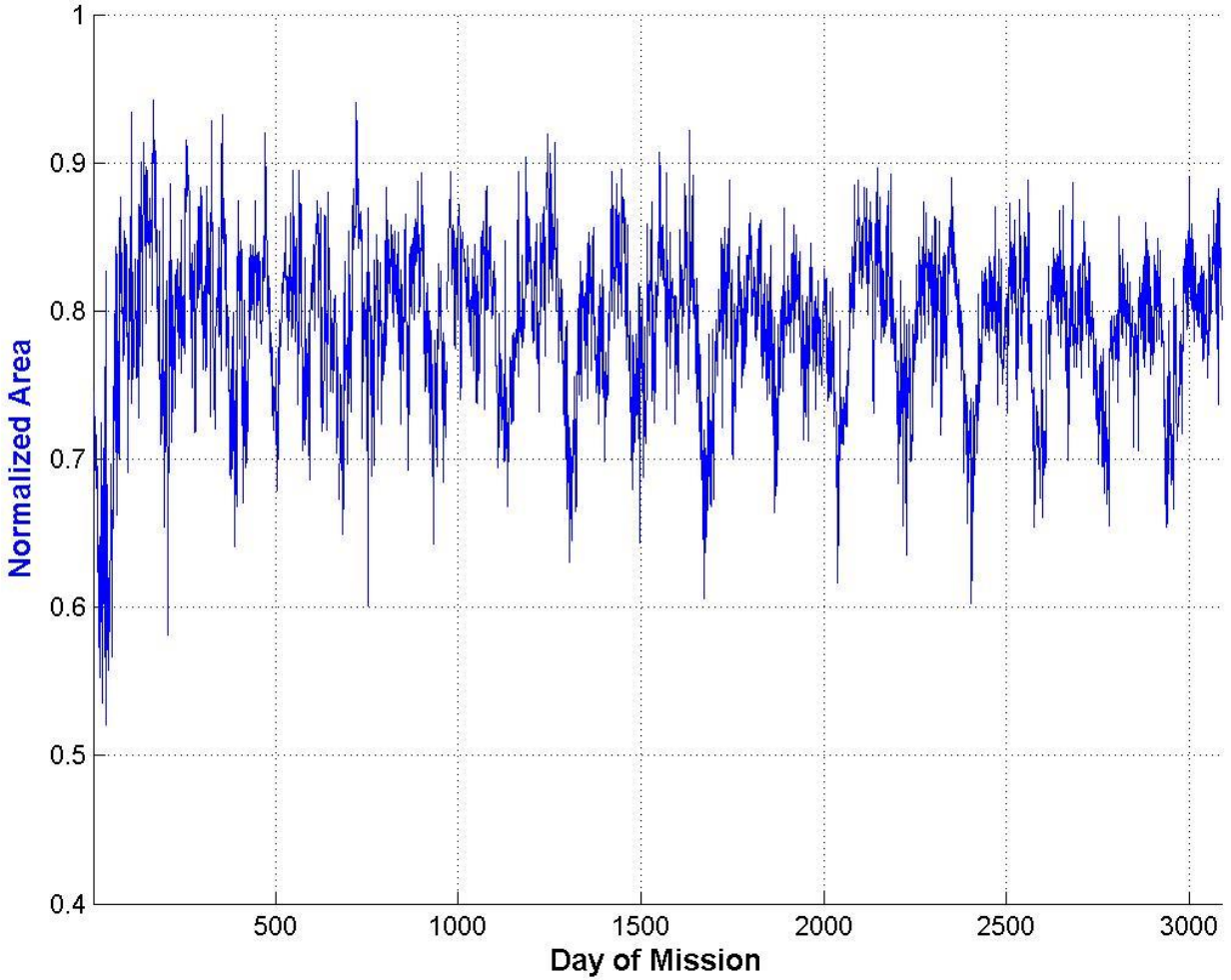

Figure 4.1. Mission Duration Normalized Area

A method to integrate the attitude and altitude measurements gathered by *Swift* became the core of this analysis. This provided actual data for use instead of simulated data. *Swift* was an excellent candidate for this research due to the depth of its accumulated data and simplified model qualities. As previously presented in Figures 1.1 and 3.33 through 3.42, *Swift* has lost 12 km in the last nine years. This leads to an obvious next step of determining when *Swift* will deorbit.

Predicting the lifetime of *Swift* produced some interesting results. Different densities, coefficients of drag, and cross-sectional areas were used and compared to the actual decay. No single model accurately followed the true decay. An earliest expected deorbit date was determined to be mid-2022 for 200 km in altitude and early 2023 for 120 km in altitude. One possible explanation for this is because the internally calculated densities and the densities gathered from the NRLMSISE-00 model differ greatly. Figures 4.2 and 4.3 show the values of each used throughout *Swift*'s mission as well as the error between the two, again, as simple combinations of the yearly data presented in Figures 3.13 through 3.32. These results are far more accurate during the periods of solar maximum as opposed to solar minimum, and may point to a flaw in NRLMSISE-00. It may also be possible, however, that the problem is not in the atmospheric model, but rather in the assumptions surrounding the coefficient of drag.

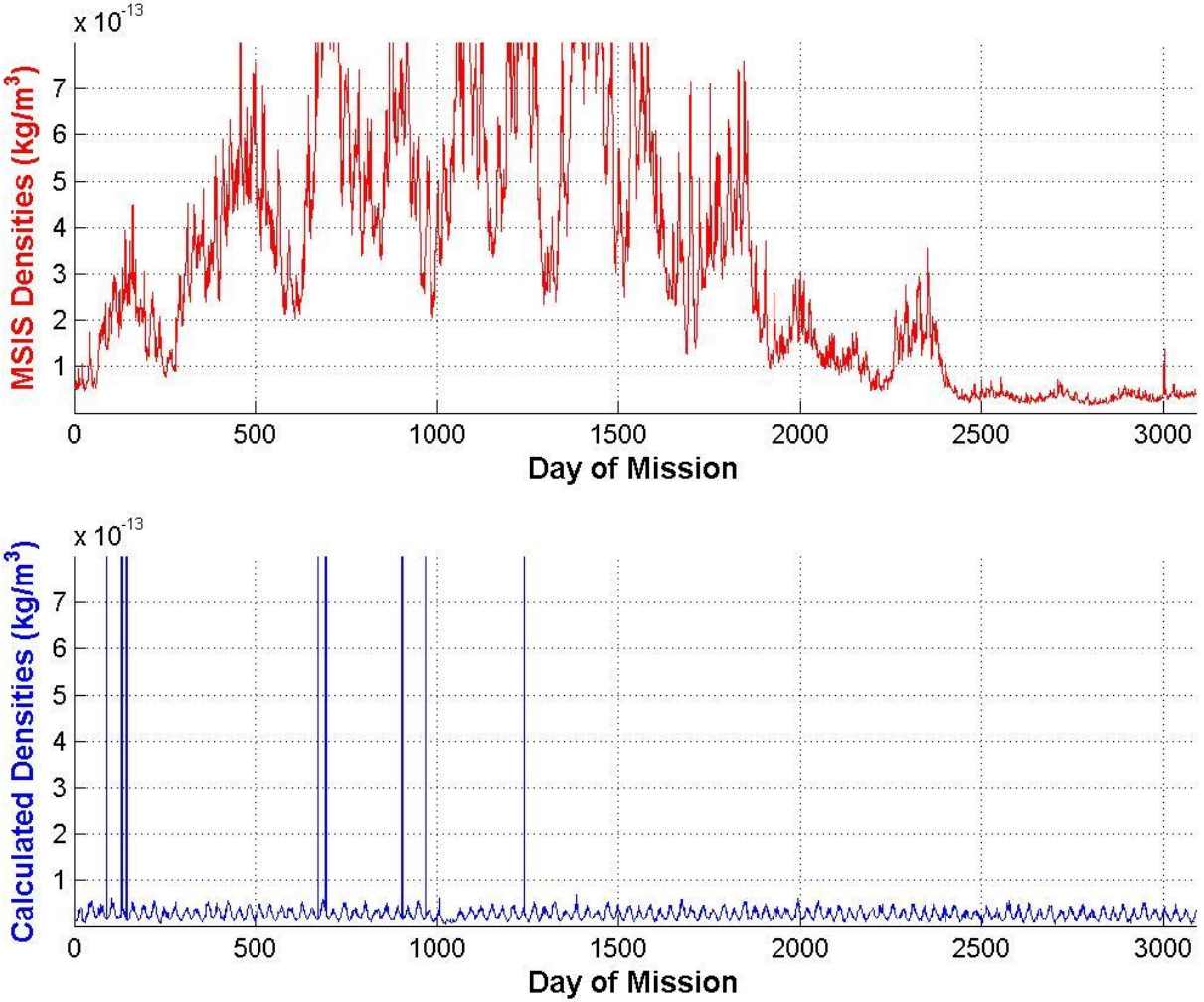

Figure 4.2. Mission Duration Calculated and MSIS Densities

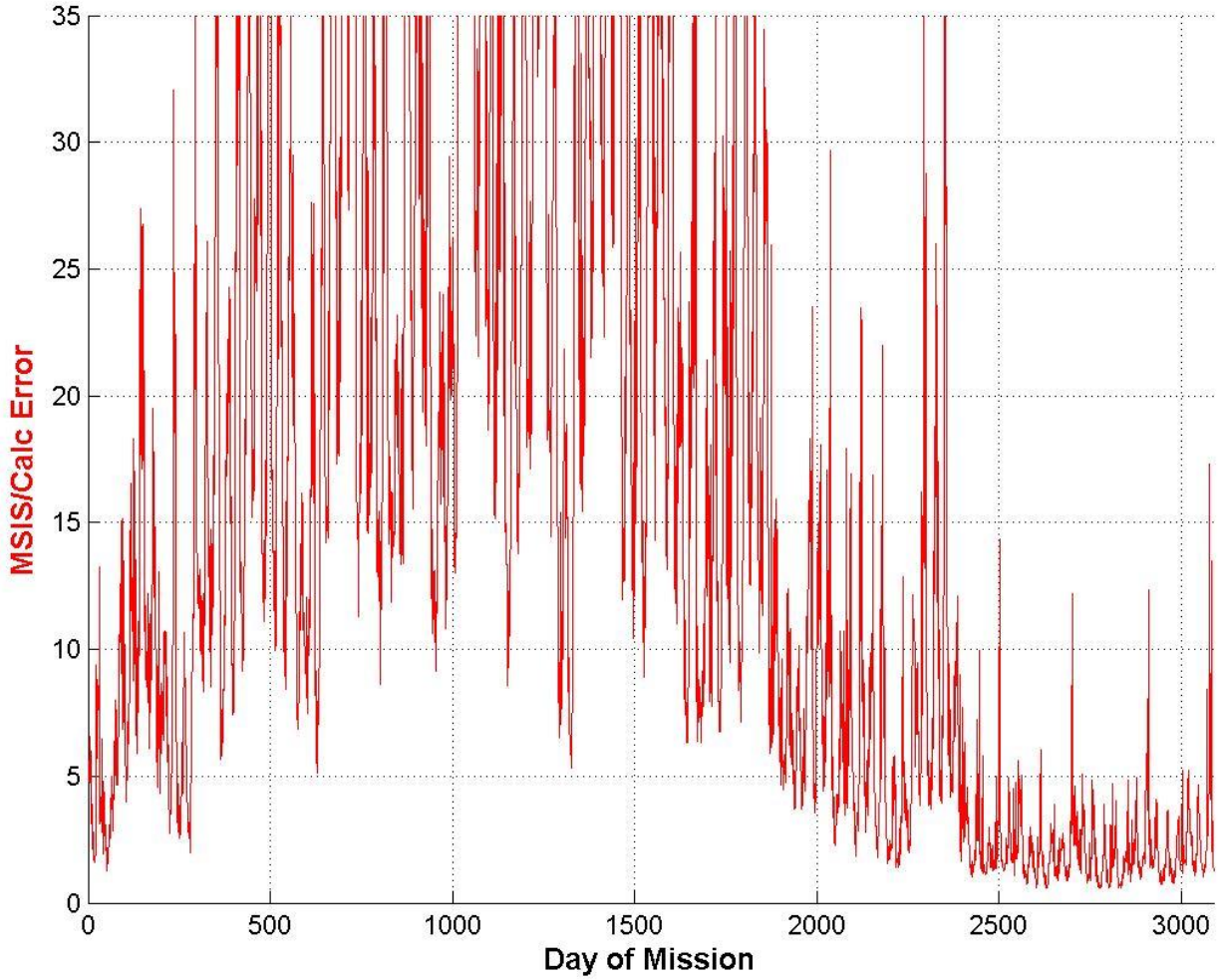

Figure 4.3. Mission Duration Density Error

The coefficient of drag was directly calculated as the focus of this research. Figure 4.4 shows the results of these calculations over the mission duration of *Swift* as a combination of the yearly calculations presented in Figures 3.52 through 3.61. It clearly shows that the assumption of a static value for the coefficient of drag deserves another look. There exists the possibility that the coefficient of drag may be more strongly tied to another factor, but that requires additional research.

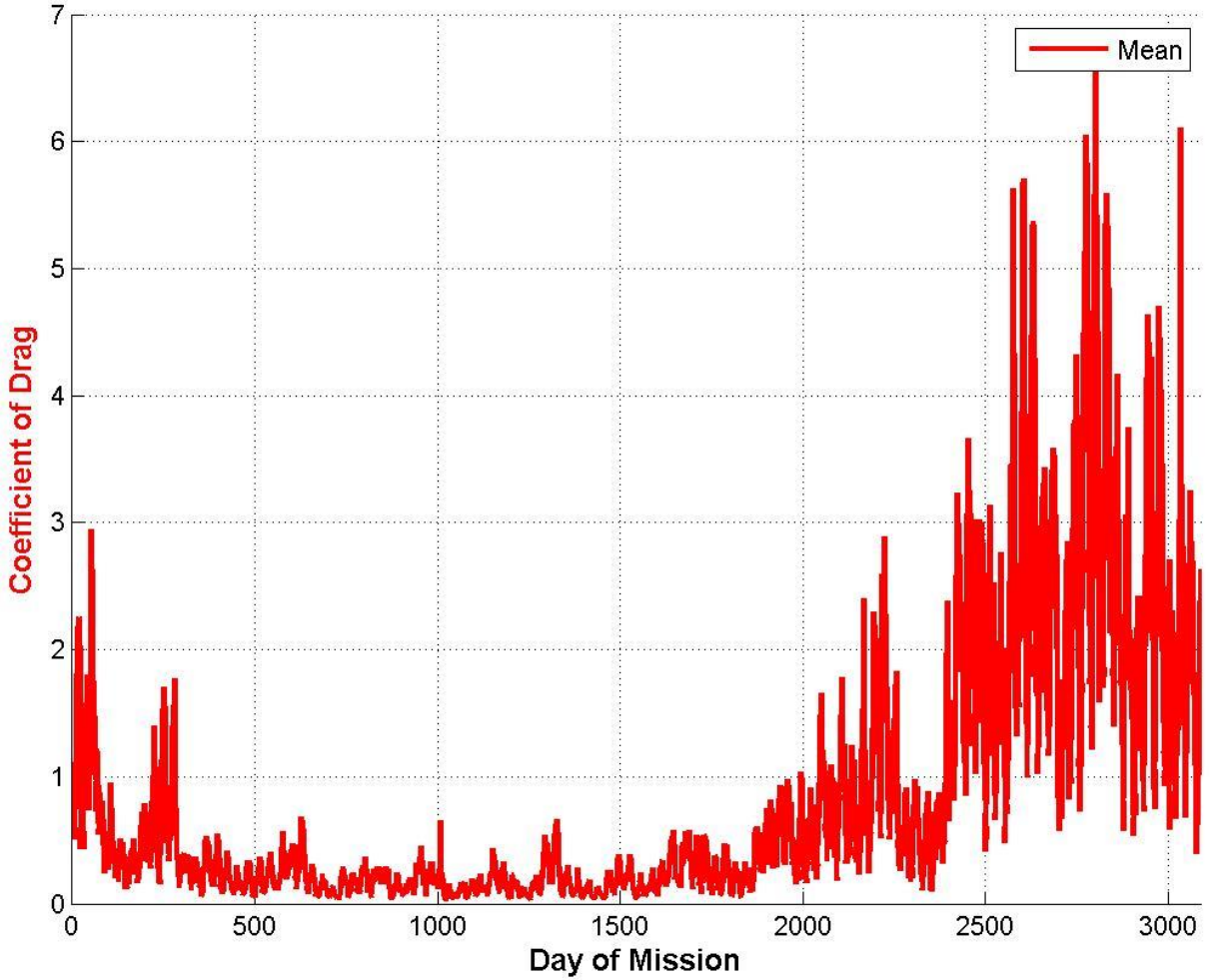

Figure 4.4. Mission Duration Coefficient of Drag

4.2 Future Work

Future applications of this research include extending the analysis to additional missions in similar orbits to see if the results are similar. In order to make this a viable possibility, portions of the software written for this research must be reworked to accommodate information from a spacecraft other than *Swift*. These include the area determination and mass definition portions.

Additionally, several other atmospheric models should be incorporated to give more options as to what is correct according to past data. Software that includes the Jacchia 71 atmospheric model and automated the gathering of the NRLMSISE-00 atmospheric density data was generated but never tested due to the October 2013 government shutdown that occurred during this phase of the research.

An extra layer of fidelity when determining the atmospheric density is also under development. The NRLMSISE-00 atmospheric model was fed limited data due to the way it was incorporated into the analysis, but additional data regarding solar flux, geomagnetic data, and accurate longitude were being worked into the analysis when the government shutdown caused the furlough of the webservers, so this portion is unfinished.

Additionally, a "live" method should be generated that can perform an update to the analysis on a daily or weekly basis. These results should be fed into easy-to-read plots so that the engineers on the *Swift* FOT and any other missions are apprised of when their spacecraft will deorbit. This method can then potentially be used to manage the decay of a spacecraft whether to speed up the decay or slow it down.

Finally, to further research into this realm, Figure 4.5 places the coefficient of drag and the solar F10.7cm radio flux on the same plot. This portion presents a strong correlation but does not explain all variations, implying that there are errors in both the density model and the calculation of the coefficient of drag, but it is unknown how much to assign to each

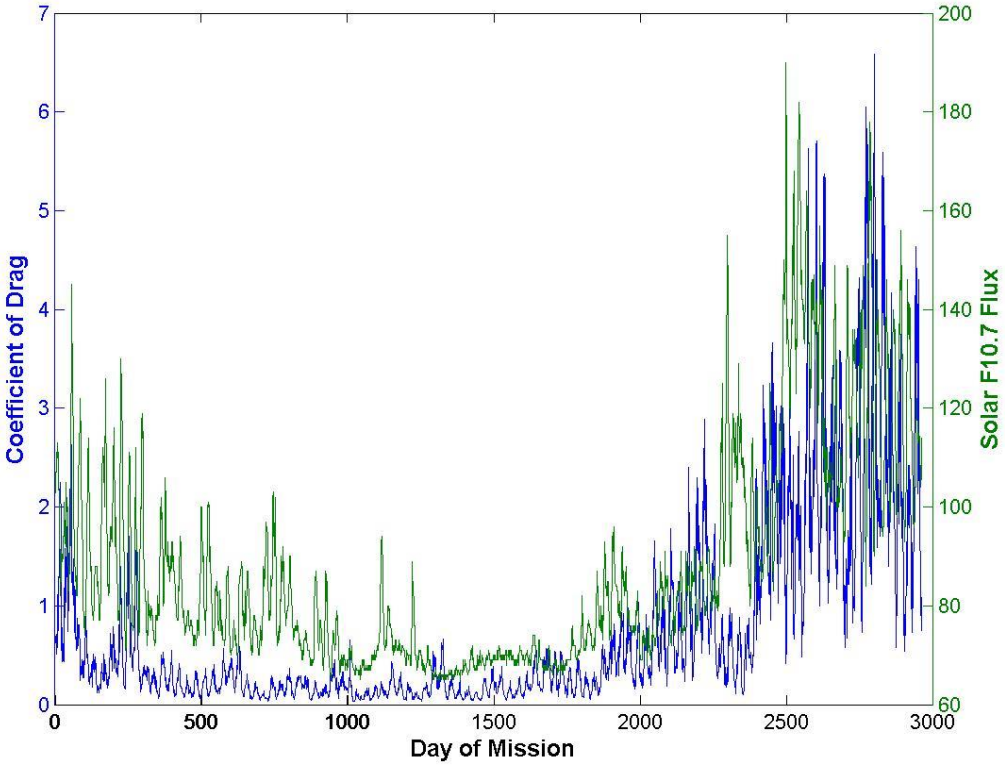

Figure 4.5. Coefficient of Drag versus F10.7 Solar Flux

References

Bird, G. 1994. "Molecular gas dynamics and the direct simulation of gas flows." Oxford Engineering Science 42. Clarenden Press, Oxford.

Chao, C., Gunning, G., Moe, K., Chastain, S., Settecerri, T., 1997. "An evaluation of Jacchia 71 and MSIS 90 atmosphere models with NASA ODERACS decay data." J. Astronaut. Sci. 45, 131–141.

Cook, G. 1965. "Satellite drag coefficients." Planet. Space Sci. 13, 929–946.

Cook, G. 1966. "Drag coefficients of spherical satellites." Ann. Geophys. 22, 53–64.

Curtis, H. 2010. Orbital Mechanics for Engineering Students Second Edition. Elsevier, Burlington, MA.

Gaposchkin, E. 1994. "Calculation of Satellite Drag Coefficients." Technical Report 998. MIT Lincoln Laboratory, MA.

Goodman, F., Wuchman, W. 1976. Dynamics of Gas-Surface Stuttering. Academic Press, New York.

Groÿekatthöfer, K., Yoon, Z. 2012. "Introduction into quaternions for spacecraft attitude representation." Technical University of Berlin.

Hedin, A. 1987. "MSIS-86 Thermospheric Model. Journal of Geophysical Research." 92:A5, 4649–4662.

Legendre, P., Deguine, B., Garmier, R., Revelin, B. 2006. "Two Line Element Accuracy Assessment Based on a Mixture of Gaussian Laws." AIAA 2006-6518.

Moe, K., Moe, M. 2005. "Gas–surface interactions and satellite drag coefficients." J. Planetary and Space Science 53 (2005) 793-801.

Pardini, C., Anselmo, L. 2001. "Comparison and accuracy assessment of semi-empirical atmosphere models through the orbital decay of spherical satellites." J. Astronaut. Sci. 49, 255–268.

Picone, J., Hedin, A., Drob, D., Aikin, A. 2002. "NRLMSISE-00 empirical model of the atmosphere: Statistical comparisons and scientific issues." J. Geophys. Res. 107 (A12).

Saltsburg, H., Smith, Jr., J., Rogers, M. 1967. "Fundamentals of Gas–Surface Interactions." Passim. Academic, New York.

Trilling, L. 1967. “Theory of gas–surface collisions.” Fundamentals of Gas–Surface Interactions. Academic Press, NY and London, pp. 392–421.

Vallado, D. 2007. Fundamentals of Astrodynamics and Applications Third Edition. Microcosm, Hawthorne, CA.

Vallado, D., Finkleman, D. 2013. “A Critical Assessment of Satellite Drag and Atmospheric Density Modeling.” Acta Astronautica. http://dx.doi.org/10.1016/j.actaastro.2013.10.005.

Zuppardi, G., 2004. “Accuracy of the Maxwell’s theory in space application.” Dipartimento di Scienza ed Ingegneria dello Spazio. ‘‘Luigi G. Napolitano’’, Universita di Napoli ‘Frederico II’’, Naples, Italy.